THE

LONDON, EDINBURGH, AND DUBLIN

PHILOSOPHICAL MAGAZINE

AND

JOURNAL OF SCIENCE.

[SEVENTH SERIES.]

AUGUST 1934.

XVII. *Two Problems arising in Practical Applications of Heat Theory.* By E. N. Fox, *M.A., B.Sc.**

WHEN endeavouring to apply results obtained from the mathematical theory of heat conduction to practice, one often finds that the assumptions of the theory do not fit the facts with sufficient accuracy, and it then becomes desirable to modify, if possible, the theory in order to allow to some extent for the discrepancies. Two problems arising in this manner will be considered in the present paper.

(a) *Boundary Law at a Lagged Surface.*

It is usual when considering a surface exposed to air to assume as the boundary condition Newton's law, viz., that the rate of loss of heat is proportional to the excess of the surface temperature above the external temperature, since this law is mathematically simple and in good agreement with fact. However, one often finds in practice that the main mass under consideration is not exposed directly to the air, but is covered by one or more layers of lagging, and it is then necessary to consider the boundary law under such conditions. One could, of course, in such cases seek exact solutions for the heat flow in each layer

* Communicated by the Director of Building Research, Building Research Station, Garston, Herts.

as well as in the main mass, but the labour involved would be very great and the results very cumbersome and complex.

Fortunately, however, this is rarely necessary, since the effect of the heat capacity of the lagging is usually small compared with that of its conductivity, and we find that, if the former is neglected, the heat losses from the boundary of the main mass obey Newton's law. Nevertheless, it is often very useful to be able to correct, even though approximately, for the effects of heat capacity in the lagging, and we shall, therefore, now derive an expression for the boundary law at a lagged surface when the effects of heat capacity are included to a first approximation. In general the lagging will be formed by one or more plane layers of different materials, but, when considering the heat flow through such layers, it is simpler to regard them as forming a special case of a lagging in which the conductivity and heat capacity/unit volume are functions of one space coordinate x. Consider such a lagging bounded internally by the plane $x=0$ and externally by the plane $x=a$, at which latter surface Newton's law holds.

Let

$\kappa(x)$=conductivity,
$\sigma(x)$=heat-capacity/unit volume,
E′=emissivity of the outer surface,
T=temperature in the lagging,
$T_0(t)$=temperature at $x=0$,
$T_A(t)$=external air temperature at $x=a$,
$H_0(t)$=rate of heat flow/unit area across $x=0$.

We consider one-dimensional flow parallel to Ox, and in order to obtain the boundary law at the surface of the mass bounded by the lagging we require an expression for H_0 in terms of T_0, T_A and the constants of the lagging only.

The equation of heat flow in the lagging is

$$\frac{\partial}{\partial x}\kappa(x)\frac{\partial T}{\partial x}=\sigma(x)\frac{\partial T}{\partial t}, \quad . \quad . \quad . \quad . \quad . \quad (1)$$

while the most general type of initial condition is

$$T=\chi(x), \quad \text{when } t=0. \quad . \quad . \quad . \quad . \quad . \quad (2)$$

At $x=0$ we have

$$T=T_0(t), \quad . \quad . \quad . \quad . \quad . \quad . \quad . \quad . \quad (3)$$

and at $x=a$

$$-\kappa(a)\frac{\partial T}{\partial x}=E'\{T-T_A(t)\}. \quad . \quad . \quad . \quad (4)$$

Integrating (1) with regard to x, we obtain

$$-\kappa(x)\frac{\partial T}{\partial x}=-\int_0^x \sigma(x)\frac{\partial T}{\partial t}dx$$

$$=H_0(t)-\int_0^x \sigma(x)\frac{\partial T}{\partial t}dx \quad . \quad . \quad . \quad (5)$$

by the definition of H_0.

Integrating again, and using (3), we obtain

$$T(x,t)=T_0(t)-H_0(t)\int_0^x \frac{dx}{\kappa(x)}$$

$$+\int_0^x \frac{1}{\kappa(x)}\int_0^x \sigma(\xi)\frac{\partial T(\xi,t)}{\partial t}d\xi\,dx.$$

This we simplify by putting

$$\int_0^x \frac{dx}{\kappa(x)}=\phi(x) \quad . \quad . \quad . \quad . \quad . \quad . \quad (6)$$

and integrating by parts, whence we have

$$T(x,t)=T_0(t)-H_0(t)\phi(x)+\int_0^x \{\phi(x)-\phi(\xi)\}\sigma(\xi)\frac{\partial T(\xi,t)}{\partial t}d\xi.$$

$$. \quad . \quad . \quad (7)$$

Substituting in (4) from (5) and (7), we obtain

$$H_0(t)-\int_0^a \sigma(\xi)\frac{\partial T(\xi,t)}{\partial t}d\xi$$

$$=E'\Big[T_0(t)-T_A(t)-H_0(t)\phi(a)$$

$$+\int_0^a \{\phi(a)-\phi(\xi)\}\sigma(\xi)\frac{\partial T(\xi,t)}{\partial t}d\xi\Big],$$

whence, putting

$$\frac{1}{E}=\frac{1}{E'}+\phi(a)=\frac{1}{E'}+\int_0^a \frac{dx}{\kappa(x)}, \quad . \quad . \quad . \quad (8)$$

we obtain

$$H_0(t)=E\{T_0(t)-T_A(t)\}+\int_0^a\{1-E\phi(\xi)\}\sigma(\xi)\frac{\partial T(\xi,t)}{\partial t}\,d\xi. \quad . \quad . \quad . \quad (9)$$

Substituting from (9) for H_0 in (7), we obtain, after simplification,

$$T(x,t)=\{1-E\phi(x)\}T_0(t)+E\phi(x)T_A(t) -\int_0^a K'(x,\xi)\frac{\partial T(\xi,t)}{\partial t}\,d\xi, \quad . \quad . \quad (10)$$

where

$$\left.\begin{aligned} K'(x,\xi)&=\{1-E\phi(x)\}\phi(\xi)\sigma(\xi), \quad 0\leq\xi\leq x\\ &=\{1-E\phi(\xi)\}\phi(x)\sigma(\xi), \quad x\leq\xi\leq a\end{aligned}\right\}. \quad (10a)$$

Equation (10) is an integral equation in x and a differential equation in t which, combined with equation (2), is completely sufficient to determine T as a function of x and t*.

For the case where the heat capacity of the lagging is small the terms containing σ will be small, and the first approximation is obtained by putting $\sigma(x)\equiv 0$.

We then have from (9)

$$H_0(t)=E\{T_0(t)-T_A(t)\}, \quad . \quad . \quad . \quad . \quad (11)$$

thus showing that the heat losses from the inner surface obey Newton's law. The temperature in the lagging in this first approximation is from (10)

$$T(x,t)=\{1-E\phi(x)\}T_0(t)+E\phi(x)T_A(t). \quad . \quad . \quad (12)$$

To obtain the second approximation to H_0 correct to the first order in σ we substitute in the small integral term of (9) the value of T given by the first approximation (12), and we then have

$$H_0(t)=E\{T_0(t)-T_A(t)\}+\frac{dT_0}{dt}\int_0^a\{1-E\phi(\xi)\}^2\sigma(\xi)\,d\xi +\frac{dT_A}{dt}\int_0^a\{1-E\phi(\xi)\}E\phi(\xi)\sigma(\xi)\,d\xi. \quad (13)$$

Further approximations correct to the second or higher orders in σ may be similarly obtained, although in practice sufficient accuracy will generally be obtained by using (13).

* *Cf.* Carslaw, 'The Conduction of Heat,' Macmillan 1921, ch. 12.

Deferring until later the estimation of the errors involved in the approximation, let us consider further equation (13), which, with the suffix 0 dropped, gives for a lagged mass a boundary law of the form

$$H=E\left\{T-T_A+F\frac{dT}{dt}+G\frac{dT_A}{dt}\right\}, \quad . \quad . \quad (14)$$

where E, F, G, are constants of the lagging, T is the temperature at the surface of the mass, T_A is the external temperature outside the lagging, and H is the rate of heat flow per unit area from the surface of the mass. The constants E, F, G can be determined from the definite integrals in (8) and (13), and in the general case of a lagging composed of n homogeneous layers, in which the rth layer from the inner surface has thickness d_r, conductivity κ_r, and heat capacity per unit volume σ_r, these integrals can be evaluated, and we obtain

$$\left.\begin{aligned}\frac{1}{E}&=\sum_{r=1}^{n}\frac{d_r}{k_r}+\frac{1}{E'},\\ F&=E\sum_{r=1}^{n}\left(\nu_r^2+\frac{d_r^2}{12\kappa_r^2}\right)\sigma_r d_r,\\ G&=\sum_{r=1}^{n}\nu_r\sigma_r d_r-F,\end{aligned}\right\} \quad . \quad . \quad . \quad (15)$$

where

$$\nu_r=\frac{d_r}{2\kappa_r}+\sum_{q=r+1}^{n}\frac{d_q}{\kappa_q}+\frac{1}{E'}. \quad . \quad . \quad . \quad (15a)$$

Let us now consider the effect, when obtaining theoretical solutions of heat flow, of using the boundary law (14) in place of Newton's law (11). Firstly, it must be noted that the G term introduces no theoretical complexity, since we may take $G=0$ provided we replace the actual air temperature T_A by the quasi air temperature

$$T'_A\equiv T_A-G\frac{dT_A}{dt}.$$

Analytically, therefore, we need consider, in place of (14), the equally general form

$$H=E\left(T-T_A+F\frac{dT}{dt}\right). \quad . \quad . \quad . \quad . \quad (16)$$

Secondly, since the F term is linear in T, it follows that any method of solution of a particular problem involving Newton's law will generally apply also if the boundary law is (16), but the algebra involved will be much more complex. In practice the F term is usually not sufficiently important to warrant the labour of evaluating the more complex solution, and we therefore proceed by taking $F=0$ and evaluating the temperature T' (say) at the boundary, whence we can include F with sufficient practical accuracy by replacing T_λ by the quasi air temperature $T_\lambda - F\frac{dT'}{dt}$. It may be further noted that for cases where the temperature gradient in the mass is small it is generally sufficiently accurate, and certainly quicker, to use for T' the value of T calculated on the assumption that the mass has an infinite conductivity, and is, therefore, at a uniform temperature.

Turning now to the consideration of the errors involved in neglecting the terms in σ of order higher than the first, we see, by substituting for T_λ in (9) from the exact expression (10) instead of the first approximation (12), that the neglected term in H_0 is

$$-\int_0^a \{1-E\phi(\xi)\}\sigma(\xi)\int_0^a K'(\xi,\lambda)\frac{\partial^2 T(\lambda,t)}{\partial t^2}\,d\lambda\,d\xi. \qquad (17)$$

Consider first the following theorem :—

"The maximum temperature attained in a non-heat-evolving mass during any time interval will occur either at the commencement of the time interval or at some point on the boundaries of the mass."

The truth of this is easily seen, for if the maximum temperature is reached not at a boundary, but at some point within the mass, then, since the temperature is a maximum in space, there will be a net flow of heat from the point, the temperature must, therefore, be decreasing, and cannot be a maximum in time unless it occurs at the commencement of the time interval considered. Conversely, if the maximum occurs later in time it must occur at some point on a boundary, and furthermore, at this point the temperature of the external medium at the time of the maximum must be at least as great as this maximum, for otherwise there would be a net flow of heat from the point both to the mass and the external

medium, whence the temperature would be decreasing and could not be a maximum in time. It follows as a corollary that :

" Given the initial temperature of a non-heat-evolving mass, the temperature at some of the boundaries, and the external temperature at the remainder, then the maximum temperature attained in the mass during any subsequent time interval cannot be greater than the greatest of (1) the maximum initial temperature, (2) the maximum given boundary temperature, and (3) the maximum given external temperature."

A similar result holds for the minimum temperature also, and hence for the maximum modulus of the temperature.

Returning to the problem in hand, we know that, since equations (1) to (4) are linear in T, we can put

$$T = T' + T'', \quad . \quad . \quad . \quad . \quad . \quad . \quad (18)$$

where T' is the temperature when $\chi(x) \equiv 0$ and T'' is the temperature when $T_0(t) \equiv T_A(t) \equiv 0$. It also follows that $\frac{\partial^2 T'}{\partial t^2}$ will be the temperature in the mass when the initial temperature is zero, and T_0, T_A are replaced by $\frac{d^2 T_0}{dt^2}$, $\frac{d^2 T_A}{dt^2}$ respectively. Hence, since the preceding corollary will apply also to the maximum modulus of the temperature, we have

$$\left| \frac{\partial^2 T'}{\partial t^2} \right| \leq M,$$

where M is the greater of the maximum moduli of $\frac{d^2 T_0}{dt^2}$ and $\frac{d^2 T_A}{dt^2}$. Hence the contribution of T' to the neglected term (17) is in modulus

$$\leq M \int_0^a \{1 - E\phi(\xi)\}\sigma(\xi) \int_0^a K'(\xi, \lambda)\, d\lambda\, d\xi. \quad . \quad (19)$$

Considering now the contribution of T'' to (17), we note that in the case of $T_0 \equiv T_A \equiv 0$ the term (17) is equal to H_0, and hence by (9) it also equals

$$\int_0^a \{1 - E\phi(\xi)\}\sigma(\xi) \frac{\partial T''(\xi, t)}{\partial t} d\xi. \quad . \quad . \quad . \quad (20)$$

Now, since the equations of heat flow are linear, $\frac{\partial T''}{\partial t}$ will be the temperature for the case of zero T_0 and T_λ and initial temperature

$$\left(\frac{\partial T''}{\partial t}\right)_{t=0} = \frac{1}{\sigma(x)} \frac{\partial}{\partial x} \kappa(x) \frac{\partial \chi}{\partial x} = f(x) \quad \text{(say)}.$$

Let M_1 be the maximum of $|f(x)|$ and T_1 be the temperature in the case of zero T_0 and T_λ and initial temperature M_1 throughout the mass. Then

$$\left|\frac{\partial T''(\xi, t)}{\partial t}\right| \leq T_1(\xi, t), \quad \ldots \quad (21)$$

for $T_1 - \frac{\partial T''}{\partial t}$, $T_1 + \frac{\partial T''}{\partial t}$, are the temperatures in the cases of initial positive temperature distributions $M_1 - f(x)$, $M_1 + f(x)$, respectively, and $T_0 \equiv T_\lambda \equiv 0$.

From (10) we now have for T_1

$$\left.\begin{aligned} T_1(x, t) &= -\int_0^a K'(x, \xi) \frac{\partial T_1(\xi, t)}{\partial t} d\xi, \\ T_1 &= M_1, \quad \text{when } t = 0. \end{aligned}\right\} \quad \ldots \quad (22)$$

$K'(x, \xi)$ is not a symmetric kernel, but

$$K(x, \xi) = \left(\frac{\sigma(x)}{\sigma(\xi)}\right)^{\frac{1}{2}} K'(x, \xi)$$

is symmetric.

Hence, if λ_n, $u_n(x)$ are the characteristic numbers and normalized orthogonal solutions* respectively of the homogeneous integral equation

$$u(x) = \lambda \int_0^a K(x, \xi)\, u(\xi)\, d\xi,$$

then the solution† of (22) will be

$$T_1(x, t) = \{\sigma(x)\}^{-\frac{1}{2}} \sum_{n=1}^{\infty} C_n u_n(x) e^{-\lambda_n t},$$

* *Cf.* Bôcher, 'An Introduction to the Study of Integral Equations,' Cambridge Tracts in Mathematics and Mathematical Physics, No. 10, 1926.

† *Cf.* Carslaw, *loc. cit.*

where

$$C_n = \int_0^a \{\sigma(x)\}^{\frac{1}{2}} M_1 u_n(x)\, dx.$$

Hence

$$M_1 \int_0^a \sigma(x) T_1(x, t)\, dx = \sum_{n=1}^{\infty} C_n^2 e^{-\lambda_n t} \leq e^{-\lambda_1 t} \sum_{n=1}^{\infty} C_n^2$$

$$\leq e^{-\lambda_1 t} \int_0^a M_1^2 \sigma(x)\, dx$$

by Bessel's inequality (Bôcher, *loc. cit.* p. 55).

Hence we have

$$\int_0^a \sigma(x) T_1(x, t)\, dx \leq M_1 e^{-\lambda_1 t} \int_0^a \sigma(x)\, dx. \quad . \quad . \quad (23)$$

The modulus of the contribution to (17) from T″ is thus, by (20), (21), and (23),

$$\leq \int_0^a \{1 - E\phi(\xi)\}\sigma(\xi) T_1(\xi, t)\, d\xi$$

$$\leq \int_0^a \sigma(\xi) T_1(\xi, t)\, d\xi$$

$$\leq M_1 e^{-\lambda_1 t} \int_0^a \sigma(\xi)\, d\xi. \quad . \quad . \quad . \quad (24)$$

Now we know (Bôcher, *loc. cit.* p. 56) that

$$\lambda_1^2 \geq \frac{1}{\int_0^a \int_0^a [K(x, \xi)]^2\, d\xi\, dx}, \quad . \quad . \quad . \quad . \quad (25)$$

and hence $\frac{1}{\lambda_1}$ is small, of order σ, and, therefore, $\lambda_1 t$ will become large for quite small values of t; e. g. for a lagging formed of one-inch slag wool $\frac{1}{\lambda_1}$ is of order ≤ 7 minutes.

Thus the effects of the initial temperature distribution in the lagging will become negligible after a short time, and subsequently the error in the boundary law (14) will be given by (19) only. Furthermore, when calculating the error at any particular time M may be chosen with reference only to the values of $\frac{d^2 T_0}{dt^2}$ and $\frac{d^2 T_A}{dt^2}$ occurring

in the preceding interval t of time, where t is just large enough to ensure that the error term (24) is negligible. Thus, isolated large values of $\frac{d^2T_0}{dt^2}$ and $\frac{d^2T_A}{dt^2}$ can give a large error term (19) for a short period only following their occurrence.

For the case of a lagging composed of n homogeneous layers the integrals in (19), (24), and (25) may be evaluated, and we obtain

$$\text{Error} \leq M\left[\tfrac{1}{2}E(G^2-F^2)\right.$$
$$+E\sum_{r=1}^{n}\left\{\sigma_r d_r\left(\nu_r^2+\frac{d_r^2}{12\kappa_r^2}\right)\left(\sum_{q=1}^{r-1}\sigma_q d_q+\frac{\sigma_r d_r}{2}\right)\right\}-E\sum_{r=1}^{n}\left.\frac{\sigma_r^2 d_r^3 \nu_r}{6\kappa_r}\right]$$
$$+M_1 e^{-\lambda_1 t}\sum_{r=1}^{n}\sigma_r d_r, \quad \ldots\ldots \quad (26)$$

where

$$\frac{1}{\lambda_1^2}\leq F^2+2\sum_{r=1}^{n}\left[\sigma_r d_r\left(\nu_r^2+\frac{d_r^2}{12\kappa_r^2}\right)\right.$$
$$\left.\times\left\{\sum_{q=1}^{r-1}\sigma_q d_q(1-2E\nu_q)+\sigma_r d_r(\tfrac{1}{2}-E\nu_r)\right\}\right]$$
$$-\sum_{r=1}^{n}\frac{\sigma_r^2 d_r^3 \nu_r(1-E\nu_r)}{3\kappa_r}-E\sum_{r=1}^{n}\frac{\sigma_r^2 d_r^5}{60\kappa_r^3}. \quad \ldots \quad (27)$$

The foregoing results have been obtained for slab lagging, but the general analysis will apply also to cylindrical lagging of bounding radii a and b $(>a)$ if we change the integration limits from $(0, a)$ to (a, b) and employ the substitution

$$\left.\begin{aligned}\kappa(x)&=\frac{x}{a}\kappa'(x),\\ \sigma(x)&=\frac{x}{a}\sigma'(x),\\ E'&=\frac{b}{a}E'',\end{aligned}\right\} \quad \ldots\ldots \quad (28)$$

which transforms the equation of slab flow to the equations of cylindrical flow. The values of E, F, and G for layer lagging can thus be deduced, as before, by evaluating the corresponding integrals, but the results will be much

more complex than in the slab case. For only one layer of radii a and b ($>a$), conductivity κ, heat capacity/unit volume σ, and emissivity E' we find

$$\left.\begin{aligned} E &= \frac{E'\theta}{\eta' \log\theta + 1}, \\ F &= \frac{Ea^3\sigma}{4\kappa^2\eta'^2}\big[\eta'^2\{\theta^2-1-2\log\theta-2(\log\theta)^2\} \\ &\qquad +\eta'(2\theta^2-2-4\log\theta)+2(\theta^2-1)\big], \\ G &= \frac{Ea^3\sigma}{4\kappa^2\eta'}\big[\eta'\{(\theta^2+1)\log\theta-\theta^2+1\}+2\theta^2\log\theta-\theta^2+1\big], \end{aligned}\right\} \quad . \quad . \quad . \quad (29)$$

where

$$\left.\begin{aligned} \theta &= b/a, \\ \eta' &= E'b/\kappa, \end{aligned}\right\} \quad . \quad . \quad . \quad . \quad . \quad . \quad . \quad (21a)$$

and the error in the boundary law is

$$\begin{aligned} \leq M\frac{E^2\sigma^2a^5}{64\kappa^3\eta'^2}\big[&\eta'^2\{(3\theta^4+4\theta^2-7)\log\theta-4\theta^4+8\theta^2-4-4(\log\theta)^2\} \\ &+\eta'\{4(3\theta^4+2\theta^2-2)\log\theta-13\theta^4+20\theta^2-7\} \\ &+16\theta^4\log\theta-12\theta^4+16\theta^2-4\big] \\ &+M_1e^{-\lambda_1 t'\sigma}\frac{b^2-a^2}{2a}, \quad . \quad . \quad . \quad . \quad . \quad . \quad . \quad (30) \end{aligned}$$

where

$$\begin{aligned} \frac{1}{\lambda_1^2} \leq\ & \frac{E^2\sigma^2a^6}{128\kappa^4\eta'^2} \\ &\big[\eta'^2\{4(\theta^4+1)(\log\theta)^2-10(\theta^4-1)\log\theta+8\theta^4-16\theta^2+8\} \\ &+\eta'\{16\theta^4(\log\theta)^2-(32\theta^4-8)\log\theta+22\theta^4-32\theta^2+10\} \\ &+32\theta^4(\log\theta)^2-48\theta^4\log\theta+28\theta^4-32\theta^2+4\big] \quad . \quad . \quad (31) \end{aligned}$$

The solution for the case of spherical lagging can be likewise deduced from the general analysis by changing the limits of integration to (a, b) and employing the substitution

$$\left.\begin{aligned} \kappa(x) &= \frac{x^2}{a^2}\kappa'(x), \\ \sigma(x) &= \frac{x^2}{a^2}\sigma'(x), \\ E' &= \frac{b^2}{a^2}E'', \end{aligned}\right\} \quad . \quad . \quad . \quad . \quad . \quad (32)$$

which transforms the equations of slab flow to the equations of spherical flow. For one layer of radii a, b, $(>a)$ and thermal constants κ, σ, E′ we find

$$\left.\begin{aligned} \mathrm{E} &= \frac{\mathrm{E}'\theta^2}{1+\eta'(\theta-1)}, \\ \mathrm{F} &= \frac{\mathrm{E}\sigma a^3}{3\kappa^2\eta'^2\theta^2}\{\eta'^2(\theta-1)^3+\eta'(\theta^3-3\theta+2)+\theta^3-1\}, \\ \mathrm{G} &= \frac{\mathrm{E}\sigma a^3}{6\kappa^2\eta'\theta}\{\eta'(\theta-1)^3+2\theta^3-3\theta^2+1\}, \end{aligned}\right\} \quad (33)$$

where

$$\left.\begin{aligned} \theta &= b/a, \\ \eta' &= \mathrm{E}'b/\kappa, \end{aligned}\right\} \quad . \quad . \quad . \quad . \quad . \quad . \quad (33a)$$

while the error term is

$$\begin{aligned} \leq \mathrm{M}\frac{\mathrm{E}^2\sigma^2a^5}{360\kappa^3\eta'^2\theta^2}&\left[\eta'^2\{15\theta(\theta-1)^5-8(\theta-1)^6\}\right. \\ &+\eta'\{28\theta^6-81\theta^5+60\theta^4+10\theta^3-33\theta+16\} \\ &\left.+40\theta^6-72\theta^5+40\theta^3-8\right]+\mathrm{M}_1e^{-\lambda_1t'}\sigma\frac{b^3-a^3}{3a^2}, \quad (34) \end{aligned}$$

where

$$\begin{aligned} \frac{1}{\lambda_1^2} \leq \frac{\mathrm{E}^2\sigma^2a^6}{90\kappa^4\eta'^2\theta^2}&\left[\eta'^2(\theta-1)^6+2\eta'(2\theta^6-9\theta^5+15\theta^4-10\theta^3+3\theta-1)\right. \\ &\left.+10\theta^6-36\theta^5+45\theta^4-20\theta^3+1\right]. \quad . \quad . \quad . \quad (35) \end{aligned}$$

All the results, both for the cylindrical and spherical cases, approximate to those of the slab case when $\theta \doteqdot 1$, *i. e.*, when the thickness of the lagging is small compared with the radii of its surfaces.

(*b*) *Extension of One-dimensional Solutions to allow for Subsidiary Transverse Heat Flow.*

The second problem we wish to consider arises from the fact that solutions of problems of two- or three-dimensional heat flow, if obtainable, usually take the form of doubly or triply infinite series respectively, and as such necessitate very great labour in numerical evaluation. As a consequence the most widely used solutions are those for

one-dimensional flow; but while it is generally true in practice that the flow of heat is mainly in one direction, it is, nevertheless, often desirable to be able to apply a correction for the subsidiary heat flow in transverse directions. We shall endeavour to show in the present paper how such a correction may be applied under certain conditions. We consider the general case of a homogeneous isotropic medium bounded by the cylindrical surface $f(x, y)=0$ and the planes $z=\pm c$, and we assume that all surfaces obey a boundary law of type (16), but that the heat exchanges at the end planes are small compared with those at the cylindrical surface. In order to increase the range of application of the results we include also the effect of heat evolution within the medium subject to the rate of evolution being a function of the time only.

Let

T = temperature in the medium,

$\epsilon(t)$ = rate of heat evolution/unit volume,

κ = conductivity,

σ = heat capacity/unit volume,

$h^2=\dfrac{\kappa}{\sigma}$ = diffusivity.

Then within the medium we have

$$h^2\nabla^2\mathrm{T}=\frac{\partial \mathrm{T}}{\partial t}-\frac{1}{\sigma}\epsilon(t), \quad . \quad . \quad . \quad . \quad (36)$$

while we assume an initial temperature distribution of form

$$\mathrm{T}=\mathrm{F}(x, y) \text{ when } t=0. \quad . \quad . \quad . \quad . \quad (37)$$

At the cylindrical surface $f(x, y)=0$ we have, in accordance with (16), an equation of the form

$$-\kappa\frac{\partial \mathrm{T}}{\partial n}=\mathrm{E}_0\left(\mathrm{T}-\mathrm{T}_{A_0}+\mathrm{F}_0\frac{\partial \mathrm{T}}{\partial t}\right), \quad . \quad . \quad . \quad (38)$$

where ∂n is in the direction of the outward normal to the surface, while at the end planes we have

$$\left.\begin{aligned} -\kappa\frac{\partial \mathrm{T}}{\partial z}&=\mathrm{E}_1\left(\mathrm{T}-\mathrm{T}_{A_1}+\mathrm{F}_1\frac{\partial \mathrm{T}}{\partial t}\right), \quad z=c,\\ \kappa\frac{\partial \mathrm{T}}{\partial z}&=\mathrm{E}_2\left(\mathrm{T}-\mathrm{T}_{A_2}+\mathrm{F}_2\frac{\partial \mathrm{T}}{\partial t}\right), \quad z=-c. \end{aligned}\right\} \quad (39)$$

where E_1 and E_2 are small.

Now since the variation of temperature is small in the direction Oz, it is not usually of great importance to know the actual variation, and we therefore consider only the average temperature in this direction. In this respect the present theory is analogous to the theory of thin plates in which the stresses considered are average values taken through the thickness of the plate.

Let

$$\frac{1}{2c}\int_{-c}^{+c} \mathrm{T}\,dz = \overline{\mathrm{T}},$$

and integrate (36), (37), and (38) with regard to z. We then obtain

$$h^2\left(\frac{\partial^2\overline{\mathrm{T}}}{\partial x^2}+\frac{\partial^2\overline{\mathrm{T}}}{\partial y^2}\right)+\frac{h^2}{2c}\left[\frac{\partial\mathrm{T}}{\partial z}\right]_{-c} = \frac{\partial\overline{\mathrm{T}}}{\partial t}-\frac{1}{\sigma}\epsilon(t), \quad . \quad (40)$$

$$\overline{\mathrm{T}} = \mathrm{F}(x, y) \quad \text{when } t=0, \quad . \quad . \quad . \quad . \quad (41)$$

$$-\kappa\frac{\partial\overline{\mathrm{T}}}{\partial n} = \mathrm{E}_0\left(\overline{\mathrm{T}}-\mathrm{T}_{\lambda_0}+\mathrm{F}_0\frac{\partial\overline{\mathrm{T}}}{\partial t}\right) \quad \text{when } f(x, y)=0. \quad (42)$$

Substituting in (40) from (39), we obtain

$$h^2\left(\frac{\partial^2\overline{\mathrm{T}}}{\partial x^2}+\frac{\partial^2\overline{\mathrm{T}}}{\partial y^2}\right)-\frac{1}{2c\sigma}\left\{\mathrm{E}_1\left(\mathrm{T}-\mathrm{T}_{\lambda_1}+\mathrm{F}_1\frac{\partial\mathrm{T}}{\partial t}\right)_{z=c}\right.$$
$$\left.+\mathrm{E}_2\left(\mathrm{T}-\mathrm{T}_{\lambda_2}+\mathrm{F}_2\frac{\partial\mathrm{T}}{\partial t}\right)_{z=-c}\right\} = \frac{\partial\overline{\mathrm{T}}}{\partial t}-\frac{1}{\sigma}\epsilon(t). \quad (43)$$

The last term on the left-hand side of (43) depends on the transverse heat flow and is small, since E_1 and E_2 are small, and for the same reason the differences $[\overline{\mathrm{T}}-\mathrm{T}]_{z=\pm c}$ are small, and to the first order we can put $\overline{\mathrm{T}}$ for T_c and T_{-c} in (43). Deferring until later the consideration of the magnitude of the error thereby introduced, we see that (43) then becomes of the form

$$h^2\left(\frac{\partial^2\overline{\mathrm{T}}}{\partial x^2}+\frac{\partial^2\overline{\mathrm{T}}}{\partial y^2}\right)$$
$$=\alpha\overline{\mathrm{T}}+(1+\mathrm{M})\left(\frac{\partial\overline{\mathrm{T}}}{\partial t}\right)-\alpha_1\mathrm{T}_{\lambda_1}-\alpha_2\mathrm{T}_{\lambda_2}-\frac{1}{\sigma}\epsilon(t), \quad (44)$$

where

$$\left.\begin{aligned}&\alpha_1/\mathrm{E}_1=\alpha_2/\mathrm{E}_2=1/2c\sigma;\\ &\alpha=\alpha_1+\alpha_2; \quad \mathrm{M}=\alpha_1\mathrm{F}_1+\alpha_2\mathrm{F}_2.\end{aligned}\right\} \quad . \quad (45)$$

Let

$$\left.\begin{gathered}\overline{\mathrm{T}}e^{\alpha t}=\mathrm{T}'\ ;\quad \mathrm{T}_{A_0}e^{\alpha t}=\mathrm{T}'_{A_0}(1-\alpha\mathrm{F}_0)\ ;\\ \mathrm{E}_0(1-\alpha\mathrm{F}_0)=\mathrm{E}'_0\ ;\quad \mathrm{F}_0/(1-\alpha\mathrm{F}_0)=\mathrm{F}'_0\ ;\quad h^2/(1+\mathrm{M})=h'^2\ ;\\ e^{\alpha t}\left\{\frac{\epsilon(t)}{(1+\mathrm{M})\sigma}+\alpha_1\mathrm{T}_{A_1}+\alpha_2\mathrm{T}_{A_2}\right\}=\frac{1}{\sigma}\epsilon'(t).\end{gathered}\right\} \quad . \ . \ . \quad (46)$$

Then, neglecting second-order terms in α such as α^2, $\alpha\mathrm{M}$, the equations (44), (41), and (42) become

$$\left.\begin{gathered}h'^2\left(\frac{\partial^2\mathrm{T}'}{\partial x^2}+\frac{\partial^2\mathrm{T}'}{\partial y^2}\right)=\frac{\partial\mathrm{T}'}{\partial t}-\frac{1}{\sigma}\epsilon'(t),\\ \mathrm{T}'=\mathrm{F}(x,\,y)\text{ when }t=0,\\ -\kappa\frac{\partial\mathrm{T}'}{\partial n}=\mathrm{E}_0\left(\mathrm{T}'-\mathrm{T}'_{A_0}+\mathrm{F}_0\frac{\partial\mathrm{T}'}{\partial t}\right)\quad\text{when }f(x,\,y)=0.\end{gathered}\right\} \quad (47)$$

Thus T′ satisfies equations similar to those which T would satisfy if there were no heat flow parallel to the z-axis. Hence, if the problem admits of solution for the case of no flow in the direction Oz, then we can solve (47) for T′, and thence from (45) and (46) we can obtain the solution for $\overline{\mathrm{T}}$—the average temperature for a given $(x,\ y)$ and varying z—which includes to a first approximation the additional complexity of a small heat flow parallel to Oz.

Consider now the three main types of one-dimensional flow and let us see whether the above results can be used to advantage. Firstly, if we consider the most symmetrical type of flow, viz., radial flow in a sphere, then there is only one boundary at which heat exchanges can occur, and the conditions of the present problems do not apply. Secondly, if we consider the one-dimensional case of radial flow in a circular cylinder, there being no axial flow of heat, then the conditions of the present problem apply directly, and we can, therefore, extend the one-dimensional solution to give $\overline{\mathrm{T}}$, the axial average of the temperature, for the case of an additional relatively small axial flow in the cylinder.

Thirdly, if we consider the case of heat flow parallel to one direction Ox, there being no flow in the perpendicular directions Oy, Oz, then we can from the preceding results extend the one-dimensional solution to give $\overline{\mathrm{T}}$ in the case

of small heat flow in either or both the transverse directions Oy, Oz. For suppose we have small transverse heat flow in both directions Oy, Oz, then, regarding the mass as a cylinder with generators parallel to Oz, we can, by substitutions of type (46), reduce the problem to one in which there is no heat flow in the direction Oz. Thence, taking this simplified problem, and regarding the mass as a cylinder with generators parallel to Oy, we can by (46) reduce this problem to the case of no heat flow in the direction Oy also, *i. e.*, to the case of one-dimensional flow parallel to Ox. Conversely, from the one-dimensional solution we can obtain the modified solution for $\overline{\mathrm{T}}$—the average temperature over any section perpendicular to the main heat flow when there is subsidiary heat flow in the transverse directions. Since the modifications are small, the combined effect will be additive, *e. g.*, for α we take the sum of the α's for the y and z directions, and we need not, therefore, correct for both directions separately.

In each case the solution is obtained by writing down the one-dimensional solution for the case of no subsidiary heat flow, changing therein T, $\epsilon(t)$, etc., to T′, $\epsilon'(t)$, etc., and then substituting for these latter symbols their expressions given by (46), whence the required solution will be the expression for $\overline{\mathrm{T}}$ so obtained.

Turning now to a consideration of the error involved in the approximation, the term we have neglected in (43) is

$$\frac{1}{2c\sigma}\left\{\mathrm{E}_1\left(1+\mathrm{F}_1\frac{\partial}{\partial t}\right)(\overline{\mathrm{T}}-\mathrm{T}_c)+\mathrm{E}_2\left(1+\mathrm{F}_2\frac{\partial}{\partial t}\right)(\overline{\mathrm{T}}-\mathrm{T}_{-c})\right\}, \quad . \quad . \quad . \quad (48)$$

where T_c, T_{-c} are the values of T at the end planes.

Now we have for any T and T_c with the same (x, y)

$$\mathrm{T}-\mathrm{T}_c=(z-c)\left(\frac{\partial \mathrm{T}}{\partial z}\right)_{\xi} \qquad c\geq\xi\geq z\geq -c,$$

whence

$$|\,\mathrm{T}-\mathrm{T}_c\,|\leq 2c\ \max\left|\frac{\partial \mathrm{T}}{\partial z}\right|,$$

the maximum being for all (x, y, z) within the mass.

Hence

$$|\overline{T}-T_c| = \left|\frac{1}{2c}\int_{-c}^{+c}(T-T_c)\,dz\right| \leq \frac{1}{2c}\int_{-c}^{c}|T-T_c|\,dz$$
$$\leq 2c \max\left|\frac{\partial T}{\partial z}\right|.$$

Similarly we have

$$\left|E_1\left(1+F_1\frac{\partial}{\partial t}\right)(\overline{T}-T_c)\right| \leq 2c \max\left|E_1\left(1+F_1\frac{\partial}{\partial t}\right)\frac{\partial T}{\partial z}\right|. \quad . \quad . \quad . \quad (49)$$

Now let

$$cE_1\left(1+F_1\frac{\partial}{\partial t}\right)\frac{\partial T}{\partial z} = T^*. \quad . \quad . \quad . \quad . \quad (50)$$

Then from equations (36) to (39) we have for T^*

$$h^2\nabla^2 T^* = \frac{\partial T^*}{\partial t},$$

$$T^* = 0 \quad \text{when } t=0,$$

$$-\kappa\frac{\partial T^*}{\partial n} = E_0\left(T^*+F_0\frac{\partial T^*}{\partial t}\right) \text{ when } f(x, y)=0,$$

$$T^* = -\frac{E_1^2 c}{\kappa}\left(1+F_1\frac{\partial}{\partial t}\right)\left(T-T_{A_1}+F_1\frac{\partial T}{\partial t}\right) \quad \text{when } z=c,$$

$$T^* = \frac{E_1E_2c}{\kappa}\left(1+F_1\frac{\partial}{\partial t}\right)\left(T-T_{A_2}+F_2\frac{\partial T}{\partial t}\right) \quad \text{when } z=-c.$$

T^* is thus the temperature in the mass under the conditions given by the above equations, and hence, by the corollary to the theorem stated in section (*a*) of the present paper, we must have

$$\left.\begin{aligned} &|T^*| \leq \text{greater of} \\ &\quad \max\frac{E_1^2 c}{\kappa}\left|\left(1+F_1\frac{\partial}{\partial t}\right)\left(T_c-T_{A_1}+F_1\frac{\partial T_c}{\partial t}\right)\right| \\ &\text{and} \\ &\quad \max\frac{E_1E_2c}{\kappa}\left|\left(1+F_1\frac{\partial}{\partial t}\right)\left(T_{-c}-T_{A_2}+F_2\frac{\partial T_{-c}}{\partial t}\right)\right|. \end{aligned}\right\} \quad (51)$$

Now, since T_c T_{-c} are special values of T, they can be replaced by T in the inequality (51), and we then obtain from (49), (50), and (51)

$$\left|\mathrm{E}_1\left(1+\mathrm{F}_1\frac{\partial}{\partial t}\right)(\overline{\mathrm{T}}-\mathrm{T}_c)\right|$$

$$\leq\frac{2c}{\kappa}\max\left|\mathrm{E}_1\left(1+\mathrm{F}_1\frac{\partial}{\partial t}\right)\mathrm{E}_s\left(\mathrm{T}-\mathrm{T}_{\mathrm{A}_s}+\mathrm{F}_s\frac{\partial t}{\partial \mathrm{T}}\right)\right|_{s=1,2}, \quad (52)$$

where the alternative suffixes denote that the suffix to be chosen is that which gives the greater maximum. A similar result with the suffixes 1 and 2 interchanged will hold for the second term in (48).

The inequality (52) contains the temperature T, which is not given *ab initio*, but by considering the equations satisfied by T and its derivatives, and by applying the corollary of section (*a*) we may show in a similar manner to that used in deriving (51) that

$$\left|\mathrm{E}_r\left(1+\mathrm{F}_r\frac{\partial}{\partial t}\right)\mathrm{E}_s\left(\mathrm{T}-\mathrm{T}_{\mathrm{A}_s}+\mathrm{F}_s\frac{\partial \mathrm{T}}{\partial t}\right)\right|_{s=1,2}\leq \mathrm{M}_r+\mathrm{M}'_r, \quad (53)$$

where M_r is the greatest of the maxima of

$$\left.\begin{array}{l}\left|\mathrm{E}_r\left(1+\mathrm{F}_r\dfrac{d}{dt}\right)\mathrm{E}_s\left(1+\mathrm{F}_s\dfrac{d}{dt}\right)\left(\mathrm{T}_{\mathrm{M}}+\mathrm{F}_u\dfrac{d\mathrm{T}_{\mathrm{M}}}{dt}-\mathrm{T}_{\mathrm{A}u}\right)\right| \\ \text{and} \qquad \mathrm{E}_r\mathrm{E}_s\,|\,\mathrm{F}(x,y)\,|\end{array}\right\}\begin{array}{l}s=1,2,\\ u=0,1,2,\end{array}$$

. . . (54)

M'_r is the greatest of the maxima of

$$\left|\mathrm{E}_r\left(1+\mathrm{F}_r\frac{d}{dt}\right)\mathrm{E}_s\left(\mathrm{T}_{\mathrm{M}}+\mathrm{F}_s\frac{d\mathrm{T}_{\mathrm{M}}}{dt}-\mathrm{T}_{\mathrm{A}s}\right)\right|_{s=1,2}, \quad . \quad (55)$$

while T_{M} is a known function of t given by

$$\mathrm{T}_{\mathrm{M}}=\frac{1}{\sigma}\int_0^t\epsilon(t)\,dt. \quad . \quad . \quad . \quad . \quad . \quad . \quad (56)$$

Hence, from (48), (52), and (53), we have, finally, that the magnitude of the neglected term is

$$<\frac{1}{\sigma\kappa}(\mathrm{M}_1+\mathrm{M}_2+\mathrm{M}'_1+\mathrm{M}'_2). \quad . \quad . \quad . \quad . \quad (57)$$

This equation enables an upper bound to the error to be estimated and shows that the error is of the second order in E_1, E_2, as assumed.

We note further that the ratio of this term to the first-order terms retained in (44) will be small provided the ratios $E_1 c/\kappa$, $E_2 c/\kappa$ are small. If c is large, of order $1/E_1$, $1/E_2$, this will not be so, which means that the term retained is also of the second order in E_1, E_2, and thus, correct to the first order, the transverse heat flow may be neglected entirely. Conversely, if the transverse heat flow be neglected entirely, we can always obtain a useful measure of the error involved by estimating an upper limit to the magnitude of the second term in (43), using for this purpose the inequality (53) with $E_r = 1$, $F_r = 0$.

Summary.

The present paper deals with two problems which arise from the fact that the assumptions involved in the simplest and most useful mathematical solutions of heat conduction are often not obeyed with sufficient accuracy in practice, and some allowance for the discrepancies is therefore necessary. In section (*a*) is considered the boundary law operating at a lagged surface, and it is shown that when the heat capacity of the lagging is small an approximate boundary law may be used which is essentially similar in form to Newton's law, but contains small additional terms which may, however, be simply taken into account when of sufficient importance. In section (*b*) is considered the problem of a medium in which the main heat flow is one-dimensional, but there is also subsidiary heat flow in transverse directions, this latter not being, however, of sufficient importance to warrant the use of a cumbersome two- or three-dimensional solution even if one be obtainable. In such cases it is shown that if we concern ourselves only with the temperature averaged in the directions of subsidiary heat flow, then the solution for this latter, correct to the first order, may be easily obtained as a simple modification of the appropriate one-dimensional solution.

XVIII. *Flame Temperatures in Methane-air Mixtures.*

By Prof. W. T. David, *Sc.D.*, *and* J. Jordan, *M.Sc.*, *Ph.D.**

IN two previous papers † we have described a method of measuring flame temperatures by means of which it was possible to correlate the temperature measurements with accurately known inflammable mixture composition, and furthermore, to delay the making of these measurements after the moment of inflammation until such time as equilibrium (or apparent equilibrium) has been established. In the second of these papers we gave the results of experiments with carbon monoxide-air mixtures at 1 atmosphere and at 5 atmospheres density over the full range of mixture strengths between the limits of inflammability. It was shown that for any given mixture composition the temperature measured at the higher density was approximately 100° C. above that measured at the lower density, but the temperatures, except in the case of very weak mixtures, were always some hundreds of degrees C. below the ideal calculated temperatures. The experiments seemed to us to prove that the overall process of conversion of chemical energy into thermal energy in flames was far from complete, and we expressed the view that a latent energy in fairly stable and long-lived form was associated with the flame gases. This appeared to us to be not out of keeping with some luminosity experiments carried out in this laboratory some years ago, in which the afterglow recorded after the gases had been completely inflamed was found to exist for some time ; indeed, in one experiment it was seen for a period of 14 seconds ‡.

In the present paper we give the results of similar experiments with methane-air mixtures of widely varying composition at densities of $\frac{1}{3}$, 1, and 5 atmospheres. In general character they are similar to those obtained with the carbon monoxide-air mixtures.

Flame temperatures measured by the sodium-line reversal method are much higher than those we have

* Communicated by the Authors.

† David, Davies, and Jordan, Phil. Mag. xii. p. 1034 (1931) ; David and Jordan, Phil. Mag. xvii. p. 172 (1934).

‡ David and Davies, Phil. Mag. ix. p. 399 (1930).

measured for all inflammable mixtures so far examined, with the exception of carbon monoxide-air mixtures on the " weak " side of the " correct " A review of the sodium temperatures obtained by various observers suggests strongly that these temperatures are higher than those corresponding to the mean molecular translational energy of the flame gases.

Method of Experimenting.

The gaseous mixture of which the flame temperature is required is introduced into a large spherical explosion vessel and ignited by means of a centrally-placed spark gap. During the resulting combustion photographic records are taken simultaneously of the pressure developed (for which purpose a diaphram indicator was used) and of the resistance of a fine platinum-rhodium wire (·0005 in. diameter and about 2 in. long) situated about $1\frac{1}{2}$ in. from the point of ignition. A Wheatstone bridge in conjunction with a sensitive torsion-string galvanometer was used for the resistance measurements, and the resistance of the wire was converted to temperature by a system of direct calibration.

When a homogeneous gaseous mixture is ignited in this way, and simultaneous pressure and temperature records obtained according to the above scheme, it is found that shortly after the passage of the igniting spark the flame reaches the wire and its temperature rises rapidly to a steady value depending on the mixture strength, and remains at this steady value until the extent of the inflammation is sufficient to produce a sensible rise of pressure. The temperature of the wire then begins to increase again owing to adiabatic compression of the gases surrounding the wire. The duration of the period of steady temperature appears to depend only upon the size of the vessel and the velocity with which the flame is propagated through the mixture. This will be seen from the two records shown in fig. 1 ; the first of these (*a*) refers to a strong mixture and the second (*b*) to a weak mixture of methane and air. Both represent tracings from actual records.

If a larger vessel were used, thus delaying still longer the point at which the pressure begins to rise, the wire temperature would have remained sensibly constant

throughout the increased period *, and it is because of this that we feel justified in applying the term flame temperature to the steady temperatures attained during the pre-pressure interval in these experiments.

Experiments at Atmospheric Density.

In fig. 2 the steady temperature attained by the wire during the pre-pressure period (Tw) is plotted against

Fig. 1.

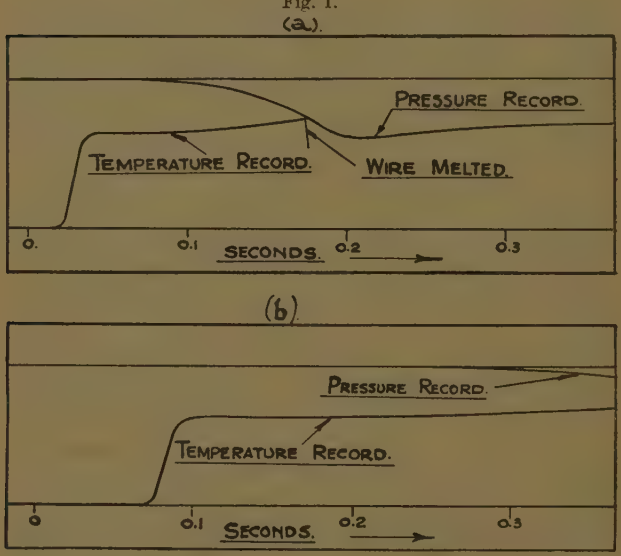

mixture strength and compared with the ideal temperature (Ti) calculated from the heat of combustion of the mixture and the specific heats of the products †. In making these calculations dissociation was neglected. On the over-rich side two curves are given accordingly

* Except in so far as the temperature of the gas is reduced by radiation. This must of course occur, but we think the effect is small both because of the numerous records of the type of fig. 1 (*b*), above which we have obtained and for reasons stated in our previous papers.

† The specific heats used are those given by Nernst and Wohl, *Z. Tech. Phys.* no. 10, p. 608 (1929). Experimental evidence justifying the use of these specific heats will be published shortly. For convenience we refer to them as the theoretical specific heats.

as carbon monoxide or hydrogen is regarded as being preferentially burnt; the true ideal temperatures will of course lie in the region between the curves. The curve *Td* shows the ideal temperature taking dissociation into account, but in this connexion it is to be noted that as the temperature measured by the wire is always well below that at which ordinary thermal dissociation begins to be appreciable, the more correct comparison would appear to be between *Tw* and *Ti*, and this view is supported

Fig. 2.

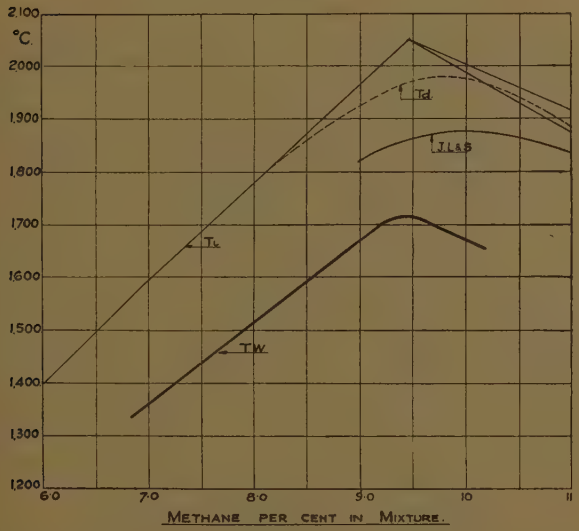

by the fact that in our experiments the maximum temperature is recorded with the mixture in which the gases are in their correct combining proportions.

In this respect the methane experiments are exactly in line with the CO experiments previously reported *, but they differ from them, however, in one important respect, viz., that whereas in the CO-air mixtures the difference between the measured and the calculated temperatures increases markedly with mixture strength,

* Phil. Mag. xvii. p. 172 (1934).

the increase in this difference with mixture strength in the case of the methane mixtures is not nearly so great.

The curve marked *J. L. & S.* (fig. 2) gives the temperatures obtained by the sodium line reversal method by Jones, Lewis, and Seaman * for methane-air mixtures burning in the open flame. These temperatures are much greater than those which we have measured, and we discuss them in a later section of the paper.

Fig. 3.

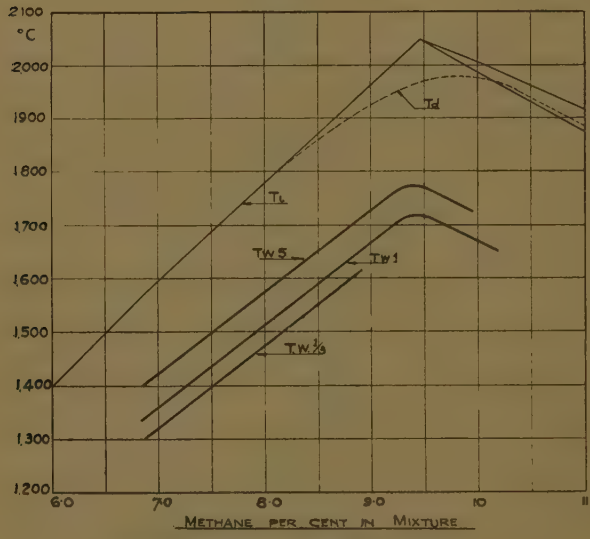

Experiments with varying Densities.

In fig. 3 we give the results of experiments with methane-air mixtures at densities of $\frac{1}{5}$ ($Tw\frac{1}{5}$) and 5 ($Tw5$) atmospheres respectively. For comparison the experiments at one atmosphere are also included ($Tw1$); the ideal curves Ti and Td are taken from fig. 2.

It will be observed that there is considerable increase (about 100° C.) in the measured flame temperatures as the density is increased from $\frac{1}{5}$ to 5 atmospheres, though the general characteristics of the results remain the same.

At first sight it might appear that these results could be explained in terms of a reduced percentage heat loss

* J. Am. Chem. Soc. liii. no. 3, p. 3993 (1931).

due to radiation as the density is increased, but the observed differences are much too large to be accounted for in this way. Indeed, as we have already shown in the case of CO-air mixtures, the total radiation loss at a density of one atmosphere is in itself very small (probably not exceeding 2 per cent. of the heat of combustion at the maximum measured temperatures). Furthermore, the temperature separation of the curves for different densities is sensibly independent of the temperature, and this could hardly be the case if radiation were appreciable.

Discussion.

It will be seen from a comparison of the temperatures determined by the sodium-line reversal method (curve *J. L. & S.*, fig. 2) and those determined by platinum thermometry during the pre-pressure period in explosions (curve *Tw*, fig. 2) that the former are much higher than the latter, particularly in the over-rich region. In what follows we attempt to show that the reason for this is that the sodium temperatures are higher than those corresponding to the mean molecular translational energy of the flame gases.

Jones, Lewis, and Seaman * have made some interesting experiments by the sodium method with methane-air mixtures in which small quantities of air are replaced by equivalent amounts of oxygen. We give in the table below temperatures taken from their curves for mixtures varied in this manner, each containing 9 per cent. methane.

Mixture.	Measured temperature.
9 % CH_4+91 % air	1820° C.
9 % CH_4+1 % O_2+90 % air	1830° C.
9 % CH_4+2 % O_2+89 % air	1870° C.
9 % CH_4+3 % O_2+88 % air	1935° C.

The mixtures are all on the "weak" side of the "correct" mixture (9·47 per cent. methane with atmospheric air), and there seems to be no apparent reason why the flame temperatures should vary, but, as will be seen from the table, there is a progressive increase in the sodium temperatures as the air is replaced by oxygen.

* *Loc. cit.*

Platinum thermometry experiments with similar mixtures have failed to produce similar results; indeed, we find on the contrary that very large increases in the oxygen content actually reduced the measured temperatures by a small amount, and this is consistent with the theoretical system of specific heats in which oxygen has a higher volumetric specific heat than nitrogen.

It should also be noted that the sodium temperature of the last-mentioned mixture in the table is 1935° C., which is somewhat higher than the ideal calculated temperature taking dissociation into account, but making no allowance for radiation loss.

Apart from the experiments summarized in the above table, the largest differences between sodium and platinum temperatures are generally found with over-rich mixtures. This will be seen from an inspection of the methane-flame temperature curves in fig. 2, and it is very noticeably the case in carbon monoxide flames *. With ethane, propane, and ethylene flames the sodium temperatures found by Jones, Lewis, and Seaman are so high in the very over-rich region that they greatly exceed the ideal temperatures †.

An explanation which at once occurs to the mind is that the composition of the mixture fed to the flame is affected by infiltration of secondary air, but, as against this, it is exceedingly difficult to see how secondary infiltration could reach the point (just above the inner cone) at which they measured their temperatures. Definite disproof of such an explanation seems to be afforded by the experiments of Ellis and Morgan ‡, who made sodium measurements with carbon-monoxide flames in a Smithell's separator, in which there could not possibly be any infiltration of secondary air. Their results (curve *E. & M.*) are shown in fig. 4, together with our platinum wire results (curve *D. J.*)§. In the same figure we show also the ideal temperatures calculated on the basis of the theoretical specific heats and assuming no radiation loss. It will be seen that here again the sodium temperatures in the very over-rich mixtures are above the ideal (and no reasonable system of specific heats could bring them below). With a

* Phil Mag. xvii. p. 176 (1934).
† J. Am. Chem. Soc. ciii. no. 1, p. 869 (1931).
‡ Trans. Faraday Soc. xxviii. p. 826 (1932).
§ Phil. Mag. xvii. p. 172 (1934).

50 per cent. mixture, for example, the sodium temperature is 150° C. above the ideal and about 450° C. above our platinum wire temperature.

We think the reason why the sodium temperatures are so high is that the sodium atoms are excited in flames to an extent greater than that corresponding to the mean molecular translational energy of the flame. Our platinum wire experiments indicate that there is a large amount of latent energy in the flame gases which could effect this, and it is of interest in this connexion to recall the fact that with thallium salts the spectrum-line reversal method gave flame temperatures 140° C. below those obtained with sodium and lithium *.

Fig. 4.

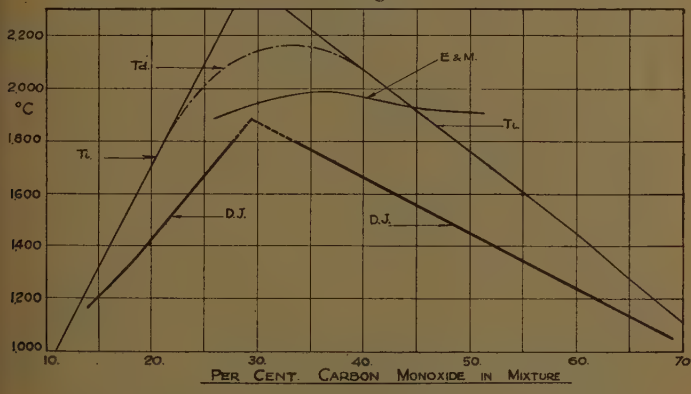

It has been shown in this paper that, as in the case of carbon monoxide flames, the steadily maintained platinum wire temperatures in methane flames are very much below the ideal calculated temperatures. When the methane flames are at atmospheric pressure the difference in these temperatures varies from about 250° C. to 300° C. Allowing about 2 per cent. for radiation loss, these measurements indicate a latent energy † in the flame gases amounting to approximately 15 per cent. of the heat of combustion. In view of the fact that the

* Jones and others, J. Am. Chem. Soc. liii. no. 1, p. 869 (1931).

† Luminosity experiments indicate that flame gases are in an abnormal condition (David and Davies, Phil. Mag. ix. p. 400 (1930); Withrow and Rassweiler, Industrial & Engineering Chemistry, xxiii. p. 769 (1931)).

temperatures increase as the density increases, it seems clear that the latent energy decreases appreciably with increase in density.

We are now making experiments with various diluent gases other than the nitrogen of the air in the hope of discovering whether the whole of this large amount of latent energy is entirely associated with the triatomic gases, formed as a result of combustion The experiments, so far as they have gone, suggest that this is the case, but we prefer to await their completion before carrying the discussion further.

XIX. *Radiation Characteristics of Open Wire Transmission Lines.* *By* T. Walmsley, *Ph.D., M.Inst.C.E.**

IN a previous communication † the author showed, *inter alia*, that the total radiation loss from long open wire radio transmission lines was not proportionately greater than from short lines. Now, although the *total* radiation loss from a balanced line need not be great, the possibility of the existence of narrow lobes of radiation of appreciable amplitude should not be overlooked. The seriousness of these narrow high amplitude lobes will not usually be great in the case of a transmitting system; but, when the lines are used for connecting an aerial with a receiver, the resulting "pick-up" from extraneous sources might conceivably have disturbing results. It is the purpose of this article to examine this possibility.

Consider a single wire, assumed to be isolated in space, carrying a non-attenuated progressive current. The amplitude ‡ of the electric field at a great distance from the wire is

$$\kappa \cot \frac{\theta_1}{2} \sin [n\pi (\cos \theta_1 - 1)], \quad . \quad . \quad . \quad (I)$$

where κ is a constant, θ_1 is the angle between the wire and the line joining the distant point to one end of the wire, and n is the length of the wire in wave-lengths.

As θ_1 varies between 0° and 180°, the expression passes

* Communicated by the Author.

† "Distribution of Radiation Resistance in Open Wire Radio Transmission Lines," Phil. Mag. xii. (Suppl.), August 1931.

‡ T. Walmsley, "Investigations into the Factors controlling the Economic Design of Beam Arrays," Journ. I. E. E. lxxiv. no. 450.

through a series of maximum and zero values, the number of rises and falls depending on the value of n.

This is shown pictorially in fig. 1 (a), which gives the three cases $n=1$, $n=5$, $n=10$. It is thus obvious that the optimum value of the amplitude increases with n, and it can be shown that it becomes infinite when n is infinite *.

Fig. 1.

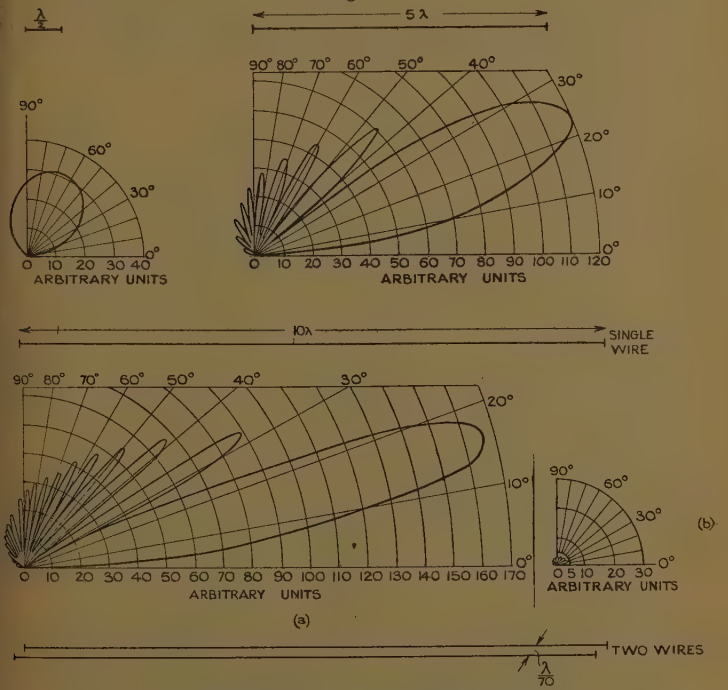

Polar radiation characteristics of transmission lines.
(a) Single wire in space. (b) Two wires in space-currents in wires antiphased.

If, now, a second wire is brought parallel to the first a fraction of a wave-length away, and having currents correctly antiphased with respect to similar currents in its companion wire, a multiplying factor is introduced which entirely changes the picture. This is shown in

* T. Walmsley, *loc. cit.*

fig. 1 (*b*) and on an enlarged scale in fig. 3 (*a*), which is the result of multiplying expresson (I) by

$$2 \sin\left(\frac{D\pi}{\lambda} \sin\theta_1 \sin\beta\right), \quad . \quad . \quad . \quad . \quad . \quad \text{(II)}$$

where D is the separation between the two wires in wave-lengths and β is the angle between the vertical and the projection on the vertical zx-plane normal to the wires of the line joining the wire to a distant point P (fig. 3).

$\frac{D}{\lambda}$ has been taken as $\frac{1}{70}$, which corresponds to a separa-

Fig. 2.

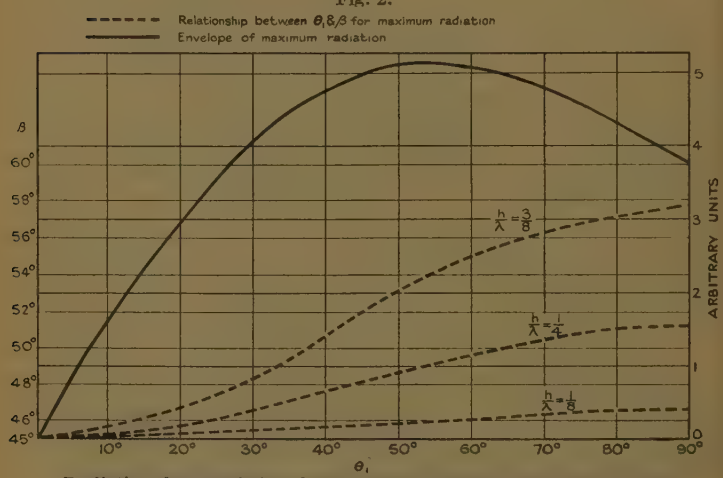

Radiation characteristics of a two-wire transmission line with perfect earth reflexion.

tion of 9″ between wires carrying current on a wave-length of 16 metres. This fraction is seldom exceeded in practice. In the case of the single wire isolated in space, the radiation diagrams in all planes having a common axis along the wire are similar; in the present case the radiation (or "pick-up" in the case of reception) varies according to the plane considered, being greatest in the plane containing the two wires, *i. e.*, when $\beta = 90°$. With this value for β and a separation of $\frac{1}{70}\lambda$, the amplitude expression (I) $\times$ (II) reduces to

$$\cdot 09\,\kappa(1+\cos\theta_1)\sin\beta.\sin[n\pi(1-\cos\theta_1)].$$

This is the condition illustrated in fig. 1 (*b*) for a value of $n=10$. In a plane normal to that containing the two wires the radiation is zero.

So far the hypothetical cases of radiation from wires isolated in space have been considered, and the effect of introducing a second wire has demonstrated how greatly the lobes of radiation are reduced in amplitude thereby.

Fig. 3.

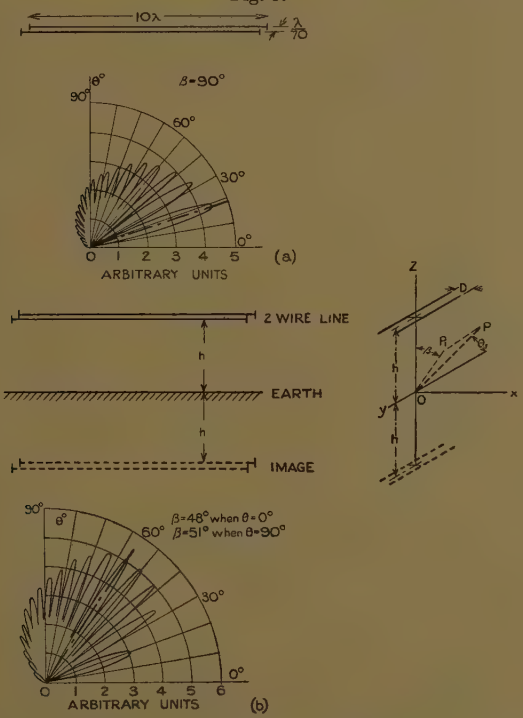

Polar radiation characteristics of a two-wire transmission line.
(*a*) Earth non-reflective. (*b*) Earth perfect reflective.

A third factor must now be introduced to take account of the reflexions due to the earth, and thus convert the problem into one of practical reality. The new factor by which (I) × (II) must be multiplied is

$$2 \sin\left(\frac{2\pi h}{\lambda} \sin\theta_1 \cos\beta\right), \quad . \quad . \quad . \quad \text{(III)}$$

where h is the height of the line above earth. Here the earth is regarded as a perfect reflector, which assumption is approximately correct for horizontal radiators.

The full expression (I) $\times$ (II) $\times$ (III) now becomes

$$\cdot 18\kappa(1+\cos\theta_1)\sin\beta \cdot \sin\left(\frac{2\pi h}{\lambda} \cdot \sin\theta_1 \cos\beta\right) \sin[n\pi(1-\cos\theta_1)]. \quad \ldots \quad \text{(IV)}$$

The last term of the expression (IV) gives the number of lobes of radiation ; the remainder of the expression gives the envelope of the amplitude of the lobes. The direction of maximum radiation is no longer such that $\beta = 90$, as in the case of two wires without reflexion ; by the usual methods of differentiation of expression (IV) it can be shown to vary in a manner indicated by the curves in fig. 2. Three cases are given, viz., when $\frac{\lambda}{h} = \frac{1}{8}$, $\frac{1}{4}$, or $\frac{3}{8}$, which covers most of the cases recurring in practice. In the same figure the envelope of the maximum radiation of the lobes as θ_1 varies between 0 and 90° is given. Within the boundary indicated by this envelope the radiation diagrams of the two-wire transmission line lie, regardless of the length of the line.

It is apparent that, as the length of the line increases, the maximum radiation occurs when $\theta_1 = 55°$ and $\beta = 46°$, 49°, or 54° approximately for values of $\frac{h}{\lambda} = \frac{1}{8}$, $\frac{1}{4}$, or $\frac{3}{8}$ respectively. To demonstrate the effect in polar form, the radiation characteristics of the two-wire line 10 wavelengths long without and with reflexion has been plotted in fig. 3.

These polar diagrams are shown on a much larger scale than those of fig. 1. Actually fig. 3 (*a*) is a reproduction of fig. 1 (*a*) drawn more accurately to scale. The main conclusion resulting from the foregoing discussion is that a perfectly balanced twin transmission line such as is used for feeding beam arrays does not produce high-amplitude lobes of radiation. Conversely, in the case of a receiving aerial system the " pick-up " of a long line of radiation arriving from any particular direction is not great relative to that of a short line.

XX. *Condensation of Thin Metallic Films: some Reflecting Observations. By* T. V. Starkey, *B.Sc., A.Inst.P., Science Research Scholar, University College, Nottingham* *.

1. Reflectivity of Thin Films.

IN many researches the variation of the reflecting powers of metallic films with thickness has been examined. Hitherto no attempt seems to have been made to correlate the results of these examinations with the processes of deposition of the films.

The present work was undertaken for the purpose of investigating the processes occurring during the early stages of growth of a condensed film by observing the variation of its reflecting power with thickness. Owing to the difficulty of obtaining consistent results with thin films no trustworthy data on these are yet available. This difficulty is no doubt due in part to the impossibility of determining film thicknesses with sufficient accuracy in such cases †.

The irregularity of the surfaces of condensed films precludes the use of interference methods for determining the film thickness. Since the density of the film bears no known relation to that of the bulk substance, absolute determinations of the thickness, made by weighing the films, are impossible, and relative determinations depending on this method are open to the objection that the density varies with the method of preparation of the films. The method described in the paper referred to above is not applicable to films as thin as those used in the present experiments. The ambiguity of specifications made in terms of thickness is avoided in the present work by measuring the time of growth of a deposit during its condensation from a molecular beam of constant density. In all previous researches the determination of the reflecting power of a film has involved its exposure to the atmosphere. The resulting contamination would produce drastic effects on the the reflectivity of the films, especially

* Communicated by Prof. Henry L. Brose.

† Tokyo Univ. Aeronaut. Research Inst., Report No. 91, p. 293 (1933): *cf.* Science Abstracts, no. 1879, May 1933.

in the earlier stages of growth. Errors due to this cause have here been eliminated by the following means :— The films are produced in a high vacuum, the residual atmosphere being of argon, and observations of the reflexion coefficients are made with the films *in situ*.

By the application of the theoretical relations deduced in later sections of this paper it becomes possible to obtain information about one aspect of the structures of metallic films formed under widely diverse conditions.

2. Apparatus.

The source of molecular rays was an iron vessel, containing a small piece of 99·9 per cent. pure cadmium, which communicated with the adsorption chamber by a small circular aperture. This vessel was surrounded by a closely-fitting quartz case around which was wound a heating spiral of several turns of platinum ribbon. Double layers of the ribbon were used at the extremities of the case to compensate the extra heat losses there. This oven was lagged with freshly roasted magnesium oxide contained in an outer brass case. The oven temperature was measured by means of a thermocouple, screwed tightly to the inner iron vessel, and a potentiometer.

The lower surface of a double-walled quartz receptacle formed the target. This surface was optically worked. Between successive experiments it was cleaned with nitric acid followed by distilled water and alcohol. During experiments the above-mentioned receptacle was filled with liquid air ; by this means the target was maintained at an appreciably constant low temperature. This vessel was waxed to the top of the adsorption chamber, and thus constituted part of the vacuum system. The adsorption chamber had two diametrically disposed windows which assisted the examination of the films formed on the target. A light-tight case surrounded this chamber. From the sides of this case, opposite the windows, projected two tubes arranged so as to facilitate the examination of the film by light specularly reflected at 30° incidence.

The adsorption chamber communicated, through a succession of drying tubes, pressure gauges, and a vapour trap, with a steel diffusion pump backed with a Hyvac. By this means the vacuum was kept high enough to eliminate disturbing collisions in the gaseous phase.

For the vapour pressures used the conditions fulfilled the requirements for the production of "Atomstrahlen."

The source of light was a 60-watt gas-filled lamp supplied from batteries giving a constant voltage. The light from this lamp passed through an Ilford micro-filter before it fell on the target. The intensity of the reflected beam was measured by means of a photo-cell combined with an electrometer. The optical system was calibrated by substituting for the target a surface of known reflecting power, and making observations of the electrometer deflexions when the incident light was reduced in known ratios by the successive interposition of a number of disks perforated with holes of different areas.

3. Theory of Reflexion.

Metallic films formed under conditions similar to those described in the previous sections are known to have a granular crystalline structure. Since crystallization has been shown to occur in such cases only on or after condensation *, the granules must range in size from that of a single atom to that of an aggregate of microscopic dimensions.

The intensity of the light reflected from a target on which such a film is adsorbed is the sum of the intensities reflected by the granules and the unobscured part of the target. If unit area of the film be considered, the intensity, I, of the reflected beam is given by

$$I = I_G . A_G + I_T . A_T, \quad . \quad . \quad . \quad . \quad . \quad (1)$$

where the suffix G refers to the granules and T to the target, A denoting the fraction of unit area in question.

If R be used to denote reflexion coefficients, equation (1) can be written

$$R = R_G . A_G + R_T . A_T. \quad . \quad . \quad . \quad . \quad . \quad (2)$$

Here R_G is a mean value of the reflexion coefficient of granules of the sizes and kind considered. If the film be formed by the condensation of a molecular beam of constant density, the first term on the right-hand side of equation (2) can obviously be written in the form $f(n_1, t)$, where n_1 is the number of granules per unit area and t is the time of growth of the film. By backing the

* Proc. Roy. Soc. A, cxli. p. 409 (1933).

target with polished metal disks of different kinds, different values, R_{T_1} and R_{T_2} of R_T, can be obtained.

At a given instant, t, using the value R_{T_1}, the observed reflexion coefficient is given by the equation

$$R_1 = f(n_1, t) + R_{T_1}.A_T. \quad . \quad . \quad . \quad . \quad . \quad (3)$$

Using the value R_{T_2} of R_T, but under otherwise identical conditions, a second value, R_2, is obtained, where

$$R_2 = f(n_1, t) + R_{T_2}.A_T. \quad . \quad . \quad . \quad . \quad . \quad (4)$$

From equations (3) and (4) the relation

$$(R_1 - R_2) = (R_{T_1} - R_{T_2})A_T \quad . \quad . \quad . \quad . \quad (5)$$

is obtained by subtraction. The validity of this equation depends on the invariance of $f(n_1, t)$ when the process is repeated. At any given instant only those aggregates above some small critical size will be effective in determining A_T. If the number of aggregates per unit area of this class be n, then, assuming the granules to be spherical, and of mean radius r,

$$A_T = 1 - n\pi r^2, \quad . \quad . \quad . \quad . \quad . \quad . \quad (6)$$

where r is given by

$$r \doteq \left(\frac{3\nu mt}{4\pi n\rho}\right)^{1/3}, \quad . \quad . \quad . \quad . \quad . \quad . \quad (7)$$

ρ being the density of the individual aggregates and ν the resultant stream density of the rays of molecules of mass m. Here νmt is the total mass deposited in time t, and this, to a first approximation, is divided between those aggregates greater than the critical size.

If $$K = n\pi\left(\frac{3\nu m}{4\pi n\rho}\right)^{2/3}, \quad . \quad . \quad . \quad . \quad . \quad (8)$$

equation (5) becomes

$$(R_1 - R_2) = (R_{T_1} - R_{T_2})(1 - K.t^{2/3}). \quad . \quad . \quad (9)$$

This may be rewritten

$$\frac{(R_{T_1} - R_{T_2}) - (R_1 - R_2)}{(R_{T_1} - R_{T_2})} = K.t^{2/3}. \quad . \quad . \quad (10)$$

In the cases dealt with in the following sections, the condition for negligible re-evaporation, stated by Cockcroft, is fulfilled *.

* Proc. Roy. Soc. A, cxix. p. 312 (1928).

For the solution of some parallel problems an alternative method based on analogous considerations could be applied. Thus equations (8) and (10) may be used in researches in which it is impossible to alter the reflecting power of the target, *e. g.*, in the study of metallic adsorption upon an opaque backing. In such cases two values of the wave-length of the incident light may be used in turn, the suffixes 1 and 2 in equation (10) signifying the reflexion of light of these wave-lengths. Here, by using two different filters for alternate readings, all the data required can be obtained from observations on a single film.

4. Experimental Results.

The following general procedure was adopted in the present investigation:—

(i.) These experiments formed a sequence characterized by the following features. If the members of this sequence be denoted by the letters *a*, *b*, *c*, etc., the experiments, when grouped in pairs, e. g., *a* and *b*, *c* and *d*, differed in that the films used in successive pairs were condensed from molecular beams of successively reduced density. The members of each pair differed only in respect of the initial reflecting power. The reduction of the stream density in the early stages of the sequence was but a negligibly small fraction of the initial stream density; in the later experiments, however, the stream density was reduced by a much larger factor, that used in the last pair of experiments being less than one-hundredth of that used in the first pair. In all these experiments a residual atmosphere of argon was used.

(ii.) A second sequence of experiments was performed which differed from the first in the use of a residual atmosphere of air.

The results of experiments (i.) are exhibited graphically in figs. 1–5, the characteristics of these several graphs being summarized below.

Fig. 1.—The variation of the reflecting power of the target and film during the formation of the latter is illustrated here. The curves are derived from alternate experiments of the sequence; these were performed in the order *a*, *c*, *e*. The dotted curve is derived from *a* and *c*; the mean values of the times required to form films of

given reflecting powers are plotted against those reflecting powers.

Fig. 2.—This graph consists of curves derived from a typical pair of experiments. In these experiments,

Fig. 1.

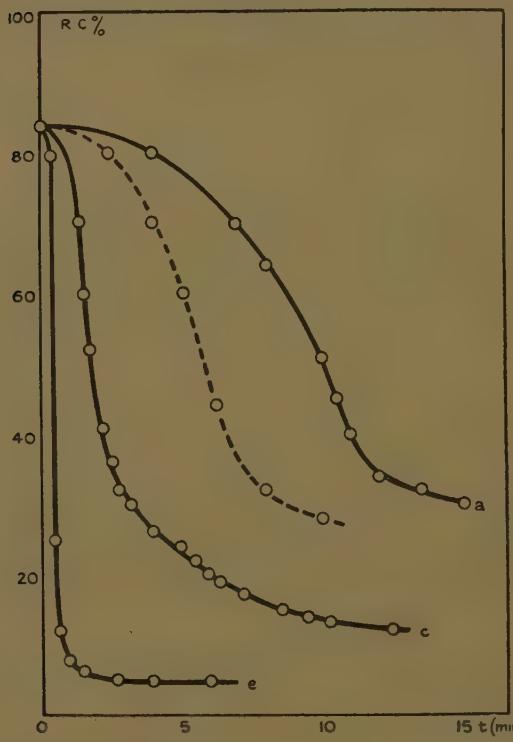

except for the initial reflecting power, all controllable conditions were identical.

Fig. 3.—The continuous curve of this figure was obtained from curves of the types *a* and *b*, fig. 2, in the manner indicated in the previous sections.

As shown by the curves of fig. 1, a continuous shortening of the process is brought about by its repetition. This

must be explained as due to a continuous sensitization of the surface, which persists in spite of the thorough cleansing between successive repetitions. In consequence of this sensitization $f(n_1, t)$, (equation (3), Section 3), is no longer invariant, and the equations of the last section

Fig. 2.

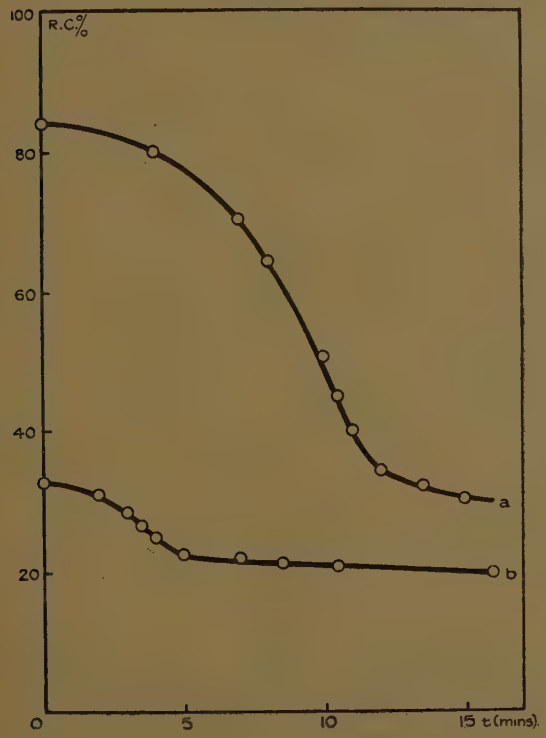

can be applied only after allowance has been made for this. An approximate correction can be made as follows. The time required to form a film of given reflecting power decreases regularly, and to a first approximation linearly, with each repetition. Hence the mean of the curves obtained from alternate experiments represents approximately the phenomena as they would occur under

conditions identical with those existing during the intermediate experiment. The dotted curve of fig. 1 is a typical mean. The correction suggested here is embodied in the dotted curve of fig. 3.

Fig. 3.

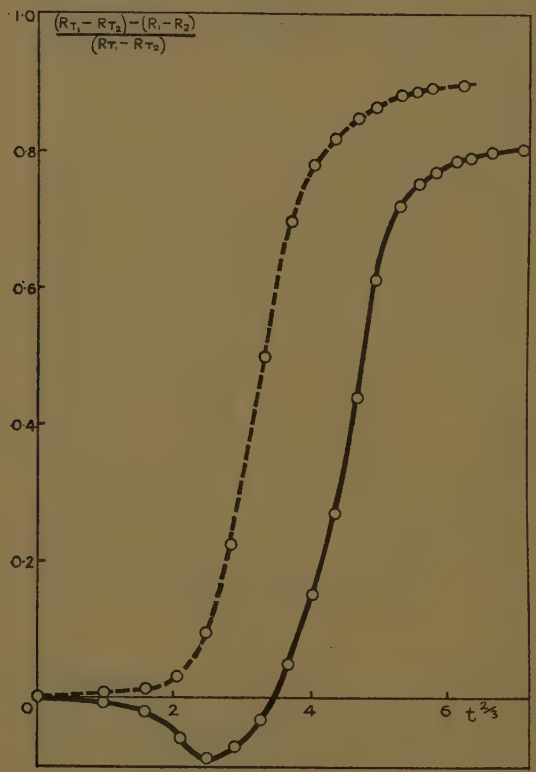

Fig. 4.—From equation (8) of Section 3, n is seen to be proportional to $K^3\nu^2$.

The continuous curve shows the variation of n, during the formation of a deposit, in the earliest stages of the sequence. According to this result, the number of aggregates greater than the critical size increases first

slowly and then more rapidly, ultimately reaching a maximum. As a result of the contact and coalescence of adjacent aggregates, the number of aggregates of this class decreases exponentially, as shown by the latter part of this curve. The broken curve illustrates the

Fig. 4.

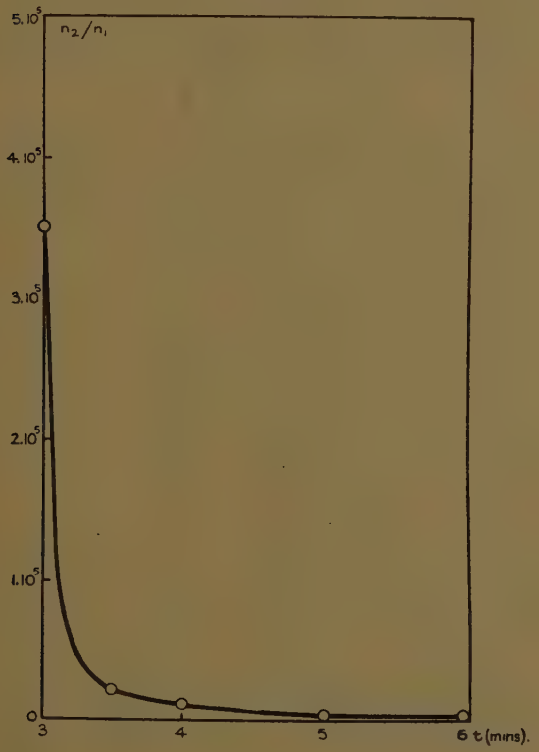

first part of this variation in the later experiments of the sequence.

Fig. 5.—The variation in the ratio of n in the later and earlier experiments respectively, with time, is shown here. This curve illustrates the combined effects upon the phenomena of sensitization and reduced stream

density. Since the ratio of the stream densities used in these experiments is a hundred to one, the effect of the reduction is shown at its maximum.

Fig. 5.

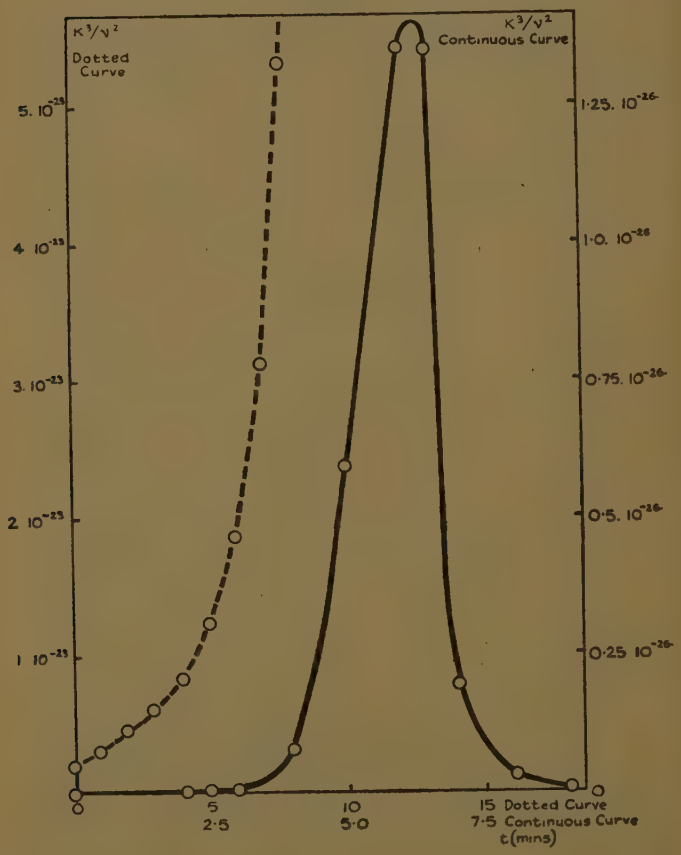

The experiments of the second series revealed no marked effect upon n of the change in the residual atmosphere.

5. Evidence regarding Processes occurring during Deposition.

(i.) *Theoretical Considerations.*

Two stages in the process of growth can readily be distinguished; these are: (*a*), in which the granules are small compared with their mean separation, and (*b*), in which the mean separation is so small that the contact and coalescence of adjacent granules becomes appreciable. These régimes are separated by a transition stage.

(a) *Granules small compared with mean separation.*

The formation of isolated aggregates is a necessary consequence of the irregularity and uneven contamination of the backing surface. An unbacked surface is known to support vapours supplied to it from its own interior structure to a depth of many molecules, and in scattered patches. Thus, except at isolated centres, the true surface forces are masked by these contaminating influences. Let the number of these active centres per unit area of the target be N, and let it be assumed that at the end of some short interval of time, t_0, all these centres are occupied. The mean volume of the aggregates, V_M, at a time t later than t_0, is given by the equation

$$V_M = V_0 + \frac{m\nu(t-t_0)}{\rho N}, \quad . \quad . \quad . \quad . \quad . \quad (1)$$

where t is the measured time of growth. Here V_0 is the mean volume at $t=t_0$. If the density, ρ, of the aggregates, and the stream density ν, of the molecular beam, remain constant, the mean volume obviously increases linearly with the time.

If the volumes of the aggregates are ranged about this mean volume according to the Gaussian error law, the number of granules, n_V, with a volume between V and V$+dV$ is given by

$$n_V = \frac{N}{2} \cdot \frac{h}{\sqrt{\pi}} \cdot e^{-h^2(V_M-V)^2} dV. \quad . \quad . \quad . \quad (2)$$

The number with a volume greater than the critical volume, V_C, at this instant is

$$n = \frac{N}{2}\left\{1 - \int_0^{V_C} \frac{h}{\sqrt{\pi}} \cdot e^{-h^2(V_M-V)^2} dV\right\}. \quad . \quad (3)$$

The integral in equation (3) cannot be evaluated directly. Since, however, $V_C \sim V_M$ is small, the following method may be used to give approximate results.

Let $$I = \frac{h}{\sqrt{\pi}} \int_0^{V_C} e^{-h^2(V_M - V)^2} dV.$$

If $$h(V_M - V) = z, \quad dV = -\frac{dz}{h},$$

and $$I = \frac{1}{\sqrt{\pi}} \int_0^{h(V_C - V_M)} e^{-z^2} dz.$$

Replacing e^{-z^2} by the equivalent series, and integrating, the above equation becomes

$$I = \frac{h(V_C - V_M)}{\sqrt{\pi}} \left\{ 1 - \frac{h^2(V_C - V_M)^2}{3} + \frac{h^4(V_C - V_M)^4}{5.2!} - \dots \right\}.$$

$$\therefore \quad n \doteq \frac{N}{2} \left[1 - \frac{h(V_C - V_M)}{\sqrt{\pi}} \left\{ 1 - \frac{h^2(V_C - V_M)^2}{3} \right\} \right]. \qquad (4)$$

Here $$\frac{dn}{dV_M} > 0, \quad \text{and} \quad \frac{d^2n}{dV_M^2} \gtrless 0,$$

according as $V_C \gtrless V_M$.

Thus the curve represented by equation (4) has the same general form as the first part of the continuous curve of fig. 4.

The above considerations are based on the assumptions that :

(α) As a result of the irregularity and uneven contamination of the surface active centres exist.

(β) These centres are all occupied after some interval t_0, short compared with the time of growth of a visible deposit.

(γ) The volumes of the aggregates are ranged about a mean volume according to the Gaussian law of errors.

The agreement of the results of these considerations, expressed in equations (1) and (4), with the experimentally derived results shown in fig. 4 establishes the validity of the assumptions. This forms the basis of the generalizations of the present section.

(b) *Granules and mean separation comparable.*

Here n continually decreases as a result of the contact and coalescence of adjacent granules.

$$\text{Rate of coalescence} = -\frac{dn}{dt} = an, \text{ where } a \text{ is constant.}$$

$$\therefore \qquad n = e^{b-at}, \quad . \quad . \quad . \quad . \quad . \quad . \quad . \quad . \quad (5)$$

where e^b is the value of n at the beginning of this régime.

(ii.) *Nature of the Target.*

The adsorbing surface used in this work was similar in most respects to those generally used in researches at high vacuum. The existing surface irregularities considerably affect the process of film deposition in its earliest stages. This process is also modified by the contaminating gas films which such a surface is known to support. Some effects of mechanical trapping by the surface crevices, and of gas contamination, on the deposition of the initial layers of a condensed film have been discussed in considerable detail in an earlier paper *.

Further confirmatory evidence of these effects is forthcoming from the present work. Here, again, the part played by the surface irregularities in supplementing, or even greatly magnifying, the normal adhesion becomes evident. Thus, after the formation of a single film upon the surface, a permanent sensitization of that surface occurs, and by none of the less violent methods is it possible to prevent this. This effect increases with each repetition of the process in spite of a thorough cleansing of the surface with nitric acid followed by distilled water and alcohol between successive repetitions. Although the net amount of material at any instant during the later stages of growth is less in the later experiments, the number of nuclei greater than the critical size increases with each repetition of the process, as indicated by the curves of fig. 1. That this increase is very substantial becomes evident when the greatly increased "covering power" of the later films is considered.

* Proc. Roy. Soc. A, cxl. p. 136 (1933).

In terms of the theoretical relations derived in the earlier part of this section, sensitization modifies the process in a way which can be represented by a reduction in t_0 and an increase in V_0.

(iii.) *Surface Migration of Molecules.*

The equations (1) and (4) of the present section were derived on the assumption that, after some interval t_0 short compared with the time occupied by an experiment, no increase in the total number of granules occurs. Since the maximum number of granules per unit area is small compared with the number of molecules impinging on that area in a time much shorter than t_0, the probability of a capture by all the active centres is extremely high. Moreover, the probability of the replacement of the molecules of the contaminating gas by those of the metallic vapour, and the consequent formation of new adsorption nuclei, is small, since the former, partly through the agency of mechanical trapping, are strongly adsorbed upon the target. No law of the variation of n with t derived on the assumption that migration and coalescence of those granules of volume greater than V_C occurs assumes the form found experimentally (fig. 4). The nuclear structure must, hence, be the result of the migration of particles of volume smaller than V_C, and probably, since V_C is small, of particles of molecular size.

(iv.) *Structure independent of Stream Density.*

According to equation (4) of this section, for given initial conditions n is determined completely at any instant by V_M, where V_M, as shown by equation (1), is homogeneous with respect to stream density and time, *i. e.*, for a film of given mass n is independent of the rate of its formation. Hence, according to the theory, n_2/n_1 is constant if no sensitization occurs. The variation of this ratio with time, shown in fig. 5, is of the type predicted by considerations based on the assumption that the variation of n with repetition, in such a sequence as that in question, results entirely from sensitization. It is probable, then, that for a film of given mass the structure is independent of its rate of formation, as indicated by the foregoing theory.

(v.) *Structure unaffected by Adsorption in Air.*

The stability of the aggregates is shown by these experiments to be very high.

(vi.) *Summary of the Process.*

Surfaces of the kind employed in this work, as a result of their irregular structure and contamination by adsorbed or trapped atmospheric gases, favour adsorption at isolated active centres. During the early stages of film formation all these active centres become occupied by metallic nuclei (Section 5 (i.)), and the subsequent growth of the film consists in the enlargement and development of these into crystal aggregates. This granular growth is favoured by migration to the active centres of molecules incident on the gas-contaminated areas (Section 5 (iii.)). The continued growth results ultimately in the contact and coalescence of adjacent granules.

6. Summary.

A method of correlating some structural characteristics of metallic films and their reflecting powers is described (Section 3). This method is applied to the study of films condensed from a molecular beam of cadmium vapour upon a target cooled by liquid air.

The following results of the processes occurring during the condensation of such films are inferred :—

(i.) As a result of the surface irregularities and the uneven contamination of the target, active centres exist (Section 5 (i.)).

(ii.) All these centres become occupied in a time short compared with the time of growth of the film (Section 5 (i.)).

(iii.) The volumes of the aggregates forming at these centres are ranged about a mean volume according to the Gaussian law of errors (Section 5 (i.)).

(iv.) As a result of mechanical trapping a permanent sensitization of the surface occurs. This sensitization persists in spite of the cleaning of the surface with acid, and increases with each repetition of the process (Section 5 (ii.)).

(v.) The growth of the aggregates is favoured by migration to the active centres of small particles only, probably of molecules (Section 5 (iii.)).

(vi.) The number of aggregates per unit area is independent of the rate of formation of the film (Section 5 (iv.)).

(vii.) No appreciable change in the number of aggregates occurs if a residual atmosphere of air be used.

I gratefully acknowledge my indebtedness to the members of the Physics Department of University College, Nottingham, for helpful discussions during the progress of the work.

XXI. *The Ultimate Origin of the Actinium Series.* *By* Harold J. Walke, *B.Sc., Mardon Research Scholar, Department of Physics, Washington Singer Laboratories, University College, Exeter* *.

THE origin of actinium and its parent protactinium has always been a question of great interest and importance, and it is still unsettled. To account for the actinium series a branching of the uranium series was demanded, though it has also been suggested that actinium has its ultimate origin not in a branch product of the uranium series but in an isotope of uranium existing in small relative amount.

It seems clear that the main line of transformation of the uranium series is given by the scheme below:

$$\underset{92}{\mathrm{U\,I}} \xrightarrow{\alpha} \underset{90}{\mathrm{U\,X_1}} \xrightarrow{\beta} \underset{91}{\mathrm{U\,X_2}} \xrightarrow{\beta} \underset{92}{\mathrm{U\,II}} \xrightarrow{\alpha} \underset{90}{\mathrm{Io}} \xrightarrow{\alpha} \underset{88}{\mathrm{Ra}} \xrightarrow{\alpha} \text{etc.}$$

In addition to these, however, two other products whose origin is uncertain have been separated from uranium called uranium Y and uranium Z. Uranium Y (UY) is a β-ray product and has a half-value period of 24·6 hours. It seems clear that this product, which emits soft β-rays, is of atomic number 90 isotopic with uranium X_1, and forms only about 3 per cent. of the equilibrium amount to be expected if it were in the main

* Communicated by Prof. F. H. Newman, D.Sc.

line of descent. Either therefore uranium Y is a branch product at some point of the uranium series, or arises from some yet unknown radioactive isotope of uranium. It has been suggested that uranium Y is the head of the actinium series

Uranium Z is a product of weak activity which emits β-rays and is transofrmed with a half-period value of 6·7 hours. It is estimated that the amount of this product is only about 0·35 per cent. of that to be expected if it were in the main line of descent of the uranium series. In chemical properties it behaves like an element of atomic number 91, and is thus isotopic with protactinium. The exact origin of uranium Z is uncertain ; it may be either a branch product of uranium X_1, in which case the scheme of dual transformation is as shown below, or it may be one of the products of an unknown isotope of uranium of weak activity

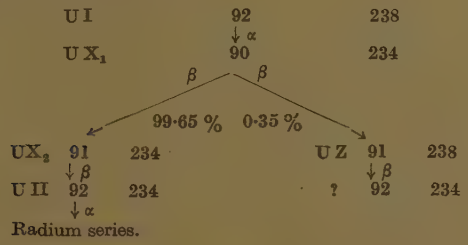

Radium series.

According to these transformations uranium Z and uranium X_2 are isotopes of the same mass, and, adopting the nuclear scheme suggested in a previous paper *, these bodies are similarly constituted, viz.,

UX_2	91	234	$45\alpha+p+53n$,
U Z	91	234	$45\alpha+p+53n$,

so that we should expect uranium II to result from the β-ray disintegration of uranium Z as well as from the disintegration of uranium X_2, the process being regarded as forming two branches, as shown,

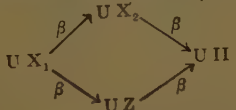

* Walke, Phil. Mag. xvii. p. 793 (1934).

similar to the branching which occurs with radium, thorium, and actinium C.

The difference in half periods of uranium X_2 and uranium Z shows that the nuclei of these elements are physically distinct, though they apparently arise from identical parent nuclei by similar disintegrations. It is difficult to imagine how this can occur except by increasing the complexity of the radioactive problem and postulating some new nuclear mechanism. It will be shown in this paper that this difficulty can be removed by supposing that uranium Z is a link in the actinium series, arising as a result of the disintegration of a heavier isotope of uranium.

Aston * examined the isotopic constitution of lead from a uranium mineral by means of a mass-spectrograph. The mass spectrum showed a strong line 206, a faint line 207, and a still fainter line 208. He concluded that the line 207 must be due in part to the end product of the actinium series. This is now generally accepted and determines the weight of all the members of the actinium series, the evidence indicating that protactinium must arise from an isotope of uranium. The simplest postulate is that this isotope, called actino-uranium of atomic number 92, has a mass 235, and is transformed by the emission of an α-particle into a β-ray product of number 90 which gives rise to protactinium. This β-ray product is identified with uranium Y.

In a previous paper † it has been shown that such transformations are consistent with the nuclear structure of these isotopes (following Landé's scheme), the absence of actino-uranium in uranium minerals being attributed to its relatively short life. This expectation follows from the theory, as its nucleus would contain an odd number of neutrons, thus :

Ac U....	92	235	$46\alpha+51n$.

Developing this theory, it is now shown that actino-uranium may itself be a transient radioactive isotope, the actinium series arising in a heavier isotope of uranium of mass 239.

* Aston, ' Nature,' March 2nd, 1929, p. 313.
† Walke, *loc. cit.*

It is suggested that this isotope, which might be termed protactino-uranium, disintegrates thus :—

	Atomic number.	Mass number.	Constitution, following Landé.
Pr Ac U ..	92	239	$46\alpha+55n$
			$\downarrow\alpha$
I	90	235	$45\alpha+55n$
			$\downarrow\beta$
II.....	91	235	$45\alpha+p+54n$
			$\downarrow\beta$
Ac U	92	235	$\begin{cases}45\alpha+p+p+53n\\45\alpha+\alpha+51n\end{cases}$
			$\downarrow\alpha$
U Y.....	90	231	$45\alpha+51n$
			$\downarrow\beta$
Pa	91	231	$45\alpha+p+50n$
			$\downarrow\alpha$
Ac	89	227	$44\alpha+p+50n$
			$\downarrow$
			Actinium series.

It is further suggested that the isotope II of atomic number 91 and mass 235, which arises from the β-ray disintegration of the product I 90 235, is uranium Z, so that the latter is to be regarded on this hypothesis as in the direct line of descent of the actinium series and not as a branch product of uranium X_1. According to this idea uranium Z has a mass 235 instead of 234, its assumed mass if it arises as a branch product of uranium X_1. The products uranium X_2 and uranium Z are thus regarded as disintegration products not of one body, uranium X_1 by a dual transformation, but of two isotopes of atomic number 91, viz., uranium X_1 of mass 234, and the new isotope of mass 235, which could by analogy be called uranium Z_1 (UZ_1). This assumption has the merit of correlating several of the radioactive transformations, and evidence in its favour will now be reviewed.

Let us first consider the branching which has been formerly assumed for uranium X_1. In all the other radioactive series branching occurs as a result of an initial β-ray disintegration, the resulting atoms emitting either β- or α-particles. The resulting nuclei then disintegrate by α- and β-ray emission respectively, the final nuclei being the same for both processes. With the supposed uranium branching, however, we have similar nuclei apparently breaking up in two distinct ways, each disintegration giving rise to β-rays following the

emission of α-rays from the parent nucleus uranium I. These differences can be shown thus :—

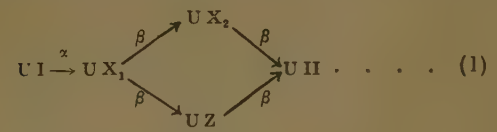

. . . . (1)

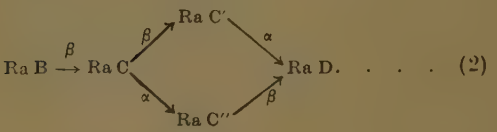

. . . . (2)

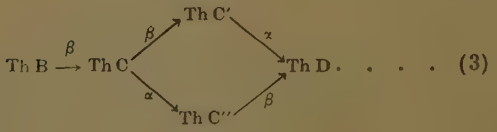

. . . . (3)

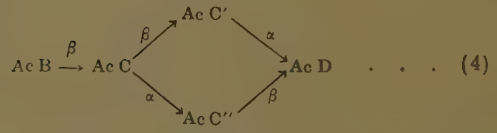

. . . . (4)

Thus the uranium branching would be quite different from the other examples, the isotopes uranium X_2 and uranium Z being physically distinct yet of the same mass. It is difficult to understand how this could occur, but if we accept the suggestion made in this paper the difficulty disappears. The branching of the isotopes RaC, ThC, and AcC has been considered in the paper already mentioned.

Further, if we assume that the disintegration electrons arise from internal conversion of γ-radiation in the negative potential field of the nucleus, as suggested by Beck *, then the energy emitted along both branches should be equal. This was shown to be true for the thorium branches by Ellis and Mott † and for radium and actinium by Beck *, using Sargent's results. Applying the theory to the supposed branching of uranium X_1

* Beck, 'Nature,' Dec. 23, 1933, p. 967.
† Ellis and Mott, Proc. Roy. Soc. A, cxli. p. 502 (1933).

Beck found a striking disagreement between the energy values on the two sides of the branch. This he concluded confirmed the view that uranium Z is not a branch product of uranium X_1, but is a derivative of a still unknown isotope of uranium. The suggestion made in this paper is in accordance with this fact.

The origin of actino-uranium from the heavy isotope by the process postulated would explain why it is not found in uranium ores, for according to the nuclear scheme adopted the nucleus of this isotope would be relatively unstable, and therefore comparatively short-lived, as shown by the odd neutron configuration. Further, the energy set free by the mass defect of the α-particle formed by the disintegration of uranium Z would tend to increase this instability. We should thus expect actino-uranium to be a short-lived product, though, if this suggestion is correct, it should be possible to detect its weak α-ray activity, because the existence of uranium Y and uranium Z seems to indicate that small quantities of this isotope exist. However, the presence of the α-particles of uranium II would probably prevent this group from being detected.

In addition, it is to be expected that protactino-uranium might occur in small quantities in uranium minerals, since to account for the existence of uranium Z this isotope should have a half-period value comparable with that of uranium I, though actino-uranium would be relatively unstable for the reasons given and would quickly decay to protactinium and actinium. It is certain, however, that such an isotope only exists in very small relative amounts, and therefore its detection would be difficult.

Further, it might be possible, though difficult, to detect the weak α-ray activity of protactino-uranium, as the α-ray group would be masked by the presence of the normal α-particles from uranium I. The record of such an α-particle disintegration would be possible in the form of a pleochroic halo in old micas, and in this connexion it is significant that Joly * has observed small "X" haloes in mica which resemble in structure the ordinary uranium haloes, but correspond to α-particle ranges which have not been found in the uranium series. In a

* Joly, Proc. Roy. Soc. A, cii. p. 682 (1923).

similar way Iimori and Yoshimura * have noted the presence of haloes, called "Z" haloes, whose radii are not in agreement with the known ranges of the α-rays from the uranium and thorium series. Their exact origin is not known, but it is possible that these haloes are due to the α-rays emitted by the uranium isotope of mass 239.

Since the atomic weight of uranium is 238·18, though the main isotope uranium I has a mass 238, it is suggested that one or more heavier isotopes exist in small quantities to account for the increased atomic weight.

In conclusion, there seems to be evidence that uranium Z and uranium Y are members of the actinium series and that the actinium series arises as a result of the disintegration of the heavy uranium isotope (protactino-uranium) of mass 239, and not, as has been previously supposed, as the result of some branching of the main uranium series.

This work was carried out under the direction of Professor F. H. Newman, D.Sc., to whom my sincere thanks are due for valuable criticism and help in preparing this paper.

XXII. *The Optical Properties of Thin Films.* *By* M. Blackman, *M.Sc., Ph.D., Otto Beit Research Scholar, Imperial College of Science and Technology* †.

1. THE properties of thin films of absorbing media have been the subject of investigations extending over a large number of years. The expressions for the optical constants were derived theoretically by Voigt ‡ and Drude § and by a large number of investigators following them ‖. In all these cases the formulæ derived have been discussed mainly in relation to the experimental work performed, *i. e.*, they were either adopted so that

* Iimori and Yoshimura, Inst. of Phys. and Chem. Res. Tokyo, v. p. 11 (1926).

† Communicated by the Author.

‡ H. Voigt, *Ann. d. Phys.* xxv. p. 95 (1885); xxxv. p. 76 (1888).

§ P. Drude, Wied. *Ann.* l. p. 595 (1893); li. p. 77 (1894).

‖ K. Försterling, *Gott. Nachrichten*, p. 451, 1911. A. Partsch and W. Hallwachs, *Ann. d. Phys.* xli. p. 247 (1913). L. Kellner geb. Sperling, *Zeit. f. Phys.* lvi. p. 223 (1929).

the optical constants (n the refractive index and κ the coefficient of absorption) could be calculated directly or the intensity of the reflected and transmitted light was calculated in a particular case and compared with the experimental values.

It was, of course, clear that the usual expression used for the reflecting power of an absorbing medium

$$R = \frac{(n-1)^2+\kappa^2}{(n+1)^2+\kappa^2}$$

held only in the case of a thick film, and that a thin film, in the limiting case, would neither absorb nor reflect any light. There does not seem to have been any general discussion of the expressions for transmission and reflexion, and in view of the large amount of experimental work,

Fig. 1.

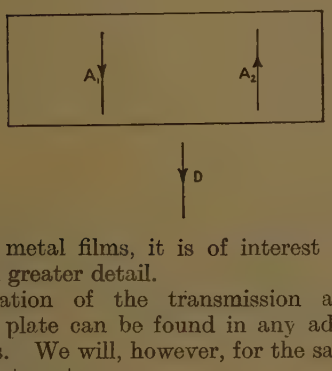

especially on metal films, it is of interest to study the expressions in greater detail.

The calculation of the transmission and reflexion of light by a plate can be found in any advanced text-book of optics. We will, however, for the sake of clarity, sketch the treatment.

We consider a plate of dielectric constant ϵ_1 placed in a medium of dielectric constant ϵ_2. Plane polarized light falls normally on the plate, and is reflected both internally and externally. We can represent the effect of all the reflected rays (taking all effects into account, *e. g.*, interference and phase-jumps) by a single reflected ray of suitable amplitude, and, similarly, for the transmitted light. In the plate we have rays going in both directions which we represent by rays in the two directions.

Now we can write down the electric and magnetic vector for each wave in each medium, as Maxwell's equations must be obeyed. Applying the usual boundary conditions at each surface we obtain a set of relations between the amplitudes of the various waves.

We take E, R, D to be the amplitudes of the incident, the reflected, and the transmitted waves respectively, λ_1 and λ_2 are the wave-lengths in the two media, and d is the thickness of the plate.

The expressions for reflexion and transmission are

$$\frac{R}{E} = \frac{i \sin \frac{2\pi d}{\lambda_2} (\epsilon_1 - \epsilon_2)}{i \sin \frac{2\pi d}{\lambda_2} (\epsilon_1 + \epsilon_2) + 2\sqrt{\epsilon_1 \epsilon_2} \cos \frac{2\pi d}{\lambda_2}},$$

$$\frac{D e^{-\frac{2\pi d i}{\lambda_1}}}{E} = \frac{2\sqrt{\epsilon_1 \epsilon_2}}{i \sin \frac{2\pi d}{\lambda_2} (\epsilon_1 + \epsilon_2) + 2\sqrt{\epsilon_1 \epsilon_2} \cos \frac{2\pi d}{\lambda_2}}.$$

These equations are quite general and hold in the case where ϵ_2 is complex. Following the method of L. Kellner * we put

$$\lambda_2 = \frac{\lambda_0}{\sqrt{\epsilon_2}} \quad \text{and} \quad \sqrt{\epsilon_2} = n + i\kappa$$

($\epsilon_2 = 1$ for a plate in air).

The substitution, which is somewhat laborious, can be seen in the paper quoted above *. It involves merely substitution and multiplication with the conjugate complex.

The final form taken by these expressions is

$$D_1 = \frac{D^2}{E^2} = e^{-\frac{4\pi\kappa d}{\lambda}} \frac{(1-R_0)^2 + 4R_0 \tan^2 \psi}{\left(1 - R_0 e^{-\frac{4\pi\kappa d}{\lambda}}\right)^2 + 4R_0 e^{-\frac{4\pi\kappa d}{\lambda}} \sin^2 (\alpha + \psi)}. \quad \ldots \quad (3)$$

$$R_1 = \frac{R^2}{E_2} = \frac{\left(1 + e^{-\frac{8\pi\kappa d}{\lambda}} - 2e^{-\frac{4\pi\kappa d}{\lambda}} \cos 2\alpha\right) R_0}{\left(1 - R_0 e^{-\frac{4\pi\kappa d}{\lambda}}\right)^2 + 4R_0 e^{-\frac{4\pi\kappa d}{\lambda}} \sin^2 (\alpha + \psi)}, \quad (4)$$

* L. Kellner geb. Sperling, *Zeits. f. Phys.* lvi. p. 223 (1929).

where $\alpha=\frac{2\pi nd}{\lambda}$ $\tan\psi=\frac{2\kappa}{n^2+\kappa^2-1}$,

$\lambda=\lambda_0$ $R_0=\frac{(n-1)^2+\kappa^2}{(n+1)^2+\kappa^2}$.

A particular case of the reflexion formula when $\kappa=0$ will be used later. In this case (4) reduces to

$$R_1=\frac{4\sin^2\frac{2\pi nd}{\lambda}\cdot\frac{(n-1)^2}{(n+1)^2}}{\left(1-\frac{(n-1)^2}{(n+1)^2}\right)^2+4\left(\frac{n-1}{n+1}\right)^2\sin^2\frac{2\pi nd}{\lambda}}$$

$$=\frac{4R_0\sin^2\alpha}{(1-R_0)^2+4R_0\sin^2\alpha}. \quad (5)$$

This is the well-known formula for the intensity of the reflexion from a thin-air film (for $n=1$).

The curves for the transmission, except in special cases, provide very little of interest, being mainly controlled by the factor $e^{-\frac{4\pi\kappa d}{\lambda}}$, so that when absorption is at all appreciable, the other factors hardly alter the value of the transmission to an appreciable extent *. An interesting special case is perhaps worthy of note. The transmission in the neighbourhood of an absorption maximum has been investigated theoretically and experimentally by Czerny † in connexion with his investigations in the infra-red absorption of NaCl; it is found that interference maxima should occur on the long wave-length side of the maximum. This effect is of importance in the experimental determination of absorption maxima where thin plates are used, as interference maxima can easily be mistaken for true absorption maxima unless precautions are taken ‡.

2. The reflexion formula provides rather interesting results. In the first place it goes over into the classical formula $R_0=\frac{(n-1)^2+\kappa^2}{(n+1)^2+\kappa^2}$ only when the reflexion from the second surface can be neglected: this is the case when the absorption is large enough to weaken the intensity of the primary beam in the crystal to such an extent that the internally reflected beam may be neglected.

* *Cf.* R. Schulze, *l. c.*

† M. Czerny, *Zeit. f. Phys.* lxxii. p. 447 (1932).

‡ Rawlins and Taylor, 'Infra-red Analysis of Molecular Structure.'

An exact estimate of when this occurs can only be given in connexion with a discussion of the reflexion formula for particular values of the absorption constant, but it can be seen from the curves given, that for values of κ of the order of unity, the formula is valid for values of $\frac{d}{\lambda}$ greater than 0·3

The formula is, however, not valid for small values of the absorption, for in that case the multiple reflexion and interference are important

It does not hold, therefore, for a parallel plate of transparent matter

In the case where the surfaces are not optically flat, and $d>>\lambda$, the reflexion, as is clear from (5), will vary rapidly between 0 and $\frac{4R_0}{(1+R_0)^2}$, *i. e.*, as $\sin^2\frac{2\pi nd}{\lambda}$ varies from 0 to 1. We may in this case put in a mean value of $\sin^2\frac{2\pi nd}{\lambda}$, *i. e.*, 1/2, in order to obtain the mean intensity of reflexion averaged over the interference effects. In this case formula (5) becomes

$$R_1=\frac{2\left(\frac{n-1}{n+1}\right)^2}{1+\left(\frac{n-1}{n+1}\right)^4}=\frac{2R_0}{1+R_0^2},$$

which is very different from the $R_0=\left(\frac{n-1}{n+1}\right)^2$ formula, which seems to be applied rather indiscriminately* to any case of reflexion.

It is readily seen that we obtain in this case roughly twice the reflexion. This is illustrated by the table.

n	1·3	1·5	2	5
R_0	1·7 %	4 %	11·1 %	61·4 %
R_1	3·4 %	8 %	22·2 %	90 %

The main features of the reflexion phenomena are the interference phenomena and the region of thickness in which they are to be expected.

* The calculation of the optical constants of a semi-transparent plate by R. W. Wood (Phys. Rev. xliii. p. 353, 1933) is therefore hardly likely to be sound.

It is clear that there are two limiting cases in the reflexion of a thin film, the first being where there is no absorption, and we would then expect marked interference fringes when the thickness is comparable with the wave-length ; the second case where the absorption is so large that the interference effects are smoothed out, and where we obtain no fluctuation of intensity as the thickness is increased.

We consider here always an optically flat plate of the material and take as variable $\frac{d}{\lambda}$ (d =thickness, λ =wave-length), as this is the natural variable for the expression of the reflexion (see formula (4)).

Taking the refractive index to be $n=1{\cdot}5$, and varying the absorption coefficient κ, the reflexion has been plotted as a function of $\frac{d}{\lambda}$. The reflexion itself is plotted in units of R_0, so that we can see when this value is reached and how the reflexion varies in relation to this quantity. It is seen that for $n=1{\cdot}5$ the value R_0 is reached for $\frac{d}{\lambda}=0{\cdot}3$ when $\kappa \geqq 1$. For small values of κ we obtain, of course, interference effects up to very large values of $\frac{d}{\lambda}$, while for $\kappa=0$ these are always present, the average value of the intensity being, however, different from R_0, as has been shown previously.

The interference effects are for $\kappa=1$ still quite marked, the maximum value of the reflexion being well above R_0. The distance between successive maxima is for a transparent film $d=\frac{\lambda}{2n}$, but the first maximum occurs for $d=\frac{1}{4n}\lambda$. The effect of absorption is to shift the first maximum to a smaller value of " d " as is shown in the figures (figs. 2 & 3).

As an example of the limiting case where the interference effects are smothered, the reflexion curve for $n=0{\cdot}15$, $\kappa=1$ (fig. 3) *, has been added.

3. An application of the above can be made to the problem of the influence of a surface layer on the optical

* In fig. 3 it should be noted that the ordinate has been reduced by half in curve 3 for the sake of convenience.

Fig. 2.

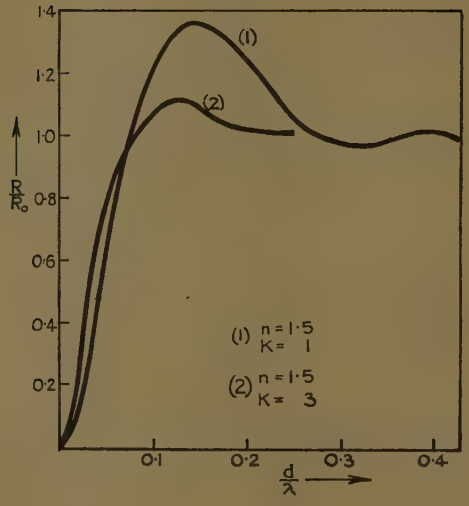
1·4
1·2
1·0
0·8
0·6
0·4
0·2
R/R₀
(1)
(2)
(1) n = 1·5 K = 1
(2) n = 1·5 K = 3
0·1
0·2
0·3
0·4
d/λ

Fig. 3.

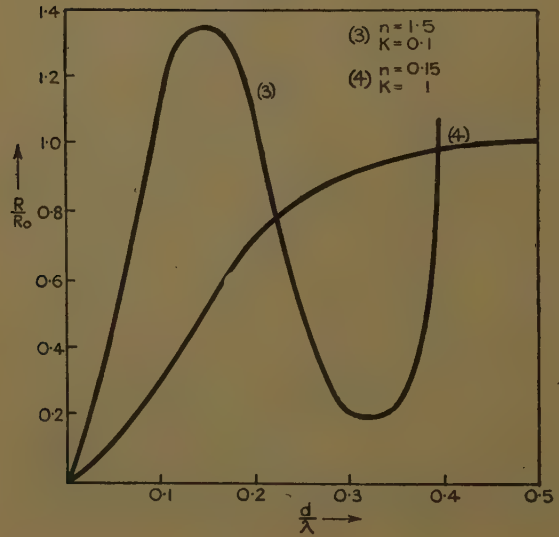
1·4
1·2
1·0
0·8
0·6
0·4
0·2
R/R₀
(3) n = 1·5 K = 0·1
(4) n = 0·15 K = 1
(3)
(4)
0·1
0·2
0·3
0·4
0·5
d/λ

properties of a substance. This is of particular interest in the case of polished metals. It has been shown that * a polished metal surface is an amorphous layer of atoms in a state similar to that of a liquid. It is of interest to see when such a layer would affect the reflecting or emitting power of a metal.

It is clear that a very heavy polish (which means a thick layer of amorphous substance) might have an effect where a thin layer could be neglected. Assuming that the layer is of thickness 10^{-6} cm. (*i. e.*, about 20 to 50 atoms and optically flat), it is seen from the given diagrams that the surface film can be neglected in the infra-red the reflexion and emission being determined solely by the properties of the metal itself. On the other hand, in the ultra-violet it is to be expected that the surface condition should be important and that different methods of preparation of the surface should yield different results. It has been found by investigators that the greatest discrepancies in the emission power do occur in the ultra-violet †. It has also been found that the reflecting power varies with the thickness of the polish ‡.

A surface layer can be considered to have no effect whatsoever when its thickness is about a hundredth of the wave-length. This holds for moderate values of $\kappa(\sim 1)$ and $n(\sim 1)$. An exception would be the case of a very large value of κ in the neighbourhood of an absorption maximum. It is clear from the diagrams that a thickness of 1/20 of a wave-length gives quite an appreciable reflexion for normal values of the optical constants.

4. A further application of the formulæ deduced above may be made in the special case of an absorption maximum of a crystal. We have already mentioned that the transmission has been calculated in the case of NaCl, and that the only interesting point here is that interference maxima become prominent on the long wave-length side of the maximum when the thickness is of the order of the wave-length

The calculation of the reflexion of a thin plate of sodium chloride has now been carried out here using the data found by Czerny An interesting property of the thin films has been found.

* R. C. French, Proc. Roy. Soc. cxl. p. 637 (1933).
† Geiger-Scheel, 'Handbuch der Physik,' xxi.
‡ E. Pfesdorf, *Ann. Phys.* lxxxi. p. 906 (1926).

It is well known * that the reflexion and transmission maxima of a crystal do not coincide, the reflexion lying in general on the short wave-length side of the "eigenfrequenzen." In particular this has been found for all the alkali halogen crystals. The theoretical derivation has been given by Försterling † and Havelock ‡.

It is, however, found that when the thickness of the plate is small compared to the wave-length, the reflexion maximum is shifted and coincides with the transmission maximum.

We can first show this theoretically by expanding formula (3) for small values of $\frac{d}{\lambda}$. It then becomes

$$R_1 = \frac{16\pi d^2}{\lambda^2}(n^2+\kappa^2) \cdot \frac{R_0}{(1-R_0)^2+4R_0 \sin^2 \psi}.$$

Now R_0 varies rather slowly in the neighbourhood of its maximum. The factors which vary rapidly are κ and n. The maximum of reflexion will therefore occur in the limiting case roughly where κ has its maximum value. We would, therefore, expect the reflexion maximum to shift from its normal position for a thick plate into a position roughly coinciding with the transmission maximum.

The curves calculated show interesting properties. First, the maximum is much sharper and the shift causes a sharp drop in the reflexion in the neighbourhood of the "Reststrahl frequenz." As the film becomes very thin (*cf.* fig. 4), the reflexion becomes very much smaller and the reflexion band much narrower. The maximum value of R is now 24 per cent. for a film of thickness $0{\cdot}2\ \mu$ compared with 90 per cent. for a thick plate.

It has been observed by Pfund and Silverman § that a powdered crystal transmits a small percentage of the incident radiation in the neighbourhood of a characteristic vibration, and shows a high "radiometric" effect, which is defined as the absorption relative to that of soot. Unfortunately there is no absolute calibration of the instrument, and the conclusion that the value of the absorption and transmission is inconsistent with any

* See, for example, the article by Born and Göppert-Mayer in the 'Handbuch der Physik,' xxiv.

† K. Försterling, *Ann. der Phys.* lxi. p. 577 (1920).

‡ T. H. Havelock, Proc. Roy. Soc. London (A), cv. p. 488 (1924).

§ Phys. Review, xxxix. p. 62 (1932).

reflexion is rather premature. It is possible that the reflexion is smaller for very fine particles on general grounds (see above), but an absolute determination is necessary before the matter can be settled definitely.

The remark by Wood * that a marble slab reflects 40 per cent. of incident radiation of wave-length 110 μ, whereas a finely ground powder reflects none, can probably

Fig. 4.

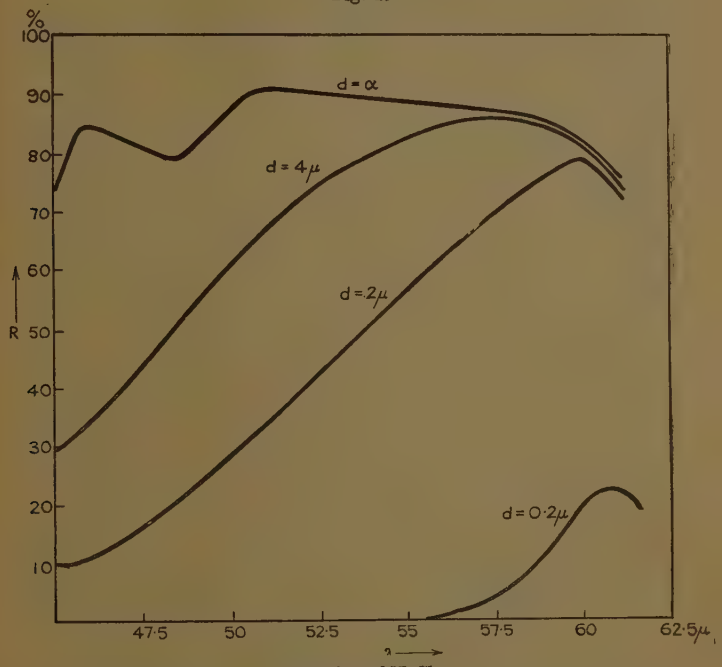

Reflexion of NaCl.

be explained by the presumably fine size of the particles, as the reflexion will then be only a fraction of its value for a thick slab, as has been shown for a thin plate.

5. If we consider several plates of NaCl which transmit a fair intensity to be placed one over the other with an air-space in between them, it is easy to show that such a system will transmit very little, but will reflect with the

* 'Physical Optics,' 1911 edition, p. 632.

reflecting power of the first plate, *i. e.*, in the case of an absorbing film with a very much smaller intensity than a thick film.

For considering the $0{\cdot}2\,\mu$ films of NaCl and a wave-length of $60\,\mu$, we see (fig. 5) that the first film reflects 24 per cent. and transmits 30 per cent. of the incident intensity; a second plate behind it could reflect back to the first only 7·5 per cent., and 2·2 per cent. would

Fig. 5.

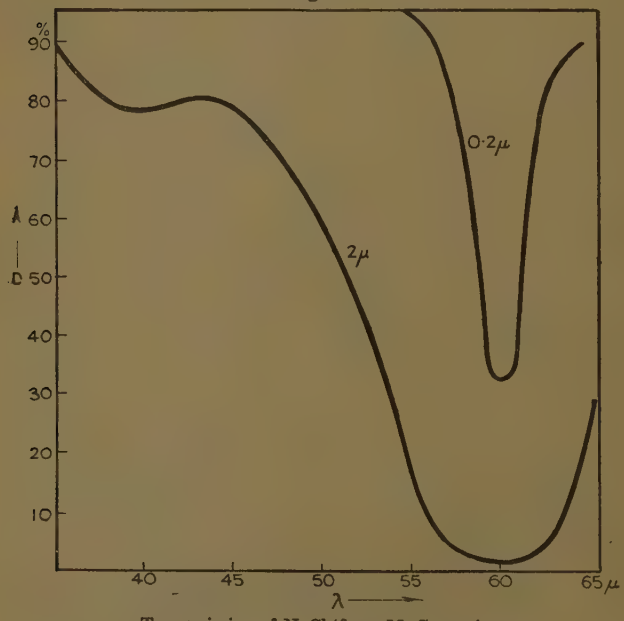

Transmission of NaCl (from M. Czerny).

get through to the surface; from a third plate only about 0·9 per cent. would get through to the top surface, and so on. For ten films the total reflected intensity would be at the most 30 per cent., while the transmitted intensity is zero.

Now a film $2\,\mu$ thick reflects 70 per cent. at the same wave-length which transmits very little. The net effect is that while the transmission for the two cases is about the same the reflexion is for a series of films very much smaller.

XXIII. *Membrane Equilibria and the Phase Rule.* *By* O. Gatty, *M.A., B.Sc.**

Introduction.

MEMBRANE phenomena are of importance in general colloid chemistry, applied chemistry, and biology. Nevertheless few workers have dealt with the equilibrium theory of systems more complicated than two component systems with a membrane permeable only to one component, in which case the phenomena are those of simple osmotic pressure. Donnan and Harris† and Donnan ‡ developed a simple thermodynamical theory of more complicated systems, and it was later realized that Willard Gibbs § had already worked out the general theory of heterogeneous systems in which at least one of the phases contains a substance unable to pass out of that phase, but able to combine with some other substance which was not subject to that restriction. More recently Hückel‖ and Donnan and Guggenheim ¶ have revised the theory to make it applicable to imperfect solutions of electrolytes and non-electrolytes. It has also been discussed in conjunction with the activity coefficient of electrolytic solutions by Liu **, but the great bulk of recent work on membrane theory has tended to investigate other factors.

Thus the effect of adsorption of solute and solvent by the membrane on the direction of osmosis of systems not in equilibrium, and a classification of such systems, has been given by Schreinemakers †† and Schreinemakers and Werre ‡‡. They also discussed the properties of mosaic

* Communicated by the Author.

† Donnan and Harris, J. C. S. xcix. p. 1554 (1911).

‡ Donnan, London Physiological Society, December 1910; *Zeit. Elektrochem.* xvii. p. 572 (1911).

§ Gibbs, 'Collected Works,' i. p. 83 (1928).

‖ Hückel, *Koll. Zeit.* (*Zsig. Festschrift*), xxxvi. p. 204 (1925).

¶ Donnan and Guggenheim.

** Liu, *Koll. Zeit.* lvii. pp. 139 & 285 (1931); lviii. p. 144 (1932).

†† Schreinemakers, *Proc. K. Akad. Wetensch. Amst.* xxxii. pp. 837–844, 1024–1031, 1305–1313 (1929); xxxiii. pp. 119–127 (1930); xxxiv. pp. 78–84, 344–347, 524–530. 823–830, 1282–1291 (1931). *Rec. Trav. Chim.* l. pp. 221–229, 883–899 (1931); li. pp. 218–232 (1932).

‡‡ Schreinemakers and Werre, *Rec. Trav. Chim.* li. pp. 51–60 (1932). *Proc. K. Akad. Wetensch. Amst.* xxxv. pp. 42–50, 162–170 (1932).

membranes whose permeability varies from point to point. The latter effect and its relationship to negative osmosis has been discussed by Söllner * and Grollman and Söllner †, while the properties of membranes that are capable of doing work have been discussed by Schreinemakers ‡ and by Straub §.

Many of the interesting properties of living membranes can be interpreted in terms of more or less complicated osmotic systems diffusing towards equilibrium, but an investigation of the more complicated types of equilibrium to be expected in many membrane systems is a necessary preliminary to a full investigation of the former type of effects. Owing to the bearing of the former set of phenomena on negative osmosis, they have received more attention than the equilibria towards which these non-equilibrium systems are diffusing. In the present paper the equilibrium theory is re-examined in terms of the number of degrees of freedom of systems containing any number of chemical components and containing any number of membranes. This is done with the concept of inert structureless membranes of a generalized type, and the possibility of the occurrence in inanimate systems and the living organism of a complicated series of equilibria is pointed out. It does not seem that the new equilibria will in general greatly alter the distribution of substances between different cells in a multicellular organism, but the positions of equilibria towards which, in the absence of any proof to the contrary, such a system may be presumed to tend, must undoubtedly conform to the conditions of Gibbs's Phase Rule as generalized to systems containing membranes.

The formulæ for equilibrium in the case of the simplest Donnan equilibrium are equivalent to those of Donnan and Guggenheim, though in this paper they are given in terms of quantities that can be obtained by observations extending over a smaller range of concentration than that necessary to establish the activity coefficients used by those authors. In the case of imperfect solutions of

* Söllner, *Zeit. Elektrochem.* xxxvi. pp. 36–47, 234–241 (1930). *Biochem. Zeit.* ccxliv. pp. 370–381 (1932).

† Grollman and Söllner, Trans. Am. Electrochem. Soc. lxi. pp. 81–88, 89–99 (1932). *Zeit. Elektrochem.* xxxviii. pp. 274–282 (1932).

‡ Schreinemakers, *Proc. K. Akad. Wetensch. Amst.* xxxiii. pp. 820–826, 1133–1139 (1930).

§ J. Straub, *Chem. Weekblad*, xxvii. pp. 672–674 (1930).

many components the labour involved in making activity determinations and extrapolating to great dilutions or saturated solutions is considerable, and should precise calculations be required it may turn out that less labour is involved if the equations are used in the form given in the present paper.

Equilibrium Conditions.

Phases which can exist together, the dividing surfaces being plane, in an equilibrium which does not depend upon passive resistance to change were called coexistent phases by Gibbs *, who gave general conditions for equilibrium between two or more such phases which may be summarized as follows. In systems where the only work done is compressional work, and where gravitational, capillary, and strain effects are negligible, the state of any homogeneous mass is completely determined by $C+2$ variables if it is considered as variable in composition, in quantity, in thermodynamic state, and as consisting of C independent chemical components.

At least one of these variables must be proportional to the total quantity of the mass present, so that in cases where quantity is of no significance the state of a homogeneous mass is determined by $C+1$ independent variables. Considering contiguous homogeneous masses, Gibbs showed that in general the conditions for equilibrium were that the pressure, the temperature, and the chemical potentials of each of the C independent chemical components of the system should be the same in all the phases. Thus, for P coexistent phases there are $(P-1)(C+2)$ equilibrium conditions, while P independent phases have $P(C+1)$ independent variations of state in addition to P independent variations of quantity which are not considered in equilibrium conditions, since the possibility of two phases being coexistent is independent of the total quantity of each phase present in the system. In consequence P coexistent phases have $P(C+1)-(P-1)(C+2)=C+2-P$ independent variations of state. This is the well-known phase rule.

Membranes.

Any surface that divides two homogeneous masses from one another will be considered as a membrane in this

* Gibbs, *loc. cit.*

paper. Since all capillary effects are negligible in the systems considered, the membranes being dealt with are to be regarded as plane surfaces, and their effect on equilibrium conditions is completely described by what passive resistances to change they can exert. It is evident that each inequality of temperature, pressure, or chemical potential that a membrane will tolerate corresponds to an additional degree of freedom of the system. If, therefore, the membranes in a system tolerate in all M independent inequalities of potential, the total number of possible independent variations of state of a system of P phases and C components is given by $C+2-P+M$. In systems with several phases it is possible for a given membrane to tolerate a given difference of potential which, however, can not be set up because equalization can occur through a series of other membranes. The total number of equalities of potential are $(P-1)(C+2)$, so that M can have any value from zero up to and inclusive of this quantity, but it can never exceed it. When $M=0$, the passive resistances to equilibrium are zero, and the system is one of P coexistent phases; when $M=(P-1)(C+2)$ the P phases may be regarded as independent. The procedure in investigating the membrane equilibria is to fix arbitrarily $C+1-P+M$ potentials and to obtain differential equations between any two of the remaining possible variations of state and composition of the different phases. Perhaps the greatest simplicity is obtained where $P=M$, because the procedure of fixing $C+1$ potentials is merely to determine all the potentials for one phase. The simple osmotic pressure phenomena correspond to $P=2$, $C=2$, and $M=2$, since the membranes tolerate an inequality of pressure and of the chemical potential of one component. The simplest Donnan equilibrium corresponds to $P=2$, $C=3$, and $M=2$, the inequalities tolerated being again the pressure and one chemical potential. The most general Donnan equilibria correspond to $P=2$, $C=C$, $M=2, 3 \ldots C-2$, or $C-1$, the restrictions being an equalization of pressure and $1, 2 \ldots$ or $C-2$ chemical potentials. The conception of the vapour-pressure of a liquid as a function of the hydrostatic pressure on the liquid implies a membrane permeable to the particles of the vapour but capable of withstanding a difference of pressure; in consequence the theory of this phenomenon would correspond to $P=2$, $C=1$, and $M=1$. (Consider,

for instance, an apparatus of the type of Callendar's vapour-pressure sieve.) Again the theory of the vapour-pressure of solutions consisting of C—C′ volatile components and C′ non-volatile components could be discussed under the case P=2, C=C, M=C′.

Donnan Equilibrium. Three Components.

In this section equations are obtained for the simplest type of Donnan equilibrium in such a way as to account for all degrees of freedom of the system. Gibbs's chemical potentials, when multiplied by the conventional molecular weights of the components, become converted to partial molal free energies, and the conditions for equilibrium will be worked out in terms of these quantities. The equations for imperfect solutions are left in terms of partial molal free energies rather than activity coefficients and molal fractions, so as to save the space necessary for the precise definition of standard states in systems consisting of three or more components. If a phase consisting of N_1, N_2, ... N_c gram molecules of components 1, 2, ... c, possessing partial molal free energies $\overline{F}_1$, $\overline{F}_2$, ... $\overline{F}_c$, is considered, all measurements of activity coefficients must ultimately rest upon measurements of

$$\left(\frac{\partial \overline{F}_r}{\partial N_s}\right)_{pTN_k},$$

where the suffix N_k indicates that all the N's other than N_s are kept constant for different values of r and s over the concentration range considered. Usually activity coefficients are only to be obtained by extrapolating down to great dilutions or by referring to saturated solutions. Thus, for complicated systems where data over the whole concentration range are lacking, equations for Donnan equilibria must either be given in terms of activity coefficients calculated from the theories of Debye and Hückel or else resort to the more readily ascertainable differential coefficients of the partial molal free energies. Guggenheim has given the equations in terms of the former quantities, and in this section they are left in the somewhat less elegant form of partial molal free energies. It may, perhaps, be pointed out that another difficulty about three or more component systems lies in the fact that the partial molal free energy of any component like the thermodynamic state of the

phase itself has four or more degrees of freedom. In two component systems activity standard states play the double function of a property that is, on the one hand, dependent only on the pressure and temperature, while, on the other hand, it is completely determined by a number of independent variables exactly one fewer than those needed to determine the partial molal free energy of the given component. In three or more component systems standard states can be chosen to fulfil either of these functions, but never both simultaneously.

Consider a system that consists of two phases α and β, separated by a membrane. Let phase α consist of $N_{1\alpha}$, $N_{2\alpha}$, $N_{3\alpha}$ gram molecules of chemical components 1, 2, and 3 at a pressure p_α and a temperature T_α. These five variables completely determine the composition, quantity, and thermodynamic state of phase α, while phase β is determined by the five similar quantities p_β, T_β, $N_{1\beta}$, $N_{2\beta}$, $N_{3\beta}$. The membrane separating the phases can tolerate a difference of pressure and is impermeable to component 3, so that it will also tolerate a difference of chemical potential of component 3. This is a case where $P=2$, $C=3$, and $M=2$, the total possible independent variations of state of the system being $C+2-P+M=5$, together with two independent variations of quantity. Denoting the partial molal free energies of component r in phases α and β by $\overline{F}_{r\alpha}$ and $\overline{F}_{r\beta}$ respectively, the conditions for equilibrium are

$$\left.\begin{aligned} \overline{F}_{1\alpha}&=\overline{F}_{1\beta},\\ \overline{F}_{2\alpha}&=\overline{F}_{2\beta},\\ T_\alpha&=T_\beta. \end{aligned}\right\} \quad . \quad . \quad . \quad . \quad . \quad . \quad (1)$$

Let the system be allowed to vary subject to the conditions that p_β, T_β, $N_{1\beta}$, $N_{2\beta}$, $N_{3\beta}$, $N_{1\alpha}$ are kept constant. Then

$$\left.\begin{aligned} &dT_\alpha=0, \quad dN_{1\alpha}=0,\\ &d\overline{F}_{1\alpha}=\overline{V}_{1\alpha}\,dp_\alpha+\frac{\partial\overline{F}_{1\alpha}}{\partial N_{2\alpha}}dN_{2\alpha}+\frac{\partial\overline{F}_{1\alpha}}{\partial N_{3\alpha}}dN_{3\alpha}=0,\\ &d\overline{F}_{2\alpha}=\overline{V}_{2\alpha}\,dp_\alpha+\frac{\partial\overline{F}_{2\alpha}}{\partial N_{2\alpha}}dN_{2\alpha}+\frac{\partial\overline{F}_{2\alpha}}{\partial N_{3\alpha}}dN_{3\alpha}=0. \end{aligned}\right\} \quad . \quad (2)$$

From these equations it is clear that there is one degree of freedom between the three variables p_α, $N_{2\alpha}$, $N_{3\alpha}$ under

these conditions. By eliminating dp_α, $dN_{2\alpha}$, and $dN_{3\alpha}$ respectively from the above equations three differential equations are obtained:

$$\left[\overline{V}_{2\alpha}\frac{\partial\overline{F}_{1\alpha}}{\partial N_{2\alpha}}-\overline{V}_{1\alpha}\frac{\partial\overline{F}_{2\alpha}}{\partial N_{2\alpha}}\right]dN_{2\alpha}$$

$$=-\left[\overline{V}_{2\alpha}\frac{\partial\overline{F}_{1\alpha}}{\partial N_{3\alpha}}-\overline{V}_{1\alpha}\frac{\partial\overline{F}_{2\alpha}}{\partial N_{3\alpha}}\right]dN_{3\alpha}, \quad . \quad . \quad (3)$$

$$\left[\overline{V}_{2\alpha}\frac{\partial\overline{F}_{1\alpha}}{\partial N_{2\alpha}}-\overline{V}_{1\alpha}\frac{\partial\overline{F}_{2\alpha}}{\partial N_{2\alpha}}\right]dp$$

$$=\left[\frac{\partial\overline{F}_{2\alpha}}{\partial N_{2\alpha}}\cdot\frac{\partial\overline{F}_{1\alpha}}{\partial N_{3\alpha}}-\frac{\partial\overline{F}_{1\alpha}}{\partial N_{2\alpha}}\cdot\frac{\partial\overline{F}_{2\alpha}}{\partial N_{3\alpha}}\right]dN_{3\alpha}, \quad (4)$$

$$\left[\overline{V}_{2\alpha}\frac{\partial\overline{F}_{1\alpha}}{\partial N_{3\alpha}}-\overline{V}_{1\alpha}\frac{\partial\overline{F}_{2\alpha}}{\partial N_{3\alpha}}\right]dp$$

$$=-\left[\frac{\partial\overline{F}_{2\alpha}}{\partial N_{2\alpha}}\cdot\frac{\partial\overline{F}_{1\alpha}}{\partial N_{3\alpha}}-\frac{\partial\overline{F}_{1\alpha}}{\partial N_{2\alpha}}\cdot\frac{\partial\overline{F}_{2\alpha}}{\partial N_{3\alpha}}\right]dN_{2\alpha}. \quad (5)$$

Similarly it may be shown that if p_β, T_β, $N_{1\beta}$, $N_{3\beta}$, T_α, $N_{1\alpha}$, $N_{3\alpha}$ are all kept constant that

$$\left[\overline{V}_{2\alpha}\frac{\partial\overline{F}_{1\alpha}}{\partial N_{2\alpha}}-\overline{V}_{1\alpha}\frac{\partial\overline{F}_{2\alpha}}{\partial N_{2\alpha}}\right]dN_{2\alpha}=\left[\overline{V}_{2\alpha}\frac{\partial\overline{F}_{1\beta}}{\partial N_{2\beta}}-\overline{V}_{1\alpha}\frac{\partial\overline{F}_{2\beta}}{\partial N_{2\beta}}\right]dN_\beta.$$

$$. \quad . \quad . \quad (6)$$

These are the equations for Donnan equilibrium. Equations (2) may be put in another way by considering the properties of phase α if it is allowed to come to equilibrium with phase β; some of it is pipetted out at $p_\alpha+dp_\alpha$ and allowed to come to p_α and is then examined. The observed charges in $\overline{F}_{1\alpha}$ and $\overline{F}_{2\alpha}$ are clearly given by

$$\left[\begin{matrix}(\delta\overline{F}_{1\alpha})_{p_\alpha}=-\overline{V}_{1\alpha}dp_\alpha,\\(\delta F_{2\alpha})_{p_\alpha}=-V_{2\alpha}dp_\alpha\end{matrix}\right]_{T_\alpha N_\alpha}, \quad . \quad . \quad . \quad (7)$$

which is equivalent to Donnan and Guggenheim's equations, and since $[\Sigma N_r d\overline{F}_r]_{pT}=0$ for all phases, these give

$$\left[(\delta F_{3\alpha})_{p_\alpha}=\frac{N_1\overline{V}_1+N_2\overline{V}_2}{N_3}dp_\alpha\right]_{T_\alpha N_\alpha} \quad . \quad . \quad . \quad (8)$$

For perfect solutions equations (3) to (6) are readily simplified, for in this case

$$\overline{F}_r = \overline{F}^0_r(p, T \text{ only}) + RT \ln \frac{N_r}{\Sigma N}; \quad . \quad . \quad . \quad (9)$$

$$\therefore \left(\frac{\partial F_r}{\partial \overline{N}_s}\right)_{p T N_k} = -\frac{RT}{\Sigma \overline{N}} \text{ if } s \neq r,$$
$$= RT\left[\frac{1}{N_s} - \frac{1}{\Sigma \overline{N}}\right] \text{ if } s = r. \quad . \quad (10)$$

Equations (3) to (6) then become

$$[N_{1\alpha}\overline{V}_{1\alpha} + N_{2\alpha}\overline{V}_{2\alpha} + N_{3\alpha}\overline{V}_{1\alpha}]\, dN_{2\alpha} = -N_{2\alpha}[\overline{V}_{2\alpha} - \overline{V}_{1\alpha}]\, dN_{3\alpha}, \quad . \quad . \quad . \quad (11)$$

$$[N_{1\alpha}\overline{V}_{1\alpha} + N_{2\alpha}\overline{V}_{2\alpha} + N_{3\alpha}\overline{V}_{1\alpha}]\, dp_\alpha = RT\, dN_{3\alpha}, \quad . \quad . \quad . \quad (12)$$

$$N_{2\alpha}[\overline{V}_{2\alpha} - \overline{V}_{1\alpha}]\, dp_\alpha = -RT\, dN_{2\alpha}, \quad . \quad . \quad . \quad (13)$$

$$\frac{dN_{2\alpha}}{N_{2\alpha}\Sigma N_\alpha}[N_{1\alpha}\overline{V}_{1\alpha} + N_{2\alpha}\overline{V}_{2\alpha} + N_{3\alpha}\overline{V}_{1\alpha}]$$
$$= \frac{dN_{2\beta}}{N_{2\beta}\Sigma N_\beta}[N_{1\beta}V_{1\alpha} + N_{2\beta}V_{2\alpha} + N_{3\beta}V_{1\alpha}]; \quad (14)$$

while equation (7) becomes

$$\left.\begin{aligned} RT d \ln x_{1\alpha} &= -\overline{V}_{1\alpha}\, dp_\alpha, \\ RT d \ln x_{2\alpha} &= -\overline{V}_{2\alpha}\, dp_\alpha, \end{aligned}\right\}, \quad . \quad . \quad . \quad . \quad (15)$$

where $$x_{2\alpha} \equiv \frac{N_{2\alpha}}{\Sigma N_\alpha}.$$

Using compressibilities to give them a mean value for the partial molal volume, equations (15) were given in an integrated form by Donnan and Guggenheim.

If

$$N_{1\alpha} >> N_{2\alpha} \quad \text{and} \quad N_{1\alpha} >> N_{3\alpha},$$

equations (11) to (13) become respectively

$$\frac{dN_{2\alpha}}{dN_{3\alpha}} = -\frac{N_{2\alpha}}{V_\alpha}(\overline{V}_{2\alpha} - \overline{V}_{1\alpha}), \quad . \quad . \quad . \quad (11a)$$

$$\frac{dN_{3\alpha}}{dp_\alpha} = \frac{V_\alpha}{RT}, \quad . \quad . \quad . \quad . \quad . \quad . \quad . \quad . \quad . \quad (12a)$$

$$\frac{dN_{2\alpha}}{dp_\alpha} = -\frac{N_{2\alpha}}{RT}(\overline{V}_{2\alpha} - \overline{V}_{1\alpha}), \quad . \quad . \quad . \quad (13a)$$

where V_α is the total value of phase α, equation (12*a*) being the same as the ordinary expression for osmotic pressure. These equations also hold if

$$N_{1\alpha} \approx N_{2\alpha} >> N_{3\alpha}.$$

If components 2 and 3 be supposed to dissociate completely into other substances that form perfect solutions, equations (2) to (8) are still valid. But equations (9) and (10) have to be altered, and, therefore, equations (11) to (15). Thus, if components 2 and 3 be supposed to be two completely dissociated binary $z-z$ valent electrolytes with a common ion, and the effects of interionic attraction are neglected,

$$\overline{F}_1 = \overline{F}^0_{1\alpha} + RT \ln \frac{N_1}{N_1 + 2N_2 + 2N_3}, \quad . \quad . \quad (16)$$

$$\overline{F}_2 = \overline{F}_2 + RT \ln \frac{N_2(N_2+N_3)}{(N_1+2N_2+2N_3)^2}, \quad . \quad . \quad (17)$$

so that

$$\left.\begin{aligned} \frac{\partial \overline{F}_1}{\partial N_2} &= -\frac{2RT}{N_1+2N_2+2N_3} = \frac{\partial \overline{F}_1}{\partial N_3}, \\ \frac{\partial \overline{F}_2}{\partial N_2} &= \frac{RT}{N_2} + \frac{RT}{N_2+N_3} - \frac{4RT}{N_1+2N_2+2N_3}, \\ \frac{\partial \overline{F}_2}{\partial N_3} &= \frac{RT}{N_2+N_3} - \frac{4RT}{N_1+2N_2+2N_3}. \end{aligned}\right\} \quad . \quad (18)$$

These values, when substituted in expressions (2) to (8), would give the equations for Donnan equilibrium for solutions of this type. For more complicated dissociations the expressions for

$$\left(\frac{\partial F_r}{\partial N_s}\right)_{N_k pT}$$

become more complicated, but after calculation may be substituted in the general equations (2) to (8) which are valid also in the case of imperfect solutions. Using the values for $\frac{\partial \overline{F}_r}{\partial N_k}$ given by expression (18), equations (3) to (5) become, if $N_{1\alpha} >> N_{2\alpha}$ and $N_{1\alpha} >> N_{3\alpha}$,

$$V_\alpha dp_\alpha = -RT\, dN_{2\alpha}\left[2 + \frac{2N_3}{N_2}\right] = +RT\, dN_{3\alpha}\frac{\left[2+\frac{2N_3}{N_2}\right]}{\left[2+\frac{N_3}{N_2}\right]}.$$

If the further condition $N_{2\alpha} >> N_{3\alpha}$ be imposed, they become

$$V_\alpha dp_\alpha = -2RT\,dN_{2\alpha} = +RT\,dN_{3\alpha}.$$

Donnan Equilibrium. Four Components.

In this case let the membrane be impermeable to component four only, and let phase α contain $N_{1\alpha}$, $N_{2\alpha}$, $N_{3\alpha}$, $N_{4\alpha}$ gram molecules of components 1–4 and phase β $N_{1\beta}$–$N_{4\beta}$ give molecules of components 1–4.

If p_β, T_β, $N_{1\beta}$, $N_{2\beta}$, $N_{3\beta}$, $N_{4\beta}$ and $N_{1\alpha}$ and T_α are kept constant, the conditions for equilibrium become

$$\left.\begin{aligned} 0 = d\overline{F}_{1\alpha} &= \overline{V}_{1\alpha}\,dp_\alpha + \frac{\partial \overline{F}_{1\alpha}}{\partial N_{2\alpha}} dN_{2\alpha} + \frac{\partial \overline{F}_{1\alpha}}{\partial N_{3\alpha}} dN_{3\alpha} + \frac{\partial \overline{F}_{1\alpha}}{\partial N_{4\alpha}} dN_{4\alpha}, \\ 0 = d\overline{F}_{2\alpha} &= \overline{V}_{2\alpha}\,dp_\alpha + \frac{\partial \overline{F}_{2\alpha}}{\partial N_{2\alpha}} dN_{2\alpha} + \frac{\partial \overline{F}_{2\alpha}}{\partial N_{3\alpha}} dN_{3\alpha} + \frac{\partial \overline{F}_{2\alpha}}{\partial N_{4\alpha}} dN_{4\alpha}, \\ 0 = d\overline{F}_{3\alpha} &= \overline{V}_{3\alpha}\,dp_\alpha + \frac{\partial \overline{F}_{3\alpha}}{\partial N_{2\alpha}} dN_{2\alpha} + \frac{\partial \overline{F}_{3\alpha}}{\partial N_{3\alpha}} dN_{3\alpha} + \frac{\partial \overline{F}_{3\alpha}}{\partial N_{4\alpha}} dN_{4\alpha}, \end{aligned}\right\} \quad . \quad . \quad . \quad (19)$$

which reduces, as before, to

$$(d\overline{F}_{r\alpha})\,p_\alpha \text{ const.} = -\overline{V}_r\,dp_\alpha \quad \text{for } r = 1, 2, \text{ or } 3, \quad (20)$$

$$(d\overline{F}_{4\alpha})\,p_\alpha \text{ const.} = -\frac{N_1\overline{V}_1 + N_2\overline{V}_2 + N_3\overline{V}_3}{N_4}\,dp_\alpha. \quad . \quad (21)$$

Equations (20) have already been given by Donnan and Guggenheim. It is possible to obtain six equations of the type

$$dN_3 \begin{vmatrix} \frac{\partial \overline{F}_{1\alpha}}{\partial N_{3\alpha}} & \overline{V}_{1\alpha} & \frac{\partial \overline{F}_{1\alpha}}{\partial N_{2\alpha}} \\ \frac{\partial \overline{F}_{2\alpha}}{\partial N_{3\alpha}} & \overline{V}_{2\alpha} & \frac{\partial \overline{F}_{2\alpha}}{\partial N_{2\alpha}} \\ \frac{\partial \overline{F}_{3\alpha}}{\partial N_{3\alpha}} & \overline{V}_{3\alpha} & \frac{\partial \overline{F}_{3\alpha}}{\partial N_{2\alpha}} \end{vmatrix} + dN_4 \begin{vmatrix} \frac{\partial \overline{F}_{1\alpha}}{\partial N_{4\alpha}} & \overline{V}_{1\alpha} & \frac{\partial \overline{F}_{1\alpha}}{\partial N_{2\alpha}} \\ \frac{\partial \overline{F}_{2\alpha}}{\partial N_{4\alpha}} & \overline{V}_{2\alpha} & \frac{\partial \overline{F}_{2\alpha}}{\partial N_{2\alpha}} \\ \frac{\partial \overline{F}_{3\alpha}}{\partial N_{4\alpha}} & \overline{V}_{3\alpha} & \frac{\partial \overline{F}_{3\alpha}}{\partial N_{2\alpha}} \end{vmatrix} = 0,$$

. . . (22)

from equation (19).

Donnan Equilibrium excepting for Pressure Equalization.

In this case the system becomes parallel to the system sodium chloride in water-alcohol mixtures in contact with its own vapour, which is supposed to be sodium-chloride free.

Three-phase Donnan Equilibrium.

Here the conditions are more complicated, because two membranes have to tolerate inequalities of a given potential if equalization of that potential throughout the system is to be obstructed and if all the three phases are contiguous. If all the three membranes tolerate inequalities of a given potential they then add two degrees of freedom to the system.

As an illustration, consider the system of three phases α, β, γ, where there are five components.

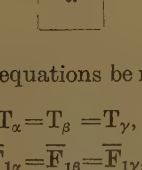

Let the equilibrium equations be nine, and as follows :—

$$\left.\begin{aligned} T_\alpha &= T_\beta = T_\gamma, \\ \overline{F}_{1\alpha} &= \overline{F}_{1\beta} = \overline{F}_{1\gamma}, \\ \overline{F}_{2\alpha} &= \overline{F}_{2\beta} = \overline{F}_{2\gamma}, \\ \overline{F}_{3\alpha} &= \overline{F}_{3\gamma}, \\ \overline{F}_{4\alpha} &= \overline{F}_{4\beta}, \\ \overline{F}_{5\beta} &= \overline{F}_{5\gamma}. \end{aligned}\right\} \quad . \quad . \quad . \quad . \quad . \quad (23)$$

Take p, T, N_1, N_2, N_3, N_4, and N_5 as the seven variables of a phase so that the system has 21 variables. Let the eleven quantities T_α, p_α, $\overline{F}_{1\alpha}$, $\overline{F}_{2\alpha}$, $\overline{F}_{4\alpha}$, $N_{1\alpha}$, $N_{1\beta}$, $N_{4\beta}$, $N_{1\gamma}$, $N_{4\gamma}$, $N_{5\gamma}$ be fixed at constant values. The conditions for equilibrium are then

$$d\bar{F}_{1\alpha}=0=\frac{1\alpha}{2\bar{\alpha}}dN_{2\alpha}+\frac{1\alpha}{3\bar{\alpha}}dN_{3\alpha}+\frac{1\alpha}{4\bar{\alpha}}dN_{4\alpha}+\frac{1\alpha}{5\bar{\alpha}}dN_{5\alpha}+odp_{\beta}+odN_{2\beta}+odN_{3\beta}+odN_{5\beta}+odp_{\gamma}+odN_{2\gamma}+odN_{3\gamma},$$

$$d\bar{F}_{2\alpha}=0=\frac{2\alpha}{2\bar{\alpha}}dN_{2\alpha}+\frac{2\alpha}{3\bar{\alpha}}dN_{3\alpha}+\frac{2\alpha}{4\bar{\alpha}}dN_{4\alpha}+\frac{2\alpha}{5\bar{\alpha}}dN_{5\alpha}+odp_{\beta}+odN_{2\beta}+odN_{3\beta}+odN_{5\beta}+odp_{\gamma}+odN_{2\gamma}+odN_{3\gamma},$$

$$dF_{3\alpha}-dF_{3\gamma}=0=\frac{3\alpha}{2\bar{\alpha}}dN_{2\alpha}+\frac{3\alpha}{3\bar{\alpha}}dN_{3\alpha}+\frac{3\alpha}{4\bar{\alpha}}dN_{4\alpha}+\frac{3\alpha}{5\bar{\alpha}}dN_{5\alpha}+odp_{\beta}+odN_{2\beta}+odN_{3\beta}+odN_{5\beta}-V_{3\gamma}dp_{\gamma}-\frac{3\gamma}{2\gamma}dN_{2\gamma}-\frac{3\gamma}{3\gamma}dN_{3\gamma},$$

$$d\bar{F}_{4\alpha}=0=\frac{4\alpha}{2\bar{\alpha}}dN_{2\alpha}+\frac{4\alpha}{3\bar{\alpha}}dN_{3\alpha}+\frac{4\alpha}{4\bar{\alpha}}dN_{4\alpha}+\frac{4\alpha}{5\bar{\alpha}}dN_{5\alpha}+odp_{\beta}+odN_{2\beta}+odN_{3\beta}+odN_{5\beta}+odp_{\gamma}+odN_{2\gamma}+odN_{3\gamma},$$

$$dF_{1\beta}=0=odN_{2\alpha}+odN_{3\alpha}+odN_{4\alpha}+odN_{5\alpha}+\bar{V}_{1\beta}dp_{\beta}+\frac{1\beta}{2\bar{\beta}}dN_{2\beta}+\frac{1\beta}{3\bar{\beta}}dN_{3\beta}+\frac{1\beta}{5\bar{\beta}}dN_{5\beta}+odp_{\gamma}+odN_{2\gamma}+odN_{3\gamma},$$

$$d\bar{F}_{2\beta}=0=odN_{2\alpha}+odN_{3\alpha}+odN_{4\alpha}+odN_{5\alpha}+\bar{V}_{2\beta}dp_{\beta}+\frac{2\beta}{2\bar{\beta}}dN_{2\beta}+\frac{2\beta}{3\bar{\beta}}dN_{3\beta}+\frac{2\beta}{5\bar{\beta}}dN_{5\beta}+odp_{\gamma}+odN_{2\gamma}+odN_{3\gamma},$$

$$d\bar{F}_{4\beta}=0=odN_{2\alpha}+odN_{3\alpha}+odN_{4\alpha}+odN_{5\alpha}+V_{4\beta}dp_{\beta}+\frac{4\beta}{2\bar{\beta}}dN_{2\beta}+\frac{4\beta}{3\bar{\beta}}dN_{3\beta}+\frac{4\beta}{5\bar{\beta}}dN_{5\beta}+odp_{\gamma}+odN_{2\gamma}+odN_{3\gamma},$$

$$dF_{5\beta}-d\bar{F}_{5\gamma}=0=odN_{2\alpha}+odN_{3\alpha}+odN_{4\alpha}+odN_{5\alpha}+V_{5\beta}dp_{\beta}+\frac{5\beta}{2\bar{\beta}}dN_{2\beta}+\frac{5\beta}{3\bar{\beta}}dN_{3\beta}+\frac{5\beta}{5\bar{\beta}}dN_{5\beta}-\bar{V}_{5\gamma}dp_{\gamma}-\frac{5\gamma}{2\gamma}dN_{2\gamma}-\frac{5\gamma}{3\gamma}dN_{3\gamma},$$

$$d\bar{F}_{1\gamma}=0=odN_{2\alpha}+odN_{3\alpha}+odN_{4\alpha}+odN_{5\alpha}+odp_{\beta}+odN_{2\beta}+odN_{3\beta}+odN_{5\beta}+\bar{V}_{1\gamma}dp_{\gamma}+\frac{1\gamma}{2\gamma}dN_{2\gamma}\frac{1\gamma}{3\gamma}dN_{3\gamma},$$

$$d\bar{F}_{2\gamma}=0=odN_{2\alpha}+odN_{3\alpha}+odN_{4\alpha}+odN_{5\alpha}+odp_{\beta}+odN_{2\beta}+odN_{3\beta}+odN_{5\beta}+\bar{V}_{2\gamma}dp_{\gamma}+\frac{2\gamma}{2\gamma}dN_{2\gamma}+\frac{2\gamma}{3\gamma}dN_{3\gamma},$$

where

$$\frac{j\alpha}{r\alpha} \equiv \left(\frac{\partial F_{j\alpha}}{\partial N_{r\alpha}}\right)_{N_{kpr}} \qquad (\alpha, \beta, \gamma).$$

From the above equations

$$\frac{dN_{3\alpha}}{dN_{3\beta}} = -\frac{D_1}{D_2},$$

where D_1 is the numerical value of the determinant

$$\begin{vmatrix}
0 & \frac{1\alpha}{2\alpha} & \frac{1\alpha}{3\alpha} & \frac{1\alpha}{4\alpha} & \frac{1\alpha}{5\alpha} & 0 & 0 & 0 & 0 & 0 & 0 \\
0 & \frac{2\alpha}{2\alpha} & \frac{2\alpha}{3\alpha} & \frac{2\alpha}{4\alpha} & \frac{2\alpha}{5\alpha} & 0 & 0 & 0 & 0 & 0 & 0 \\
0 & \frac{3\alpha}{2\alpha} & \frac{3\alpha}{3\alpha} & \frac{3\alpha}{4\alpha} & \frac{3\alpha}{5\alpha} & 0 & 0 & 0 & -\overline{V}_{3\gamma} & -\frac{3\gamma}{2\gamma} & -\frac{3\gamma}{3\gamma} \\
0 & \frac{4\alpha}{2\alpha} & \frac{4\alpha}{3\alpha} & \frac{4\alpha}{4\alpha} & \frac{4\alpha}{5\alpha} & 0 & 0 & 0 & 0 & 0 & 0 \\
\frac{1\beta}{3\beta} & 0 & 0 & 0 & 0 & \overline{V}_{1\beta} & \frac{1\beta}{2\beta} & \frac{1\beta}{5\beta} & 0 & 0 & 0 \\
\frac{2\beta}{3\beta} & 0 & 0 & 0 & 0 & \overline{V}_{2\beta} & \frac{2\beta}{2\beta} & \frac{2\beta}{2\beta} & 0 & 0 & 0 \\
\frac{4\beta}{3\beta} & 0 & 0 & 0 & 0 & \overline{V}_{4\beta} & \frac{4\beta}{2\beta} & \frac{4\beta}{5\beta} & 0 & 0 & 0 \\
\frac{5\beta}{3\beta} & 0 & 0 & 0 & 0 & \overline{V}_{5\beta} & \frac{5\beta}{2\beta} & \frac{5\beta}{5\beta} & -\overline{V}_{5\gamma} & -\frac{5\gamma}{2\gamma} & -\frac{5\gamma}{3\gamma} \\
0 & 0 & 0 & 0 & 0 & 0 & 0 & 0 & \overline{V}_{1\gamma} & \frac{1\gamma}{2\gamma} & \frac{1\gamma}{3\gamma} \\
0 & 0 & 0 & 0 & 0 & 0 & 0 & 0 & \overline{V}_{1\gamma} & \frac{2\gamma}{2\gamma} & \frac{2\gamma}{3\gamma}
\end{vmatrix}$$

and D_2 is the numerical value of the determinant

$$\begin{vmatrix}
\frac{1\alpha}{3\alpha} & \frac{1\alpha}{2\alpha} & \frac{1\alpha}{4\alpha}^{*} & \frac{1\alpha}{5\alpha} & 0 & 0 & 0 & 0 & 0 & 0 & 0 \\
\frac{2\alpha}{3\alpha} & \frac{2\alpha}{2\alpha} & \frac{2\alpha}{4\alpha} & \frac{2\alpha}{5\alpha} & 0 & 0 & 0 & 0 & 0 & 0 & 0 \\
\frac{3\alpha}{3\alpha} & \frac{3\alpha}{2\alpha} & \frac{3\alpha}{4\alpha} & \frac{3\alpha}{5\alpha} & 0 & 0 & 0 & 0 & -\overline{V}_{3\gamma} & -\frac{3\gamma}{2\gamma} & -\frac{3\gamma}{3\gamma} \\
\frac{4\alpha}{3\alpha} & \frac{4\alpha}{2\alpha} & \frac{4\alpha}{4\alpha} & \frac{4\alpha}{5\alpha} & 0 & 0 & 0 & 0 & 0 & 0 & 0 \\
0 & 0 & 0 & 0 & \overline{V}_{1\beta} & \frac{1\beta}{2\beta} & \frac{1\beta}{3\beta} & \frac{1\beta}{5\beta} & 0 & 0 & 0 \\
0 & 0 & 0 & 0 & \overline{V}_{2\beta} & \frac{2\beta}{2\beta} & \frac{2\beta}{3\beta} & \frac{2\beta}{5\beta} & 0 & 0 & 0 \\
0 & 0 & 0 & 0 & \overline{V}_{4\beta} & \frac{4\beta}{2\beta} & \frac{4\beta}{3\beta} & \frac{4\beta}{5\beta} & 0 & 0 & 0 \\
0 & 0 & 0 & 0 & \overline{V}_{5\beta} & \frac{5\beta}{2\beta} & \frac{5\beta}{2\beta} & \frac{5\beta}{5\beta} & -V_{5\gamma} & -\frac{5\gamma}{2\gamma} & -\frac{5\gamma}{3\gamma} \\
0 & 0 & 0 & 0 & 0 & 0 & 0 & 0 & \overline{V}_{1\gamma} & \frac{1\gamma}{2\gamma} & \frac{1\gamma}{3\gamma} \\
0 & 0 & 0^{*} & 0 & 0 & 0 & 0 & 0 & \overline{V}_{2\gamma} & \frac{2\gamma}{2\gamma} & \frac{2\gamma}{2\gamma}
\end{vmatrix}$$

If, now, the condition $d\overline{F}_{5\beta}=d\overline{F}_{5\gamma}$ is no longer supposed to hold, so that the system becomes the superposition of two two-phase five-component Donnan equilibria, the degrees of freedom of the system are increased by unity. If the system then be subjected to the additional restraint

$$dN_{4\alpha}=0, \qquad \frac{dN_{3\alpha}}{dN_{3\beta}}=-\frac{D_1'}{D_2'},$$

where D_1' and D_2' are respectively the numerical values of the determinants formed from determinants D_1 and D_2 by striking out the column corresponding to $dN_{4\alpha}$ and the row corresponding to the equation $d\overline{F}_{5\beta}-d\overline{F}_{5\gamma}=0$, which have been marked by asterisks in the figures for D_1 and D_2.

It seems probable that in general $\frac{D_1}{D_2} \cdot \frac{D'_2}{D'_1}$ would differ appreciably from the value unity, in which case the "three-phase" Donnan equilibrium set up by the condition $d\overline{F}_{5\beta}=d\overline{F}_{5\gamma}$ would have an appreciable effect on the position of equilibrium.

Since every cell is surrounded by a membrane, the solution inside it may be regarded as a separate phase, and this view is really too simple owing to the colloidal nature of cell-contents. The possibility of vital processes, which are further complicated by capillary and disequilibrium effects, tending towards polyphase equilibria of the type outlined above, depends on whether the permeability of all the cell-walls is identical or whether it varies. Cells with different functions, and, therefore, presumably with different permeabilities, often occur adjacent to one another in living organisms. In addition, a number of cases have been quoted from time to time which suggest that marked changes in permeability of cell-wall occur during the life of a single cell, and that these changes are associated with specific changes in normal activity. Examples of this type are found in the text-books of Bayliss* and Lillie†, although it is doubtful how far some of the evidence is free from criticism. Nevertheless, McClerdon‡, Mitchell and Wilson§, and Blackman and Paine‖ have all shown that changes in the permeability of a living cell can be induced by stimulation and fatigue. It is therefore reasonable to conclude that polyphase Donnan equilibria will represent end-points towards which certain vital processes may be expected to tend, in the absence of evidence to the effect that the second law of thermodynamics does not apply to living systems. How far the polyphase equilibria are likely to differ from the mere superposition of two-phase Donnan effects is hard to predict, but the effects may turn out to be appreciable. It seems improbable, however, that an effect of this nature could account for the ratio in which two similar elements like sodium and potassium are taken up by living tissues. This is so both because of the diffi-

* Bayliss, 'Principles of General Physiology,' 4th ed. (Longmans, 1927).
† Lillie, 'Protoplasmic Action and Nervous Action' (Chicago).
‡ McClerdon, American Journ. Phys. xxix. p, 302 (1912).
§ Mitchell and Wilson, Journ. Gen. Phys. iv. p. 45 (1921).
‖ Blackman and Paine, Ann. Bot. xxxii. p. 69 (1918).

culty of devising any polyphase system that would account for it on these grounds alone and because the phenomenon has also been observed in the case of unicellular organisms like Valonia.

Summary.

The Phase Rule has been extended to systems in which membranes operate. The equations for Donnan equilibrium in certain simple cases have been deduced. They are similar to those given by Donnan and Guggenheim where these authors have calculated a corresponding equation, but are given in terms of quantities which may turn out to be obtained with less experimental labour. A simple three-phase Donnan equilibrium is discussed and the possibility of polyphase membrane equilibria playing a rôle in vital processes is pointed out.

XXIV. *Alternating and Pulsating Currents in a Loaded Telephone Cable.* *By* Mario Marro, *Dr.Ing.**

THE tests described in the following note were made to prove that a pulsating current behaves, during its propagation through a loaded cable, in a manner very differently from an alternating current. In other words, the attenuation of a loaded cable when operated by a pulsating current is substantially the same for all frequencies comprised between voice-frequencies range; whereas the same cable, operated by alternating current, has an attenuation which depends on the frequency of this alternating current.

In order to demonstrate this assertion, I sent into a loaded cable alternating current generated by a "Standard" transmission set, which has an output of 1 milliwatt at all frequencies. I employed a pair of a loaded telephone cable between Turin and Vercelli, 80 km. long.

The constants of the cable were:

$r = 27$ ohms
$L = 0{\cdot}0006$ henry
$g = 1 \times 10^{-6}$ mho
$C = 0{\cdot}036 \times 10^{-6}$ farad

per km. at 800 cycles per second.

* Communicated by the Author.

When the cable was operated by alternating current, of which the frequency varied from 100 to 2200 cycles per second, I obtained the following attenuation values :—

Frequency.	Attenuation (nepers).
200	0·925
500	0·965
1000	1·035
1500	1·120
2000	1·350
2200	1·430

The same cable when operated by a pulsating current gave the following attenuation values :—

Frequency.	Attenuation (nepers).
200	1·795
500	1·780
1500	1·765
1700	1·770
2000	1·795
2200	1·890

The pulsating current which I used was obtained from the alternating current generated by the "Standard" transmission set, current rendered pulsating by means of a copper oxide rectifier (Westinghouse). The alternating current entered the cable through a transformer 1/1.

The diagrams show that the attenuation of the pulsating current remained about the same for all frequencies between 100 and 2000 cycles per second, and then the curve began to move upward (fig. 1).

The attenuation diagrams have the same O point, as it was only necessary to represent the attenuation low for an alternating current and for a pulsating current.

In fact, if I rectify an alternating current, by suppressing one-half a wave, I have a direct component and an alternating component of the same frequency as that of the rectified alternating current. I suppose the cable divided into some T sections, and I calculate the voltage decay at these knots. It is sufficient to examine what arrives in one section. I suppose applied an alternating e.m.f. represented by vector OV. This e.m.f. gives rise to a current, which will have a phase-angle α. This current will give rise to a voltage decay $AB=rI$. This vector

Fig. 1.

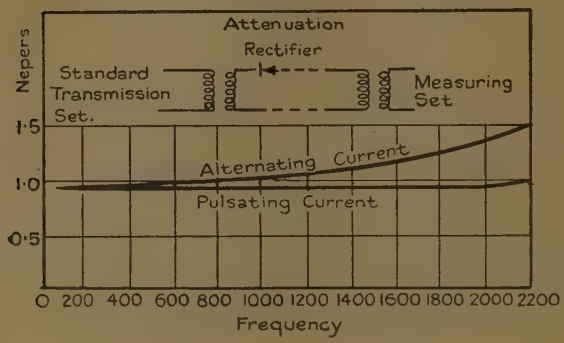
Attenuation
Rectifier
Standard Transmission Set.
Measuring Set
Nepers
1·5
1·0
0·5
Alternating Current
Pulsating Current
0 200 400 600 800 1000 1200 1400 1600 1800 2000 2200
Frequency

Fig. 2.

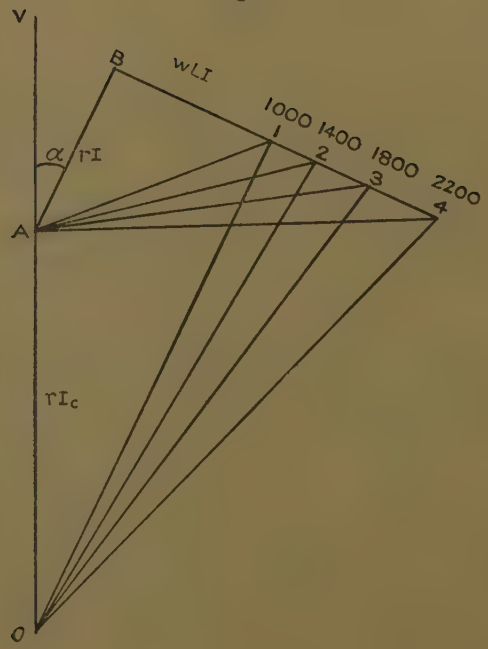
V
B
wLI
1000 1400 1800 2200
1
2
3
4
α
rI
A
rIc
O

will have the same phase-angle α with respect to the applied e.m.f., and it will be also a voltage decay $B1=wLI$, at 90 degrees with respect to the latter one. The resulting voltage decay will be represented by vector A1. Now I suppose that the frequency of the applied e.m.f. will change 100~to 1400, 1800, 2000. The voltage decay rI will remain the same—it does not depend on the frequency of the applied e.m.f. The voltage decay wLI will change with the frequency. The resulting voltage decay will be now A1, A2, A3, A4. The vectors are proportional to the values of the attenuation diagram for a loaded cable, with a cut-off frequency of 2800 cycles, when operated by a sinusoidal alternating current (fig. 2).

If I rectify the alternating current I have a direct component. The current produced by this component will have the same direction of vector OV of the applied e.m.f. It will give rise to a voltage decay $OA=rI_c$. Vector O1 is chosen so that O1 is the double of vector A1. In fact, by rectifying the alternating current I sent into the cable only one-half a wave, that is, only one-half of the energy generated by "Standard" set.

We can see how the difference between vectors O4 and O1 is much less than the difference between vectors A4 and A1.

From the experimental results we see that for a loaded telephone cable, with mH=177 loading coils, at 1 mile one from the other, the attenuation for a pulsating current is about the same for all frequencies between 100 and 2000 cycles per second, that is, between the voice-frequencies range.

XXV. *The Structure of Thin Celluloid Films.*—III. *By* E. Taylor Jones, *D.Sc., Professor of Natural Philosophy in the University of Glasgow* *.

[Plate IV.]

In two recent papers † on this subject some diffraction patterns, obtained by transmission of cathode rays through thin films of celluloid, were described, which

* Communicated by the Author.

† Phil. Mag. xvi. pp. 793, 953 (1933). These papers will here be referred to as I. and II.

were shown to be composed of simpler patterns of two fundamental types, viz. :—

1. A principal pattern in which the "first ring," *i. e.*, the ring on which the six spots nearest the centre lie, is elliptical in form, four of the six spots being nearer the centre than the other two.

2. A secondary pattern in which also the first ring is elliptical, but is larger than that of the principal pattern, completely enclosing it in fact, with its major axis at right angles to that of the first ring of the principal pattern.

The ratio of the diametral distances of the nearest spots which lie on the principal axes of the ellipse is 2 : 3 for the principal and 4 : 3 for the secondary pattern, and it was further shown that the two patterns can be regarded as being due to scattering of rays transmitted through the same lattice in two directions inclined at 60° to each other—that is, due to two portions of the film in which the lattice is turned through a relative angle of 60° about a line parallel to the plane of the film. From the fact that many of the spots of the secondary pattern appear to be formed by twice-diffracted pencils it was concluded that the two portions of the film concerned form superposed layers through which the rays pass in succession. The measurements of the patterns, when compared with other available data, indicated that the axis about which the rotation takes place is parallel to the length of the molecular chains of the film.

The spots of the secondary pattern can be easily distinguished from those of the principal one, not only by their positions, but also by the fact that in the more central parts of the pattern they are generally of much less intensity. The secondary pattern seems to appear only as an accompaniment of the principal pattern; at least, no photograph has yet been obtained by the writer which shows the secondary pattern alone. Whether the principal pattern can be formed without the secondary is more doubtful. Certainly many photographs have been obtained which show one or more principal patterns and no trace of the secondary, but in these photographs all spots outside the first ring are rather faint (owing perhaps to unsuitable curvature of the film), and in these

circumstances the absence of a visible secondary pattern can scarcely be regarded as conclusive. As far as the writer has observed, the secondary pattern is always visible if the principal pattern is well developed both on and outside the first ring.

As to the place of origin of the secondary pattern, we have inferred from the photographs that this is in a layer of the film which is superposed upon the main portion and has its molecular arrangement rotated relatively to that of the main portion. Further support of this view is found in the circumstance that, if the molecular arrangement of the main layer is that suggested in I. p. 807, the angle of rotation which would allow the molecular chains

Fig. 1.

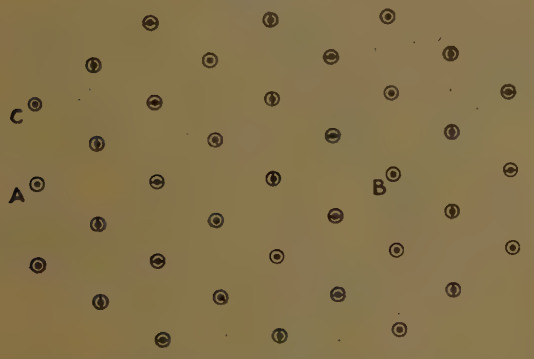

Projection of principal lattice.
The points ⊙, ⊕, and ⊕ are in different layers.

in the lower surface of the rotated layer to conform most closely to those of the upper surface of the main layer below it is 60°, and this is just the amount of rotation required to give the secondary pattern.

In fig. 1 is shown the projection on the (horizontal) plane of the film of the lattice which was suggested to account for the principal pattern (I. pp. 797, 807). The molecular chains, supposed parallel to the plane of the film, have their lengths parallel to AC, those marked ⊙ being all in the same layer, those indicated by ⊕ being in the layer above it, and those by ⊕ in the second layer above the first. In the fourth layer the chains are

vertically above those of the first layer, and so on. The length AC from ring to ring along a chain is 4·95 Å.U., the distance from chain to chain in the same layer, *i. e.*, the width of the space occupied by one ring, is one-half the distance AB, and is 11·04 Å.U., and the perpendicular distance between the layers is 4·256 Å.U. This arrangement of the chain molecules, each ring being supposed to act as a scattering centre, gives correctly within about 1 per cent. the positions of all the spots of the principal pattern.

Fig. 2.

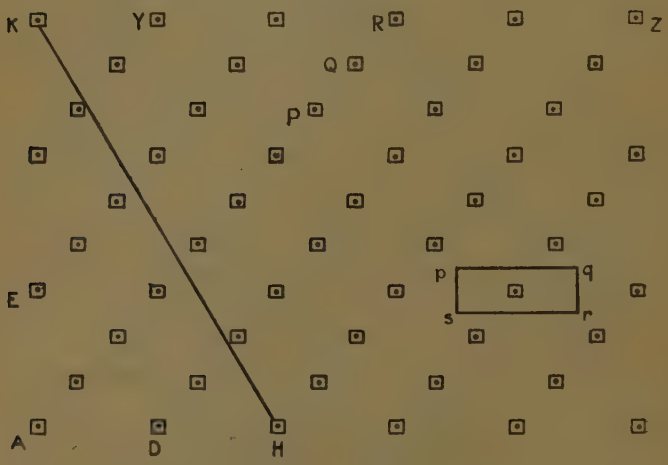

Normal section of principal lattice.

Fig. 2 shows a section of the lattice by a normal plane at right angles to the length of the chains (*e. g.* by a normal plane through AB in fig. 1), the positions of the chains being indicated by the points ⊡.

It will be seen from fig. 2 that each chain, such as Q, has as its nearest neighbours those next to it in the same inclined row PR, and the lateral adhesive forces between the layers may be supposed to be greatest in this direction. Similar adhesive forces, acting between the chains in the lower surface of the film and the water, are doubtless

partly responsible for the ease with which the film is spread over the water surface upon which it is deposited.

Now if another film, having its lattice rotated about a line parallel to the length of the chains, is to be attached to the upper surface KZ of the film of fig. 2, it will naturally set itself so as to be attached to this film at as many points as possible. The interfacial energy of the two films will be a minimum in these circumstances. It may also be expected that the chains of the superposed layer will attach themselves to those of the layer KZ much in the same way as R is attached to Q or Q to P.

The problem is therefore to find what inclined layer of fig. 2 has its chains at distances apart corresponding most closely with those of the layer KZ.

Let HK be the inclined layer required (fig. 2), and let AH be N_1a and AK be N_2h, where a is the shortest *horizontal* distance between chains (*i. e.*, $\frac{1}{3}$ AD), h is the perpendicular distance between the layers (*i. e* , $\frac{1}{3}$ AE), and N_1, N_2 are integers. The condition that the chains H and K should after rotation coincide with, or rather occupy the positions of, chains in the layer KZ is

$$\sqrt{N_1^2a^2+N_2^2h^2}=N_3a,$$

where N_3 is another integer.

Thus

$$\frac{N_3^2-N_1^2}{N_2^2}=\frac{h^2}{a^2}=\frac{4}{3}, \quad . \quad . \quad . \quad . \quad . \quad (1)$$

since

$$h=2a/\sqrt{3}.$$

The smallest value of N_3 divisible by 3 which satisfies equation (1) is the solution required. Passing over the first solution

$$N_1=N_3, \quad N_2=0,$$

which represents merely the superposition of an exactly similar layer upon the existing main layer, we find the next solution in order to be

$$N_1=2, \quad N_2=3, \quad N_3=4,$$

or common multiples of these numbers.

The smallest value of N_3 divisible by 3 is therefore 12, with $N_1=6$, $N_2=9$. This is the solution represented by HK in fig. 2. The distance HK is $12\,a$, so that if a layer

parallel to HK is placed in contact with KZ the chains H and K can take the places of two chains in KZ at $12a$ apart, such as Y and Z. The tangent of the angle AHK (fig. 2) is $3h/2a$, *i. e.*, $\sqrt{3}$, and the angle of relative rotation of the lattices in the two attached films is therefore 60°.

With a main layer of the type shown in fig. 2 a layer having its lattice inclined to this at 60° could be attached to the horizontal surface KZ in a more stable manner than any layer having its lattice inclined at a different

Fig. 3.

Normal section of principal layer, with superposed layer.

angle. This is therefore the configuration a superposed layer would take up which, while preserving the relative positions of its own molecular chains, must adapt itself as well as possible to the conformation of the layer below it *.

In fig. 3 is shown the main layer with the superposed layer attached to it, the figure again representing a normal

* The next solution of equation (1) is

$$N_1=1, \quad N_2=6, \quad N_3=7,$$

which indicates a rotation of $\tan^{-1} 4\sqrt{3}$, *i. e.*, 81° 47′. In this case the shortest distance between the points of attachment of the superposed layer is $21a$, and this layer would not give the secondary pattern.

section of the film at right angles to the length of the chains. It will be seen that the distance between the vertical rows of chains, which is a in the lower layer, is reduced to $a/2$ in the upper layer, this being the condition for the formation of the secondary pattern. The points of attachment of the two layers are Y and Z, the chains in these positions being regarded as belonging to both layers. The arrangement of the chains in the upper layer is in fig. 3 continued down to the interface KZ, but probably the chains L, M, N would be absent, as their lateral dimensions would not allow them to approach as closely as there shown to the chains K, R, S beneath them.

The two layers of fig. 3 together account for the whole of a principal and a secondary pattern, *i. e.*, the pattern shown in II. pl. xxix. fig. 6. Rays which are scattered only in the main layer give rise to the principal pattern. Those scattered only in the superposed layer account for a few of the spots of the secondary pattern (see I. p. 802, and II. p. 958). The large majority of the spots of the secondary pattern are produced by rays which are scattered by both layers, as explained in the two previous papers.

In one of the previous papers (I. p. 805) it was explained that it is impossible to determine completely the form and dimensions of the lattice from the principal and secondary patterns alone, and that a further observation or assumption is required for this purpose. The assumption there made was that the molecular chains are arranged in the main portion of the film as indicated in fig. 2, the layer AH being parallel to the plane of the film. With this arrangement a counter-clockwise rotation of the lattice through 60° about a line parallel to the chain length would, as explained, give the set of normal planes required to produce the secondary pattern.

Another conceivable arrangement of the chains is indicated in the normal section of a principal layer shown in fig. 4. A layer of chains which in fig. 2 is parallel to the plane of the film is in fig. 4 inclined to it at an angle ϕ. The distance Oα must still be equal to a (*i. e.*, 3·68 A.U.), and the length of the chains is unaltered. If h is the distance between consecutive layers measured along the normal to the film (*i. e.*, the distance Oβ in fig. 4), the conditions that a counter-clockwise rotation θ of the

lattice about a normal to the plane of fig. 4 would diminish to one-half the spacing of normal planes parallel to the chain length, and therefore give the secondary pattern, are represented by the equations

$$\cos(\theta+\phi)=\tfrac{1}{2}\cos\phi, \quad . \quad . \quad . \quad . \quad . \quad . \quad (2)$$

$$h\sin\theta=\mathrm{N}a/2, \quad . \quad . \quad . \quad . \quad . \quad . \quad (3)$$

where N is any positive integer. The value 2 is chosen for N because it leads to a more probable value of the density than other integers *. The cross-section of the

Fig. 4.

Normal section of inclined lattice.

space occupied by one chain is $3a\times h$, i. e., $3a^2/\sin\theta$.

If the arrangement is that of fig. 2, then $\phi=0$, $\theta=60°$, and the cross-section (*i. e.*, the area *pqrs* in fig. 2) is $2a^2\sqrt{3}$. The length of one ring along the chain being 4·95 Å.U., and the composition being taken as $C_6H_8O_3(NO_3)_2$, the density of the substance is 1·8 gm./c.c., as previously stated (I. p. 808).

* If the coordinates of any chain such as P in fig. 4 are na and $mh+ny$ (y being $a\tan\phi$), and if $la-2$ is the horizontal coordinate of this chain after rotation, it can be shown that $n-l=2m$. The three integers n, m, l may be positive or negative or zero. If they are all zero the chain is of course the one at the origin O about which the rotation is supposed to take place.

If we assume the value $\phi = 15°$, then θ is 46° 7′ and h is 1·387 a. The cross-section is therefore 4·161 a^2, and, the chain length being unaltered, the density for the same composition is 1·498 gm./c.c. This is the case illustrated in fig. 4. The density of the substance, if the molecular arrangement is of the type of fig. 4, is therefore less than that of the film which we have assumed to have the arrangement of fig. 2.

In the same way, by suitably choosing the angle ϕ (fig. 4) the value of h and the density could be made to have other values; for example, if ϕ is 6° 24′ and h is 1·238 a the rotation θ is 53° 84′ and the density (again for the same composition) would be 1·68 gm./c.c. This was the value found for the density of a specimen of nitro-cotton containing 12·2 per cent. of nitrogen. The percentage of nitrogen in this substance is between that of the dinitrate (11·11 per cent.) and that of the trinitrate (14·14 per cent.) of cellulose, and the composition must be different in the different ring groups of which the molecules of the substance are built up. It is highly probable that a variation of composition from ring to ring exists also in the celluloid films used in the present experiments, and since the spacings in these films are remarkably definite and constant it appears that the density of such a film is to be regarded as varying from point to point.

The density of these thin celluloid films has not been determined, but it is probably less than the value 1·8 gm./c.c. which we have arrived at on the basis of the arrangement of fig. 2 and the assumed composition $C_6H_8O_3(NO_3)_2$, *i. e.*, dinitrocellulose. Such difference, if it exists, might conceivably be explained by assuming the lattice to be inclined, as in fig. 4, but to the writer it seems more probable that a film formed by evaporation on water would take up the configuration of fig. 2, in which a much larger number of the molecular chains are in contact with, or as close as possible to, the water surface. On this view the density of the film at a part where the composition is that of dinitrocellulose is 1·8 gm./c.c., though the average density of an extended portion of the film may be considerably less than this value.

The diffraction pattern obtained with celluloid films is usually composed of two, three, or more of the simple

forms which we have called the principal and secondary patterns. Another example is shown in fig. 5 (Pl. IV.), in which there are in all eight principal patterns, some of which are accompanied by visible secondary patterns. The photograph of fig. 5 (Pl. IV.) was taken at a maximum potential of 40 kv. The spots on the first ring are seen more clearly if the photograph is taken at a lower potential. Fig. 6 (Pl. IV.) shows a photograph taken with the same film at 10 kv.* The drawing in fig. 7 shows the heads of all the spots of the first ring of the pattern of figs. 5 and 6 (Pl. IV.) numbered in groups according to the principal pattern to which they belong †. The spots are arranged on two concentric circles, sixteen on the

Fig. 7.

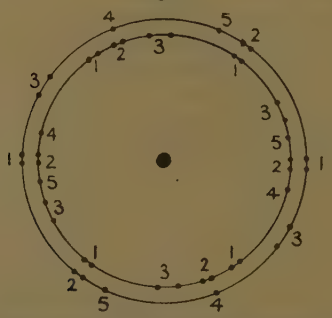

First ring of pattern of fig. 5, Pl. IV.
The spots are on two circles of diameters in the ratio 1·11.

larger and, with allowance for some overlapping, twice as many on the smaller. The ratio of the diameters of the two circles is 1·11, the spots on the outer circle being at the ends of the major axes, those on the inner circle at the ends of pairs of equal diameters of the elliptical first rings of the principal patterns to which they belong.

It is evident that the whole pattern of fig. 5 (Pl. IV.) is formed in a portion of the film in which there are eight adjacent areas having their crystalline axes set in different directions. The most prominent group of spots on the first ring are one of the pair marked 1 (fig. 7). This

* *I. e.* the 3 mm. sparking potential between 10 cm. diameter spheres.

† Closely neighbouring spots on the same ring in fig. 7 are included in the same number.

group has a well-marked secondary pattern, and its axes are in fact parallel to those of the "double" pattern shown in II. pl. xxix. fig. 6, which was obtained by transmission through a neighbouring portion of the same film.

The directions of the axes of the eight groups of figs. 5 and 6 (Pl. IV.) are not distributed uniformly about the centre, and consequently the first ring in the photograph does not appear to be very accurately circular *. With a uniform distribution of the axial directions the first ring of a pattern composed of numerous groups assumes a much more nearly circular appearance, and it was remarked on a previous occasion † that in such cases the spots of the first ring are found to lie upon two circles of slightly different diameter. It is now the writer's opinion that all the apparently circular rings obtained with celluloid films are composed of elliptical rings, as illustrated in fig. 7. If this is the case, the second ring, which was formerly described as having a diameter probably $\sqrt{3}$ times that of the first ring (D_1)‡ should be analyzed into two principal pattern rings of diameters $1{\cdot}65\ D_1$ and $1{\cdot}86\ D_1$, with a possible third ring between them, of diameter $1{\cdot}75\ D_1$, belonging to the secondary pattern. In many cases, especially if the films are not extremely thin, the photographs fail to reveal these differences, and it is rather rarely that a film is obtained which shows clearly the fundamental groups which we have called the principal and secondary patterns. Still less frequently does a film give one only of each of the fundamental groups or a single principal pattern alone. A more frequently occurring type is the "quadruple" pattern of I. pl. xxiii. figs. 1 and 2. Another example, which includes this type along with three other, much weaker, principal patterns, is reproduced in fig. 8 (Pl. IV.). In all, five films have been found to give this "quadruple" type of pattern in which the two principal patterns included in it have their axes inclined to each other at about 67°.

* In some cases the axes are arranged chiefly in two directions at right angles to each other, the first ring then appearing to be roughly square.

† Phil. Mag. xii. p. 653 (Sept. 1931).

‡ *Loc. cit.* p. 655. See also 'Induction Coil Theory and Applications,' p. 170 (Pitman, 1932).

It may be added that films prepared by evaporation of a solution of nitrocotton containing 12·2 per cent. of nitrogen also give a diffraction ring in which the spots lie on two circles of slightly different diameter, and that in all probability therefore the pattern given by films of this substance is also based upon a fundamental form having an elliptical first ring, as is the case in the celluloid patterns described in this and the two previous papers.

It is remarkable that a similar pattern, having the same proportions (though not the same absolute dimensions) has been obtained by Trillat and Hirsch * with a film of paraffin. The projection on the plane of the film of the lattice of this substance is very different from that which we have assumed for celluloid, being of the " rectangular " rather than the " triangular " type of fig. 1 of the present paper. The close similarity between the patterns of paraffin and celluloid suggests the possibility of accounting for the celluloid pattern by a rectangular arrangement of the molecular rings. This possibility is worthy of careful consideration, but in the opinion of the present writer the triangular arrangement offers the more satisfactory explanation of the celluloid pattern. In the first place it accounts perfectly for the complete absence of the first and other odd orders of the (100) and (010) reflexions †, and in the second place the comparative weakness of the secondary pattern in the inner portion, and its superior intensity in the outlying parts of the pattern, seem to agree best with the hypothesis of a superposed layer and twice-diffracted pencils (see I. p. 802). It may also be noted that Meyer and Mark ‡ have suggested for native cellulose a " triangular " arrangement of the rings as that which agrees best with the results of X-ray intensity measurements.

Glasgow,
April 1934.

* *Journ. de Phys. et le Rad.* iv. (1) p. 38, pl. i. fig. 3 (Jan. 1933).

† The nearest of these vacant positions to the centre would be on a circle of radius one-half that of the larger of the two circles of fig. 7.

‡ ' Der Aufbau der Hochpolymeren Organischen Naturstoffe,' fig. 39, p. 111 (Leipzig, 1930).

XXVI. *Harmonic Analysis of Sound-Frequency Oscillations with a Stroboscopic Disk.* *By* Tihamér d. Nemes *. (Communication of the Research Laboratories of Electrical Communication, Budapest, Hungary.)

[Plate V.]

Abstract.

The experimental arrangement described demonstrates the function of the stroboscopic disk in general cases. The stroboscopic disk is used for showing not only the presence of the fundamental of any oscillation, but also for giving the harmonics quantitatively and simultaneously.

Historical Reflexions.

THE application of a stroboscopic disk for the purpose of studying sound-frequency oscillations appears to have been first described by Toepler. Rogers (cited by Toepler, Pogg. *Ann.* cxxviii. p. 109 (1866)), has applied a rotating disk with black and white spaces and illuminated the disk with the flame of the "chemical harmonica," turning the disk at a speed that makes the spaces appear to stand still. Forchhammer applies a sensitive flame as a microphone with his Phonoscope (Humboldt, vii. p. 44 (1888)). Samojloff uses an A.C. incandescent lamp as a source of intermittent light (*Ann. d. Phys.* iii. p. 353 (1900)). Benischke makes known the use of the disk in the power-current technics (*Ann. d. Phys.* v. p. 487 (1901), and E. T. Z. xx. p. 142 (1899)). Seashore's Tonoscope ('Science,' xliii. p. 592 (1916)) is not a disk, but a cylinder, as is also Forchhammer's Phonoscope. The Strobyloin of Scripture (*Ztschr. f. Sinnesphys.* lix. p. 166 (1928)) differs from these only in that a disk is again used. On Doniselli's Phonogrammoscope (*Ztschr. f. Sinnesphys.* lx. p. 195 (1928–29) the spaces are coloured. L. B. Argimbau applies a neon lamp (The Gen. Rad. Experimenter, Nov. 1930, p. 5). Others who worked at the problem besides the above mentioned are E. Günther (*Phys. Ztschr.* xxii. p. 369 (1921)); Schröter and Vieweg (*Arch. El.* xii. p. 358 (1923); H. E.

* Communicated by the Author.

Linckh and R. Vieweg (*Ztschr. f. Instr.-kunde*, xlvi. p. 31 (1926)); W. Anderson and H. Lowery (Journ. Sci. Instr. July 1933, p. 203); and M. Metfessel, 'Science,' Nov. 3, 1933, p. 416). All these authors content themselves with the demonstration of the pitch of the fundamental oscillation. They describe the secondary phenomena as a disturbing effect only, and do not mention the possibility of quantitative analysis.

Properties of the Stroboscopic Disk.

If we rotate a disk on one ring of which there are equally wide black and white spaces, and illuminate it with intermittent light, the ring appears to stand still, provided the frequency of the light corresponds with the frequency of the spaces. The very expression "it appears to stand still" is not quite correct, as we generally see indistinct patches instead of sharply bordered spaces. It must be emphasized that in certain experimental circumstances the luminous intensity of these patches is in continual proportion to the amplitude of the corresponding pure sine-wave oscillation, so that the Fourier constant of each harmonic can be determined by means of photometric or photographic valuation (T. d. Nemes, *Archiv f. El.* xxvi. p. 403 (1932)).

If there is only one ring on the disk, by slowly changing the speed at which it is turned the measurements can be accomplished successively; but we can also measure the phenomena simultaneously if we apply several rings on a disk of constant speed. This latter method is suitable for the analysis of momentary noises or other transient phenomena.

The disk may also be divided into unequal black and white spaces, which circumstance influences the result in a way easily to be followed. The white spaces may be quite narrow, in which case a variable-density oscillogram of the oscillation appears on the disk.

Another property of the disk is that it also shows the phase-angle of each component.

Description of the Experiment.

The following new experiment may justify the theory without reiterating the mathematical discussion of it.

The source of illumination giving steady light illuminates a dull screen of tissue paper, as shown in fig. 1. This dull screen figures as the real source of light of homogenous surface. Naturally the lamp cannot be supplied with an alternating current. The projecting-lens system throws the sharp image of the slot placed behind the condenser upon a disk, the edge of which is cut out in the form of a pure sine wave. If the image of the slot falls upon the disk as shown in fig. 1, then the set, while the disk is rotating, will work as a generator of a pure sinusoidal luminous flux. The width of the slot has no influence upon the sine-wave form of the luminous flux, it only changes the amplitude.

Now let us analyse this light with the aid of the stroboscopic disk. We glue the stroboscopic disk to the gener-

Fig. 1.

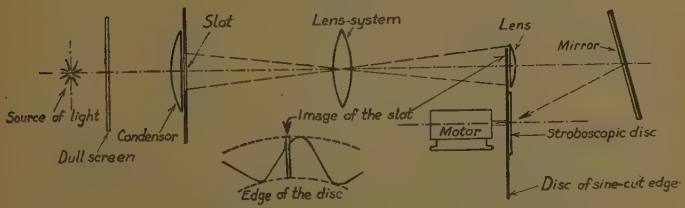

Experimental arrangement explaining properties of stroboscopic disk.

ator disk and project the light with a flat or spherical mirror upon the stroboscopic disk, so that the lens, placed close to the edge, should throw a sharp image of the dull screen upon the plane of the disk. As a result, the disk, or at least a large part of it, will be illuminated with a single large, circular, luminous spot, which, though not changing its form, alters in its totality its luminous intensity sinusoidally in a homogeneous way. After having painted as many white spaces upon the disk as there are sine lines on the edge (n), this ring will appear to stand still while rotating. If we paint several rings of $2n$, $3n$, $4n$, etc., spaces upon the disk (fig. 2, Pl. V.), these rings will appear to be equally grey, thus showing that there are no upper harmonics beside the fundamental (fig. 3, Pl. V.).

Now, for instance, if we cover the upper part of the slot with a small piece of paper, the luminous flux will lose its pure sine-wave form and the even harmonics will come forward as shown in fig. 4 (Pl. V.). This corresponds to the Fourier series of the asymmetrically distorted sine waves, for in this the even harmonics prevail. We get an oscillation in which there are merely even harmonics beside the fundamental, if we set the slot so that the opening should be narrow and then *half* cover the opening.

If, on the other hand, we cover the upper and lower ends of the slot symmetrically, only those rings will appear to stand still which correspond with the odd harmonics (fig. 5, Pl V.), since there are exclusively odd harmonics in the Fourier series of any curve symmetrical to the time-axis.

Thus we may easily demonstrate the analysis of other oscillations as well, if we use an edge formed in the corresponding curve instead of the pure sine edge. Naturally the slot must be narrow, and the piece of paper is superfluous.

Possibilities of Application.

The arrangement discussed here is primarily suitable for the illustrative demonstration of the Fourier analysis, because the analysis occurs momentarily, simultaneously and discernibly to our eyes. Besides the applicability in acoustics the set can be used for measuring television amplifiers. In this case the mirror in fig. 1 is omitted, the light, penetrating the disk, is projected upon the photocell, whilst we illuminate the stroboscopic disk with a neon lamp (or with another source of light which can be modulated with a linear characteristic). This lamp is supplied with the output current of the television amplifier, the transmitter, or of a television receiver. Thus, by means of photometry or photography, we get the linear and non-linear distortions with phase data at the examined exciting frequencies.

Accuracy.

The accuracy of the direct measuring can be increased by contrast effect up to 2 per cent. of the fundamental. The rings have to be made two-fold, so that the white spaces on one ring should correspond to the black spaces

on the neighbouring ring. The instantaneous photograph taken of the disk must be copied into a diapositive in observance of the Goldberg criterion, and then photometered through a sine mask if we want to have accurate values. If we are satisfied with ascertaining only the presence of the harmonics, we make manifold hard copies of the negative.

It must also be mentioned that the white sections of the stroboscopic disk may be substituted by electrical contacts (Barlow and Keene, Phil. Trans. Soc. London, A, ccii. p. 131 (1922), and B. G. Gates, Journ. Sci. Instr. ix. p. 380 (1932). In theory one cannot accomplish accurate measurements with them straight away, as the searching wave is a rectangular wave full of disturbing harmonics. The advantage of our disk is that by applying a sine mask the searching wave will have a pure sine shape (T. d. Nemes, *Archiv f. El.* xxvi. p. 403 (1932)).

XXVII. *The Specific Heats of Gases at High Temperatures.* *By* Prof. W. T. David, *Sc.D.*, *and* A. Smeeton Leah, *Ph.D.**

THE system of specific heats for the gases H_2, O_2, N_2, CO, CO_2, and H_2O calculated upon the basis of the Planck-Einstein quantum expression has received remarkable confirmation at temperatures up to 600° C. by the experiments of Henry †, Eucken and Mucke ‡, and Knoblauch, Raisch, and Haussen §. Tentative use of these specific heats in the interpretation of our explosion experiments has led to a growing confidence in their substantial accuracy also at very high temperatures (with the possible exception of those for H_2O at temperatures above 2000° C. or, perhaps, 2200° C.), and we bring forward in this paper evidence which would appear to us to justify their use—at any rate for industrial purposes.

The Planck-Einstein specific heats as calculated by Nernst and Wohl ‖ for H_2, N_2, CO, CO_2, and H_2O are

* Communicated by the Authors.
† Proc. Roy. Soc. A, cxxxiii. p. 492 (1931).
‡ *Zeit. f. Phys. Chem.* B, xviii. p. 167 (1932).
§ See *Zeit. Phys. Chem.* B, v. p. 257 (1929).
‖ *Zeit. f. Tech. Phys.* x. p. 613 (1929).

summarized in Table I. The values for O_2 given in the table are due to Johnstone and Walker *. It will be convenient to refer to these specific heats as the theoretical specific heats.

We have expressed the view on many occasions that the explosion method of determining specific heats at high temperatures is unreliable. In using this method it is usual to assume that combustion (defined in the sense of conversion of chemical energy into thermal or internal energy) is complete at the moment of development of maximum pressure. But it has been proved conclusively by explosion experiments in vessels of different sizes † and with mixtures at various initial densities ‡ in which both pressure and heat-loss measurements were made, that combustion in general is incomplete.

Much light has been thrown upon the nature of the incomplete combustion by luminosity experiments § and platinum thermometry experiments ||. It is somewhat complicated, but for the purpose of the present paper its exact nature need not concern us. It is sufficient for our purpose to indicate that platinum thermometry experiments in constant-pressure burning indicate that it may be decreased in any given conditions by increasing the pressure, and pressure recording in constant-volume explosions shows that for some reason or other it may be decreased by increasing the size of the vessel ¶.

* J. A. C. S. dci. p. 172 (1933).

† Phil. Mag. xiv. p. 764 (1932).

‡ Unpublished experiments. The ratio of the maximum explosion pressure to the initial pressure in an 18-inch vessel increases up to at least 3 atmospheres initial pressure in the case of carbon monoxide mixtures. In the case of hydrogen mixtures this ratio also increases in the same manner for initial pressures below atmospheric, but between the limits of initial pressure 1 and 3 atmospheres the increase in the ratio is inappreciable.

§ Phil Mag. ix. p. 390 (1930).

|| Phil. Mag. xii. p. 1043 (1931); xvii. p. 172 (1934).

¶ David, Brown, and El Din, Phil. Mag. xiv. p. 764 (1932). Maxwell and Wheeler (J. C. S. p. 882 (1933)) suggest that the conclusion reached by David, Brown, and El Din, that combustion is more complete in a large vessel than in a smaller one, cannot be maintained in the light of a comparison with their own experiments and those of Thorp (Phil. Mag. viii. p. 814 (1929)). But in correlating the explosion pressures measured by the various investigators with mixture composition (fig. 1, Maxwell and Wheeler's paper, p. 884) they did not take into account the fact that "airs" with different oxygen contents were used. Clearly, as most of their measurements relate to "over-rich" mixtures, this is most important, and, when it is taken into account, their work, as well as that of Thorp, fully confirms the conclusion of David, Brown, and El Din.

TABLE I.—Mean Specific Heats at Constant Volume over the Range 273° abs.—T° abs.

T° abs.	273	373	473	573	800	1200	1600	2000	2400	2800
H_2	4·82	4·91	4·93	4·94	4·97	5·06	5·21	5·36	5·52	5·66
N_2	4·97	4·97	4·99	5·03	5·16	5·43	5·67	5·85	6·0	6·1
CO	4·97	4·98	5·00	5·06	5·22	5·52	5·76	5·9	6·1	6·2
O_2	5·01	5·08	5·18	5·29	5·54	5·89	6·12	6·29	6·41	—
CO_2	6·63	7·18	7·67	8·08	8·84	9·77	10·37	10·8	11·1	11·4
H_2O	5·99	6·05	6·14	6·24	6·53	7·09	7·61	8	8·5	8·8

TABLE II.—$2H_2+O_2+n$ [Diluent] Explosions (Thorp).
1 atmos. initial pressure.

Inflammable mixture percentages.	Diluent gases percentages.	$\left[\frac{P_m}{P_i}\right]_{20°}$	$T_m - T_i$ ° C.	Q.	System of specific heats used.			
					Theoretical.		Partington and Shilling.	
					E.	U.E. %.	E.	U.E. %.
$20\ H_2+10\ O_2$.....	$70\ O_2$	6·45	1805	11460	10950	4·4	9870	13·9
$20\ H_2+10\ O_2$.....	$68·8\ N_2+1·2\ O_2$	6·77	1910	11460	11100	3·1	10590	7·6
$20\ H_2+10\ O_2$.....	$70\ H_2$	7·01	1990	11460	10960	4·3	11160	2·6

In the absence of exact information about the amount of incomplete combustion obtaining in explosion experiments, the direct determination of specific heats from such experiments is impossible. It does, however, seem possible to check the various specific heat systems which have been proposed by means of large numbers of explosions made with various types of mixtures. This we have attempted to do in what follows, with results, as has already been indicated, favourable to the theoretical system.

The other systems of specific heats considered in this paper are those due to Partington and Shilling *, Pier and Bjerrum †, and Goodenough and Felbeck ‡, which are all in common use in industry.

The symbols used are summarized below :—

P_i = the initial pressure.

P_m = the maximum explosion pressure.

T_i = the initial temperature in ° C.

T_m = the maximum mean temperature after explosion in ° C.

$\left[\frac{P_m}{P_i}\right]_{20°}$ = the ratio of the maximum pressure to the initial pressure corrected to the initial temperature of 20° C.

h_m = the heat loss up to maximum pressure expressed as a percentage of the heat of combustion.

Q = the heat of combustion in calories per gram-molecule.

E = the internal energy of the products of combustion in calories *per gram-molecule of original mixture.*

$\text{U.E.} = \left[\frac{(Q-E)}{Q}\, 100 - h_m\right]$, the "unaccounted energy" or incomplete combustion expressed as a percentage of the heat of combustion.

* 'The Specific Heat of Gases' (Benn).
† *Zeit. Electrochem.* xvii. p. 731 (1911); xviii. p. 101 (1912).
‡ Univ. of Illinois Bulletin, no. 139 (March 17th, 1924).

Before describing our own experiments it will be of interest to examine some hydrogen explosion experiments made by B. H. Thorp * in our laboratory some years ago. These are shown in Table II. They relate to explosions of mixtures containing the same amount of chemical energy, but with different diluents. The temperatures reached are such that there are no complications due to thermal dissociation.

In the last four columns are shown the internal energies per gram-molecule of original mixture and the estimated incomplete combustion or unaccounted energy at maximum pressure, first when the estimates are based upon the theoretical specific heat values, and secondly when these estimates are based upon the Partington and Shilling values, in which it is assumed, as in so many other systems, that the specific heats of the diatomic gases O_2 and N_2 are the same and those for H_2 nearly the same. There seems to be no reason why the amount of incomplete combustion should differ much in these mixtures, and the experiments, therefore, at once suggest the substantial relative accuracy of the mean theoretical specific heats for H_2, N_2, and O_2 over the temperature range 0° C. to 2000° C.

These experiments were made with the inflammable gases relatively dry. Wohl and Elbe † have made the interesting discovery that explosion pressures attain more closely to the ideal calculated pressures if substantial quantities of water-vapour are added to the inflammable hydrogen mixtures. They suggest that this is due to a considerable heat-loss (of the order of 3 per cent. of the heat of combustion) in the dry mixtures during explosion, but that in the wet mixtures the heat-loss is negligible. Our experiments do not confirm this view, for the heat-loss seems to be very small with both dry and wet mixtures. We think the water-vapour acts as a kind of catalyst, improving the overall process of combustion and so reducing the amount of incomplete combustion or unaccounted energy at maximum pressure (Compare the wet and dry hydrogen explosions in Table III.)

* Phil. Mag. viii. p. 814 (1929).
† *Zeit. Phys. Chem.* B. v. p. 241 (1929).

Table III.

Inflammable mixture percentages.	Diluent gases percentages.	Vessel used.	$\left[\frac{P_m}{P_i}\right]^{20°}$	h_m.	$T_m - T_i$ °C.	U.E. %, assuming the following specific heats :—			
						Theoretical.	Partington and Shilling.	Pier and Bjerrum.	Goodenough and Felbeck.
19·82 CO + 1H14·01 O_{22}	68·77 CO	18″	7·28	0·8	2085	2·6	10·6	8·4	7·2
		6″	6·94	0·85	1975	8·2	16·5	14·4	13·0
20·36 H_2 + 10·18 O_2	31·24 H_2 + 38·22 N_2 (dry)	18″	6·89	Very small—certainly less than 0·25 per cent.	1955	4·9	6·5	6·8	6·5
		6″	6·56		1845	11·0	12·9	13·6	13·2
19·08 H_2 + 9·54 O_2	34·92 H_2 + 35·89 N_2 + ·57 H_2O (wet)	18″	6·73		1885	2·3	4·4	4·8	4·7
		6″	6·39		1780	9·0	10·9	11·7	11·2

Experimental.

The explosion experiments recorded in this paper were all made in a spherical vessel 17·45 inches in internal diameter. The inflammable mixtures were ignited by means of a centrally placed spark-gap *. Both pressures and heat-losses were optically recorded simultaneously on the same photographic film. Full details of the experimental arrangements will be found in a previous paper †.

We have already indicated that by using a large explosion vessel more complete combustion at maximum pressure is secured. How much more complete the combustion is in a 17·45-inch vessel than in a 6-inch vessel will be clear from Table III. Great care was taken to secure mixtures of identical composition in each vessel. The initial pressures of the mixtures were in all cases 3 atmospheres.

The temperature of the gases before explosion varied between about 15° C. and 22° C., but since the maximum pressure ratios depend on the initial temperature, the ratios have all been corrected to the initial temperature of 20° C.

Analysis of the gases used were made in a Bone and Wheeler apparatus, and the composition of the various mixtures as given in the tables have been corrected for the small impurities found.

The heat of combustion at constant volume of CO to CO_2 has been taken to be 67,370 calories per gram-molecule ‡, and for H_2 to H_2O 57,290 calories per gram-molecule.

Specific Heats at 2000° *C.*

In Table IV. we give the results of explosion experiments with inflammable mixtures consisting of

(i.) $2CO+O_2$ diluted with O_2, N_2, CO, and CO_2 or suitable mixtures of these; in order to obtain sufficiently rapid explosions, small quantities of H_2 were added, as shown in column 1.

(ii.) $2H_2+O_2$ saturated with water-vapour at room-temperature and diluted with H_2, N_2, and CO_2;

* The heat absorption of the spark leads up to the moment of maximum pressure was experimentally determined and found to be entirely negligible when expressed as a fraction of the heat of combustion.

† Phil. Mag. (7) xiv. p. 764 (1932).

‡ This figure is the average of values determined by Rossini, Roth and Bause, Griffiths and Awberry, and Fenning and Cotton.

Table IV.

Inflammable mixture percentages.	Diluent gases percentages.	$\left[\frac{P_m}{P_i}\right]_{20°}$	h_m per cent.	$T_m - T_i$ °C.	Q.	System of specific heats used.							
						Theoretical.		Partington and Shilling.		Pier and Bjerrum.		Goodenough and Felbeck.	
						E.	U.E. %	E.	U.E. %	E.	U.E. %	E.	U.E. %
16·03 CO + 4·37 H_2 + 10·2 O_2.	69·4 O_2	6·90	1·4	1960	13300	12800	2·4	11320	13·5	11530	11·9	11740	10·4
19·82 CO + 1 H_2 + 10·41 O_2.	68·77 CO	7·31	0·8	2095	13940	13470	2·6	12350	10·6	12650	8·4	12830	7·2
15·08 CO + 5·02 H_2 + 10·05 O_2.	50·68 N_2 + 19·17 CO	7·10	0·6	2020	13040	12650	2·4	11730	9·4	11960	7·7	12200	5·8
22·94 CO + 1 H_2 + 11·97 O_2.	22·57 CO_2 + 41·52 CO ...	6·99	1·1	2030	16030	15480	2·3	14000	11·6	14520	8·4	14670	7·4
24·94 CO + 1 H_2 + 12·97 O_2.	34·59 CO_2 + 26·5 CO	6·87	1·5	2020	17370	16700	2·4	15000	12·2	15690	8·2	15810	7·5
20·84 H_2 + 10·42 O_2	67·8 H_2 + ·94 H_2O	7·29	Very small, certainly less than 0·25 %.	2095	11930	11630	2·5	11900	0·3	11930	0·0	11740	1·6
21·58 H_2 + 10·79 O_2	57·29 N_2 + 9·59 H_2 + ·75 H_2O.	7·19		2070	12340	12070	2·2	11780	4·5	11770	4·6	11900	3·6
29·10 H_2 + 14·55 O_2	40·45 CO_2 + 15·02 H_2 + ·88 H_2O.	6·93		2085	16700	16330	2·2	15600	6·6	15950	4·5	15970	4·4

severe detonation prevented the carrying out of experiments with O_2 as a diluent.

The mixtures, which were at an initial density of 3 atmospheres, were proportioned so as to give a maximum mean explosion temperature in the neighbourhood of 2000° C., and in all cases care was taken to arrange for an excess of one of the reacting gases.

Attention is directed to the unaccounted energy or incomplete combustion estimates made upon the basis of the various specific heat systems after taking measured heat-loss into account.

It will be seen that the unaccounted energies range from 0·3 per cent. to 13·5 per cent. (Partington and Shilling), 0·0 per cent. to 11·9 per cent. (Pier and Bjerrum), and 1·6 per cent. to 10·4 per cent. (Goodenough and Felbeck). But on the basis of the theoretical specific heats given in Table I., the unaccounted energies are remarkably uniform, ranging only from 2·2 per cent. to 2·6 per cent. There seems to be no reason why, in these mixtures, the amount of incomplete combustion should vary much either in the carbon-monoxide group or in the hydrogen group, and it would appear that the experiments indicate the substantial accuracy of the theoretical specific heats.

A difficulty arises, however, when these experiments are reviewed in the light of similar experiments which we have made with argon as the main diluent. In these experiments, in which both carbon-monoxide mixtures and hydrogen mixtures were used, the incomplete combustion amounted to from 5 per cent. to 6 per cent. when the estimates were made upon the basis of the theoretical specific heats for CO_2 and H_2O respectively. It would therefore seem, taking all the results into consideration, that either

(i.) the theoretical specific heats are all a little (4 to 5 per cent.) too great, or

(ii.) that the monatomic gas argon has a tendency to inhibit the overall process of combustion, or, to put the matter in another way, that it does not deactivate the abnormal CO_2 and H_2O molecules formed during combustion as effectively as do the diatomic and triatomic diluents.

There is much general evidence in favour of (ii.),

which has been reviewed by P. Pringsheim *. It is interesting, too, to recall in this connexion that Bone, Newitt, and Townend † in their high-pressure explosion experiments found that $CO-O_2$ mixtures diluted with helium yielded maximum pressures appreciably different from those yielded by similar mixtures diluted with argon. Even the monatomics, therefore, would appear to differ from one another in their ability to deactivate.

Specific Heats up to 2500° *C.*

We give in Table V. the results of three series of explosion experiments with $2CO+O_2$ mixtures diluted

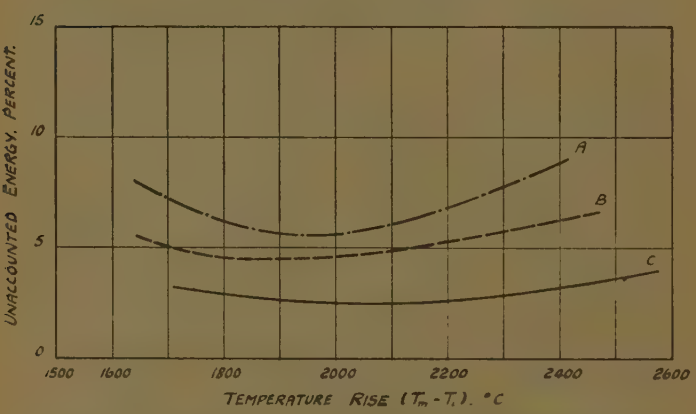

with CO, CO_2+CO, and N_2+CO, the object of the excess CO in the two latter series being to suppress dissociation. The experiments were all made at an initial density of 3 atmospheres.

It will be seen from the last column of this table that the incomplete combustion or unaccounted energy (estimated on the basis of the theoretical specific heats) is a minimum when the mixture-strengths are such that the maximum temperatures developed are in the neighbourhood of about 2000° C. to 2250° C. At lower and at higher temperatures the unaccounted energy is a little greater.

* ' Fluorescenz und Phosphorescenz ' (Springer, 1928).

† ' Gaseous Combustion at High Pressures,' p. 209 (Longmans, 1929).

Table V.

Inflammable mixture percentages.	Diluent gases percentages.	$\left[\frac{P_m}{P_i}\right]_{20°}$	h_m.	$T_m - T$ ° C.	Q.	Theoretical specific heats.	
						E.	U.E. %.
15·80 CO+1 H_2+8·4 O_2	74·80 CO	6·27	1·6	1710	11210	10670	3·2
17·82 CO+1 H_2+9·41 O_2 ...	71·77 CO	6·80	1·15	1905	12580	12080	2·8
19·82 CO+1 H_2+10·41 O_2 ...	68·77 CO	7·31	0·8	2095	13940	13470	2·6
21·86 CO+1 H_2+11·43 O_2 ...	65·71 CO	7·71	0·6	2255	15300	14800	2·7
23·56 CO+1 H_2+12·28 O_2 ...	63·16 CO	8·01	0·5	2380	16440	15820	3·3
26·12 CO+1 H_2+13·56 O_2 ...	59·32 CO	8·49	0·4	2575	18170	17410	3·7
23·00 CO+1 H_2+12·00 O_2 ...	28·47 CO_2+35·53 CO.....	6·75	1·2	1955	16070	15300	3·6
23·96 CO+1 H_2+12·48 O_2 ...	26·25 CO_2+36·31 CO	7·02	1·1	2060	16710	16140	2·3
25·00 CO+1 H_2+13·00 O_2 ...	23·08 CO_2+37·92 CO.....	7·31	1·0	2170	17410	16830	2·3
26·12 CO+1 H_2+13·56 O_2 ..	19·52 CO_2+39·80 CO.....	7·63	0·8	2295	18150	17580	2·3
26·92 CO+1 H_2+13·96 O_2 ...	14·96 CO_2+43·16 CO.. ...	7·90	0·6	2395	18660	17900	3·4
17·04 CO+1 H_2+9·07 O_2 ...	33·48 N_2+39·46 CO	6·62	1·4	1840	12060	11580	2·6
15·08 CO+5·02 H_2+10·05 O_2	50·68 N_2+19·17 CO	7·10	0·6	2020	13040	12650	2·4
18·35 CO+4·05 H_2+11·20 O_2	45·21 N_2+21·19 CO	7·62	0·8	2220	14690	14210	2·3
22·46 CO+2·0 H_2+12·23 O_2 .	40·13 N_2+23·18 CO	7·96	0·7	2365	16280	15780	2·3
25·34 CO+1 H_2+13·17 O_2 ...	35·49 N_2+25·00 CO	8·25	0·6	2520	17640	16830	2·9

The unaccounted energy curves shown in the figure are illuminating in this connexion. Curve A shows the unaccounted energy in a series of $2CO+O_2+nCO$ explosions at an initial density of $\frac{1}{4}$ atmosphere, curve B the unaccounted energy for a similar series at $\frac{1}{2}$ atmosphere, and curve C, also for a similar series, has been plotted from the figures given in the last column of Table V.

It will be seen that in curves A and B there is a fairly well-defined minimum value for the unaccounted energy. The explanation is, we think, that in the case of the lower temperature mixtures (which are fairly slow-burning mixtures) the unaccounted energy results in a large measure from incomplete *combination* at the moment of maximum pressure in the high-density film of gas in contact with the cold metal walls of the explosion vessel; it may also partly result from the fact that the hot gases tend to rise during the explosion, leaving a small amount of unburnt gas at the bottom of the vessel at maximum pressure. In the case of the high-temperature mixtures the rise in unaccounted energy would appear to result from an increasing latent energy associated with the abnormal condition of the exploded gases *; but for our present purpose the interesting fact is that as the density increases the unaccounted energy decreases, and the curves tend to flatten out. We think it exceedingly likely that had we been able to experiment with higher density mixtures (as we hope to do shortly), the unaccounted energy values would have tended to become more and more uniform.

The increase in unaccounted energy values up to 2500° C., however, is not very considerable even at 3 atmospheres initial density, and, as the estimates are based upon the theoretical specific heats, we feel justified in suggesting their substantial accuracy for the gases used in these experiments, viz., CO, N_2, and CO_2, up to about 2500° C. It seems possible that experiments at higher densities may indicate that the specific heat values for these gases can be extended to still higher temperatures.

In order to test the theoretical specific heats for the gases H_2, O_2, and H_2O it will be necessary to make explosions with hydrogen mixtures. A preliminary survey, which does not lend itself to concise presentation, of the

* See Phil. Mag. (7) xvii. p. 172 (1934).

experiments of Thorp and a few that we ourselves have made suggests that the values for H_2 and O_2 are probably substantially accurate at the higher temperatures. The values for H_2O, while probably not seriously in error up to about 2200° C., would appear to us to be doubtful at still higher temperatures.

Wohl and Elbe *, from their hydrogen explosion experiments, arrive at values for H_2O up to temperatures of 2500° C. very close to the theoretical values, but in deducing these values they assume the dissociation $H_2O \rightleftharpoons OH + \frac{1}{2}H_2$, and also dissociation of H_2 into atomic hydrogen. Such dissociation should tend to be suppressed by increasing the density, and it is difficult to draw support from our experiments at various densities for dissociation of these types on a scale sufficiently large to bring the explosion specific heats at the higher temperatures down to the theoretical values. We believe that the most satisfactory check on the H_2O specific heat values at the higher temperatures would be derived from explosions at high densities in a large vessel with hydrogen mixtures in which water-vapour is the main diluent. In order, however, to obtain such a large concentration of water-vapour in the mixtures, arrangements would have to be made for heating the vessel to high initial temperatures.

Discussion.

Making explosion experiments in such a manner as to keep down the incomplete combustion obtaining at maximum pressure to as small an amount as possible—having regard to the apparatus we have available—we have shown that the theoretical specific heats given in Table I. enable us to interpret these experiments in a thoroughly satisfactory manner. We think their use—at any rate for industrial purposes—is justified up to a temperature of at least 2500° C., though, exceptionally, we would for the present limit the temperatures to about 2200° C. in the case of H_2O.

A serious difficulty arises, however, when we compare the high speed internal combustion engine efficiencies determined by various observers with the ideal efficiencies calculated upon the basis of the theoretical specific heats. The indicated thermal engine efficiencies approach much

* *Zeit. Phys. Chem.* B, v. p. 241 (1929).

too closely to the ideal efficiencies on the basis of the generally accepted engine theory, and the theoretical specific heats would, therefore, appear to be much too large. It is true that where a direct comparison is possible between the experiments of the various observers, large differences in the engine efficiencies are sometimes noticeable *, but a comprehensive survey of high speed internal combustion engine literature suggests that the position is as stated. A possible explanation is that in high speed engines (1000 to 1500 revolutions per minute) there is insufficient time for the molecules of the diluent gases to develop their equilibrium amounts of vibrational energy, and so behave as though they had apparent specific heat values lower than the true values. Some support for this suggestion may be derived from the experiments of Kneser †, in which it was shown that specific heats determined by sound-waves decreased as the sound-wave frequency was increased.

On the other hand, in comparing measured flame-temperatures with ideal temperatures calculated upon the basis of the theoretical specific heat values, these values would not appear to be nearly large enough ‡; but it is thought that the theory of latent energy in flame-gases which has been put forward provides a satisfactory explanation.

Summary.

We think that the explosion experiments which we have made in a large spherical vessel indicate the substantial accuracy of the mean values of the theoretical specific heats of:

(1) H_2, CO, N_2, O_2, CO_2, and H_2O at 2000° C.

(2) CO, N_2, and CO_2 (and probably H_2 and O_2) up to 2500° C. There are indications in our experiments that, if explosions were carried out at higher densities than 3 atmospheres, the theoretical specific heat values for CO, N_2, and CO_2 could be extended beyond 2500° C., and we think that there is nothing in our experiments

* *E. g.*, Ricardo's efficiencies with hydrogen as a fuel ('The High Speed Internal Combustion Engine,' Blackie & Son, 1931, p. 79) are much greater than those determined by A. F. Burstall (Proc. Inst. Automobile Engineers, xxii. p. 358 (1927)) with a similar engine using the same fuel, even after making corrections for the different compression ratios.

† *Ann. Physik*, xi. p. 777 (1931).

‡ David and Jordan, Phil. Mag. xvii. p. 172 (1934).

which suggests that the values for H_2 and O_2 may not also be so extended.

The theoretical values for H_2O at temperatures above about 2000° C. would appear to us to require further investigation, but the inaccuracies resulting from their use will not be very considerable up to temperatures of 2200° C.

It would, we think, be worth while making experiments of a similar kind to those described in this paper, not only with mixtures at higher densities, but also with a still larger explosion vessel.

We wish to express our indebtedness to the Department of Scientific and Industrial Research for a grant which has enabled one of us (A. S. L.) to devote his time to this work.

XXVIII. *The Acoustical Insulation afforded by Double Partitions constructed from Similar Components.* *By* J. E. R. Constable, *M.A., Ph.D., B.Sc., Physics Department, National Physical Laboratory, Teddington, Middlesex* *.

THE provision of good acoustical insulation by partitions of small weight is a problem of very great practical importance. The many measurements of sound transmission made at the National Physical Laboratory and elsewhere have shown that the reduction of air-borne sound due to a partition of simple construction, such as a sheet of plywood or an ordinary brick wall, is determined almost entirely by its weight per unit area. It follows that good acoustical insulation can be provided by a simple partition only if the weight per unit area is large. Further, since sound produces in the human ear a sensation varying approximately as the logarithm of the intensity, even doubling the weight per square foot does not make a great deal of difference in the apparent sound reduction. Thus an increase in the effective sound reduction due to a simple partition can only be obtained by a disproportionate increase in its mass.

Several experimenters have observed that a partition constructed from two panels with an air-space between

* Communicated by Dr. G. W. C. Kaye.

them can have a sound reduction which is much greater than that possessed by a simple partition of the same weight. This construction will, therefore, provide a light-weight partition possessing a good sound reduction or, alternatively, a medium-weight partition possessing a high sound reduction.

Probably the most common example of a double partition is the double window which is often used in buildings to minimize the entrance of sound arising outside the building. Double walls are occasionally used for this purpose but, as used for exterior walls, are usually tied together at frequent intervals and are not, therefore, true examples of an air-spaced double partition. Double panels are also used, for the sake of lightness, for aeroplane cabin walls, but these usually have a filling of some light sound-absorbent material. Many other constructions in which double partitions are used occur in practice, such as telephone cabinets, gramophone audition rooms, etc.

In the following paper a relation is derived from which the sound reduction due to a certain type of double partition can be calculated from measurements made upon one of its components. The calculations apply only to a double partition the components of which are similar, mechanically isolated, flexurally rigid but subject to elastic constraints, and which have non-absorbing interior surfaces.

An interesting result of these calculations is that at any given spacing the sound reduction at frequencies which are less than a certain value and are greater than the fundamental frequency of either of the components, will decrease with increase of air-spacing. Owing to this effect it is possible for the sound reduction of a double partition to be less at some frequencies than that provided by a single one of its components.

The latter part of the paper deals with experimental measurements which show that the formula approximately represents transmission of sound through a double window, even although such a structure lies outside the limits to which the formula strictly applies.

Theoretical Treatment.

It will be appreciated that a rigorous theoretical treatment of the double partition would be extremely difficult,

mainly owing to the fact that every panel has a very large number of resonant frequencies (in the case of each of the panes of glass described in the experimental section of this paper over 150 resonances were observed at different frequencies below 4000 ~). At any one of these resonances a panel vibrates in a form which, in general, consists of a number of vibrating areas, adjacent areas being in alternate phases and separated by nodal lines.

In the following calculations a special simple case only has been considered. They relate, as stated above, to a double partition composed of two similar mechanically isolated, flexurally rigid, elastically constrained pistons. For further simplification only plane waves of sound, incident normally, are considered. It is hoped to discuss in a later paper the modifications which arise when double partitions with dissimilar components are employed.

There are two cases which may be considered in a theoretical discussion of double partitions.

(1) We may suppose that the pressure variations in the incident sound wave cause vibrations of the first component of the partition which, in turn, cause pressure variations in the interspace. These pressure variations, acting upon the second component, will cause it to vibrate and thus radiate sound energy on the other side of the partition. Obviously this supposition is subject to error in that the pressure variations are assumed to be uniform over the interspace ; this theory will not, therefore, be applicable when the sound waves have a wave-length which is less than, say, ten times the spacing between the panels.

(2) If the above condition does not hold, we may regard the process as similar to that visualized by Rayleigh in his theory of the transmission of sound through a thick partition * and assume that the vibrations of the first component cause a radiation of sound into the interspace and, acting upon the second component, this will cause a radiation of sound on the other side of the partition. Owing to internal reflexions there will be effectively two trains of waves proceeding in opposite directions within it.

Since both of the above cases are instructive and interesting, it is proposed to discuss each of them.

* Rayleigh, ' Theory of Sound,' ii. p. 86.

Case (1).—*Sound Reduction when the Separation between Components is small compared with the Wave-length.*

Infinite double components, identical in all respects, the separation between which is *small* compared with the wave-length of sound in the interspace.

For simplicity, the components also are supposed to be thin compared with the wave-length, and to have non-absorbent interior surfaces. The arrangement is represented in fig. 1. Let the pressure and density of the air on either side of the pistons be Π and ρ respectively, and let the distance between them, assuming them to be parallel, be d.

Fig. 1.

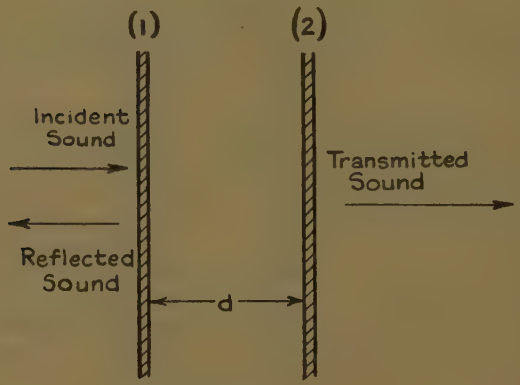

Let x_1 and x_2 be the displacements of the first and second pistons respectively, measured perpendicular to their planes, and let the elastic restoring forces be kx_1 and kx_2 per unit area. Since the pistons are assumed to be infinite in extent, their radiation resistances will be ρc, where c =velocity of sound in air.

Let the sound be incident from the left. Then it will produce a wave-train reflected from piston (1) and a transmitted wave-train radiated by piston (2). Let the particle velocities in the incident and reflected wave-trains be $\dot{y}_1$ and $\dot{y}'_1$ respectively. Then, by continuity, we have at the surface of piston (1):

$$\dot{y}_1+\dot{y}'_1=\dot{x}_1.$$

If σ = the mass per unit area of the components, we may, using the above relation, write the equations of motion of the two panels as :

Piston (1):

$$\sigma\ddot{x}_1 - 2\rho c\dot{y}_1 + \rho c\dot{x}_1 + x_1\left(k + \frac{\Pi\gamma}{d}\right) - x_2\left(\frac{\Pi\gamma}{d}\right) = 0. \quad (1)$$

Fig. 2.

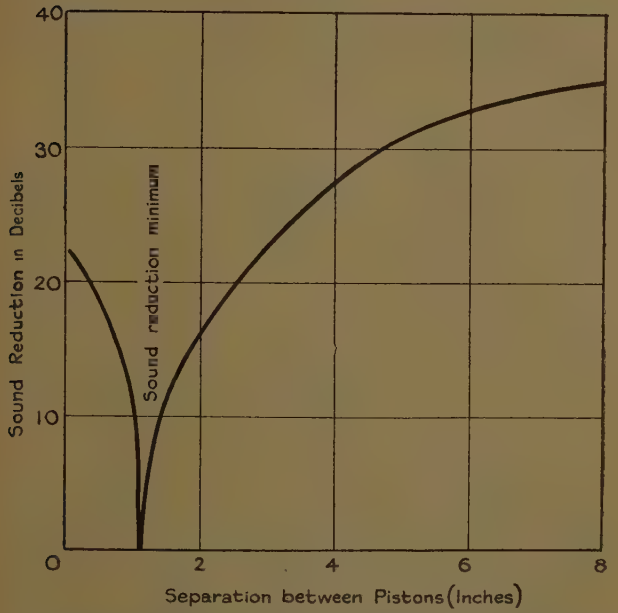

Variation with spacing of the sound reduction afforded by an idealized double partition at a frequency of 200 ~, as calculated from equation (8) (each component weighing 21 oz. per square foot and having a resonant frequency = 17 ~).

Piston (2):

$$\sigma\ddot{x}_2 + \rho c\dot{x}_2 + x_2\left(k + \frac{\Pi\gamma}{d}\right) - x_1\left(\frac{\Pi\gamma}{d}\right) = 0, \quad . \quad . \quad (2)$$

where γ = the ratio of the specific heats of air.

Putting $y_1 = y_0 e^{i\omega t}$

and substituting $x_1 = X_1 e^{i\omega t}$

and $x_2 = X_2 e^{i\omega t}$

(where X_1 and X_2 are, in general, complex), and solving for X_1 and X_2, we have

$$-\omega^2\sigma X_1 - 2i\rho c\omega y_0 + i\rho c X_1\omega + X_1(k+\beta) - X_2\beta = 0, \quad (3)$$

and

$$-\omega^2\sigma X_2 + i\rho c\omega X_2 + X_2(k+\beta) - X_1\beta = 0, \quad . \quad . \quad . \quad (4)$$

whence

$$X_1 = X_2\left\{\frac{k-\omega^2\sigma+\beta+i\omega\rho c}{\beta}\right\}, \quad . \quad . \quad . \quad . \quad (5)$$

where $$\beta = \frac{\Pi\gamma}{d}.$$

Substituting from (5) in (3) we obtain

$$X_2 = \frac{2\beta\rho c\omega y_0}{2\beta\rho c\omega + 2\alpha\rho c\omega - i(\alpha^2 - \rho^2c^2\omega^2 + 2\alpha\beta)}, \quad . \quad (6)$$

where $\alpha = \sigma(\omega_0^2 - \omega^2)$ and ω_0 is the resonant pulsatance of the pistons $\left(= \sqrt{\frac{k}{\sigma}}\right)$.

The amplitude of the second piston is thus given by

$$_0x_2 = \frac{2\beta y_0}{\sqrt{4(\alpha+\beta)^2 + \left(\frac{\alpha^2}{\rho c\omega} + \frac{2\alpha\beta}{\rho c\omega} - \rho c\omega\right)^2}}. \quad . \quad (7)$$

The vibrations of this piston will cause a radiation of sound-energy on the right-hand side of the partition at an average rate of $\frac{1}{2}\rho c\, {}_0\dot{x}_2^2$ per unit area per unit time.

The rate of incidence of energy $= \frac{1}{2}\rho c\, \dot{y}_0^2$ per unit area per unit time, and thus the sound-reduction factor of the partition, which is defined as

$$R = \frac{\text{rate of incidence of acoustical energy}}{\text{rate of radiation of acoustical energy}},$$

will be $$\dot{y}_0^2/{}_0\dot{x}_2^2.$$

Substituting for $_0x_2$, α, and β, this becomes

$$R = 1 + \frac{1}{\rho^2c^2\omega^2}\left\{\sigma(\omega_0^2-\omega^2) + \frac{\rho^2c^2\omega^2}{2\Pi\gamma}\left(1 + \frac{\sigma^2(\omega_0^2-\omega^2)^2}{\rho^2c^2\omega^2}\right)d\right\}^2. \quad . \quad . \quad . \quad (8)$$

It will be noted that, provided $\omega > \omega_0$, the sound-reduction, regarded as a function of d, will pass through a minimum at

$$d = \frac{-2\sigma(\omega_0^2 - \omega^2)\Pi\gamma}{\sigma^2(\omega_0^2 - \omega^2)^2 + \rho^2 c^2 \omega^2} \quad . \quad . \quad . \quad . \quad . \quad (9)$$

For frequencies less than ω_0, R will increase steadily with increase of d. Regarding (9) as an equation for ω, it appears that at any given spacing there are two values of ω for which R passes through a minimum (*cf.* fig. 3). The minimum values of R as calculated from equation (8) are each unity. This very low value is due to the fact that the only damping which has been considered is that due to radiation of sound. In practice other damping would occur and R would never be so small.

The variation of R with d is shown graphically in fig. 2, where R is plotted for a frequency of 200 $\sim$ and for an idealized partition, the components of which each weigh 21 oz. per sq. ft. and have a resonant frequency of 17 $\sim$. (These values of the weight and resonant frequency are chosen because of their application to the sheets of glass described in the experimental section of this paper.) It should be pointed out that the sound reduction has, following the usual practice, been plotted in logarithmic units (decibels) *.

By substituting numerical values for Π, γ, ρ, and c in equation (9), and assuming the weight of the piston to be not less than, say, 0·2 lb. per sq. ft., it appears that, in general, one value of ω given by equation (9) is very nearly equal to ω_0, whilst the other is larger than ω_0 by an amount which increases with decrease of d †. As an actual example of this it may be noted that the idealized partition referred to above would, in addition to the 17 $\sim$ resonance, have another resonance (corresponding to the greater value of ω discussed above) of about 420 $\sim$ when the spacing was reduced to $\frac{1}{4}''$. The variation of R (in decibels) with ω for this partition is shown for two different spacings in fig. 3. For comparison purposes the

* The sound reduction in decibels $= 10 \log_{10} R$.

† Fig. 2 is thus merely a description of the fact that, by suitably adjusting d, the upper resonance may be made to coincide with the frequency at which the measurement of the sound reduction is being made.

reduction due to a single piston as calculated from the formula given by Davis * is also given.

As a matter of interest it may be mentioned that even if the single components were non-resonant, the combined system would have one resonance given by

$$\omega^2 = \rho c(2\sigma c = \rho c d)/d\sigma^2$$

$$= \frac{2\rho c^2}{d\sigma} \text{ approximately.}$$

Fig. 3.

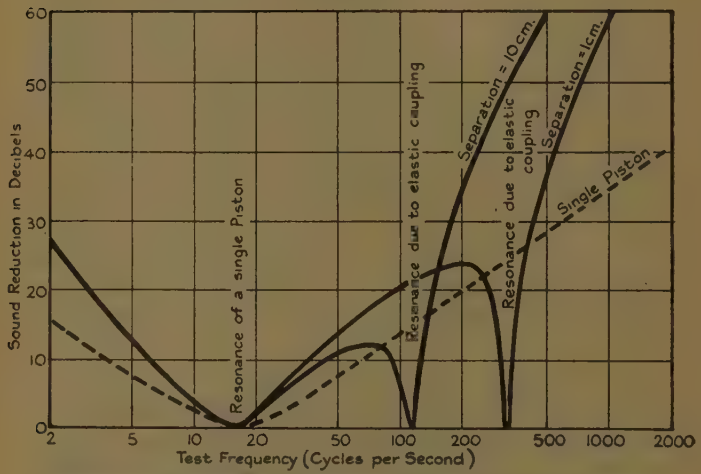

Variation with frequency of the sound reduction afforded by idealized double partitions with spacings of 1 cm. and 10 cm. respectively, as calculated from equation (8) (each component weighing 21 oz. per square foot and having a resonant frequency = 17~). The variation of the calculated sound reduction due to a single component is shown for comparison purposes.

Thus it is not necessary for the components to be resonant in order that the sound reduction shall pass through a minimum.

It will be shown later that there is an advantage in transforming equation (8) so that it provides a relationship between the sound reduction (R) due to the two pistons and the sound reduction (r) due to one of them alone.

* A. H. Davis, Phil. Mag. 7, xv. p. 309 (Feb. 1933).

An expression for r has been given by A. H. Davis *, who finds

$$r=1+\frac{\sigma^2}{4\rho^2c^2}\frac{(\omega^2-\omega_0^2)^2}{\omega^2}$$

$$=\frac{\sigma^2}{4\rho^2c^2}\frac{(\omega^2-\omega_0^2)^2}{\omega^2} \text{ approximately.}$$

Substituting this in equation (10), we obtain

$$\mathrm{R}=1+\left[\frac{(4r+1)\rho c\omega d}{2\Pi\gamma}\pm 2\sqrt{r}\right]^2 \text{ approximately,} \quad (10)$$

which may be approximated further to

$$\mathrm{R}=4\left[\frac{rd\omega}{c}\pm\sqrt{r}\right]^2, \quad . \quad . \quad . \quad . \quad (11)$$

the sign taken being that of $(\omega_0^2-\omega^2)$.

At $d=0$, (11) becomes $4r$, which is approximately the reduction to be expected from a single piston with a weight double that of either piston.

Case (2).—*Sound Reduction when the Separation between Components is large compared with the Wave-length.*

When we are no longer able to assume that the pressure is uniform throughout the interspace, a more accurate theory, leading to a more complicated formula, must be used.

The following calculation provides a formula for the reduction due to an idealized air-spaced double panel with any separation and follows the lines of Rayleigh's calculation of the sound reduction due to a thick plate †.

Let the two components, idealized as on page 324, be represented in fig. 4, and let them both be perpendicular to the axis of x, the one being at $x=0$ and the other at $x=d$. Let a train of plane waves be incident from the left and let the resulting displacements of the pistons be ζ_1 and ζ_2 respectively parallel to x. Then some sound energy will be reflected by the first piston and the remainder will be transmitted and will pass on to the second piston, where it will again split up into a reflected and a transmitted beam. The reflected wave will again be internally

* A. H. Davis, *loc. cit.*

† Rayleigh, 'Theory of Sound,' ii. p. 86.

reflected at the first piston and so on, with the final result that at any time there will be within the air-space two sets of waves travelling in opposite directions.

Let the incident sound be represented by

$$Xe^{i(\omega t - kx)}$$

and the reflected sound by

$$X_1 e^{i(\omega t + kx)},$$

where $k = \omega/c$.

Let the two wave-trains in the interspace be represented by

$Ye^{i(\omega t - kx)}$ to the right,

and $Y_1 e^{i(\omega t + kx)}$ to the left.

Fig. 4.

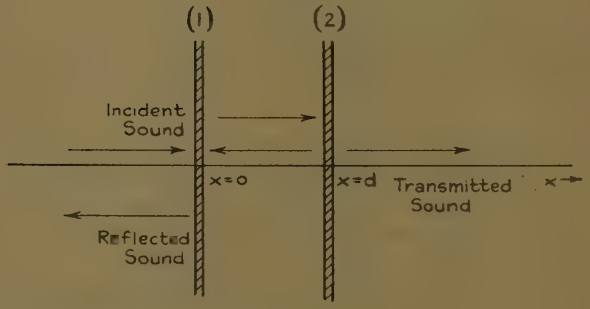

Let the transmitted sound be

$$Ze^{i(\omega t - kx)}.$$

(In the above expressions X, X_1, Y, Y_1, and Z may all be complex.)

Then by continuity we have:

At $x=0$, $\quad Xi\omega e^{i\omega t} + X_1 i\omega e^{i\omega t} = \dot{\zeta}_1$

and $\quad Yi\omega e^{i\omega t} + Y_1 i\omega e^{i\omega t} = \dot{\zeta}_1$.

At $x=d$, $\quad Yi\omega e^{i(\omega t - kd)} + Y_1 i\omega e^{i(\omega t + kd)} = \dot{\zeta}_2$

and $\quad Zi\omega e^{i(\omega t - kd)} = \dot{\zeta}_2$.

Combining the above equations, we have

$$X + X_1 = Y + Y_1$$

and $$Z - Y = Y_1 e^{2ikd}.$$

Solving these for Y and Y_1, we obtain

$$Y=\frac{(X+X_1)e^{ikd}-Ze^{-ikd}}{2i\sin kd} \quad . \quad . \quad . \quad . \quad (12)$$

and

$$Y_1=\frac{(Z-X-X_1)e^{-ikd}}{2i\sin kd} \quad . \quad . \quad . \quad . \quad (13)$$

The acoustical forces per unit area upon the pistons are

(1) $\rho c\omega e^{i\omega t}(X-X_1+Y_1-Y)$ to the right.

(2) $\rho c\omega e^{i\omega t}(Ye^{-ikd}-Y_1e^{ikd}-Ze^{-ikd})$ to the right.

By substituting for Y and Y_1 from (12) and (13), the equations of motion of the two pistons can be obtained and are

$$(1)\ \frac{\rho c\omega e^{i\omega t}}{\sin kd}\{Ze^{-ikd}-X_1e^{ikd}-Xe^{-ikd}\}=\sigma\ddot{\zeta}_1+\omega_0^2\sigma\zeta_1;$$

$$(2)\ \frac{\rho c\omega e^{i\omega t}}{\sin kd}\{X+X_1-Z\}=\sigma\zeta_2+\omega_0^2\sigma\zeta_2.$$

Eliminating X_1 between these two equations, we obtain the following relation between X and Z:

$$\frac{X}{Z}=\frac{\left(2\alpha\rho c\omega+\frac{\alpha^2}{2}\sin 2kd\right)-(2\rho^2c^2\omega^2-\alpha^2\sin^2 kd)}{2\rho^2c^2\omega^2},$$

where α, as before, $=\sigma(\omega_0^2-\omega^2)$.

Thus the reduction factor, which equals X^2/Z^2, is

$$R=1+\frac{\alpha^2}{4\rho^4c^4\omega^4}\{2\rho c\omega\cos kd+\alpha\sin kd\}^2, \quad . \quad (14)$$

which, if α is negative, will pass through an infinite number of minima which are given by

$$\tan kd=-\frac{2\rho c\omega}{\alpha} \quad . \quad . \quad . \quad . \quad . \quad . \quad (15)$$

This reduction factor may be expressed in terms of the theoretical reduction due to a single component by the formula

$$R=1+4r\{\cos kd\pm\sqrt{r}\sin kd\}^2,$$

the sign used being that of the expression $(\omega_0^2-\omega^2)$.

It may be noted that when kd is small the expression for R becomes approximately

$$R=4\left\{\frac{r\omega d}{c}\pm\sqrt{r}\right\}^2,$$

which is identical with (11).

Re-writing the expression in the form

$$R=1+2r(1+r)[1+\cos(2kd-2\epsilon)], \quad . \quad . \quad (16)$$

where $$\tan\epsilon=\frac{\alpha}{2\rho c\omega},$$

we see that the reduction will oscillate in a sinusoidal manner * between R = 1 and R = 1 + 4r(1 + r). After the first minimum (which corresponds to the minimum considered in the simple theory) minima occur at successive increases of a half wave-length in the magnitude of d. The minimum value of the reduction according to the above formula would be unity, but, as was explained on page 327, this is probably due to mechanical damping not having been taken into account.

It may be remarked that if the interior surfaces of the components of the partition are rendered sound-absorbing, the reflexion effects will be reduced and we may expect the amplitude of the variation of R with d to be correspondingly reduced. The reduction at separations large compared with the wave-length will then tend towards r^2. (This has been confirmed experimentally in the case of a pair of fibre boards.)

The above theoretical work has been carried out with an air-filled interspace in view. The elastic coupling between the two panels might equally well consist of springs or elastic material, and in this case it is possible that the simpler formula would suffice. This formula, as amended to take account of this case would be

$$R=1+\left\{\frac{\sigma(\omega_0^2-\omega^2)+\frac{d}{2Y}[\rho^2c^2\omega^2+\sigma^2(\omega_0^2-\omega^2)^2]}{\rho^2c^2\omega^2}\right\}^2,$$

where Y = Young's modulus for the elastic material if uniformly spread between the two components, or the

* The non-sinusoidal character of the theoretical curves in fig. 10 is, of course, due to the use of logarithmic ordinates.

effective Young's modulus for the elastic system if not uniformly spaced.

The effect of changing the gas in the interspace is usually small, as may be seen from equation (11), the only change being in γ, since the density of the *contained* gas does not enter into the equation. At large spacings, however, the fact that the velocity of sound in the interspace had changed would be of importance. For example, the minima which occur at intervals of $\lambda/2$ could be rendered much less important by filling the interspace with hydrogen, when the wave-length would be increased by a factor of approximately 4. Appreciably higher sound reduction should then be obtainable at high frequencies (*i.e.*, $>500\sim$).

Reducing the pressure of the gas in the interspace would also be of considerable advantage at all spacings, but constructional difficulties would probably prevent this being practicable.

The above results have been obtained from a consideration of the behaviour of a pair of pistons, each rigid and singly resonant. It is known, however, in the case of single partitions in actual practice, that the large number of resonant frequencies they possess causes departures from the sound reduction calculated for an idealized singly resonant piston, and it is to be expected that corresponding effects will occur in the case of double partitions. In actual fact experiment shows that for single partitions there is satisfactory agreement between calculated and experimental sound reductions, except at resonant frequencies, provided the weight of the partition is below about $1\frac{1}{2}$ lb. per sq. ft. At frequencies which are near to one of the resonances there may be large discrepancies, however, even for very light partitions. For example, the experiments described below show that in the case of a single sheet of glass, the weight of which lies below the above limit, the calculated and experimental sound reduction factors were for most frequencies within a decibel of each other. At one of the resonant frequencies ($500\sim$), however, the experimental value was 8 decibels smaller.

If we may assume that the presence of such resonances will affect, in like manner, a double partition constructed from two similar sheets, we may reasonably anticipate that equations (11) and (16) (which express the sound reduction due to an idealized double partition in terms

of that due to one of its components) would lead to a closer agreement between the calculated and experimental values for an actual double partition than would equations (8) and (14) (which express the sound reduction in terms of the fundamental constants) *. That this is the case will appear from the experiments described below, where equations (11) and (16) are seen to be generally satisfactory. Moreover, even at the resonant frequency of 500 $\sim$, agreement between reduction factors calculated on this basis and the experimental values is shown to be quite good.

Experimental Arrangements.

The experiments described below was designed to afford an indication of the degree of approximation associated with equations (11) and (16), from the point of view of their possible practical application, *e. g.*, to double windows.

To this end a series of experiments was made in the sound-transmission rooms at the National Physical Laboratory upon a double partition constructed from sheets of glass. The transmission rooms have already been described †, but for reference a short description is appended. They consist of two rooms which, except for a connecting aperture, are acoustically isolated by air-spaced walls and doors. In one of the rooms sound of a definite frequency is generated by a large moving-coil loud-speaker which is driven by approximately sinusoidal alternating current derived from a heterodyne oscillator. Measurements of the sound intensity generated in the second room are made by a condenser microphone. To minimize errors due to stationary wave formation both of the rooms are lined with sound-absorbent material, and the microphone and loud-speaker are used in a series of standard positions for each frequency. Measurements of the sound intensity generated in the second room are made both with and without the partition in position in

* It will be noted, in this connexion, that the resonant frequency has been eliminated in (11) and (16). It is easy to show that the relation would be exact for a pair of multi-resonant pistons provided they remained rigid. When the relation is applied to actual partitions it is only approximate, owing to the complicated form of vibration associated with resonances other than the fundamental.

† A. H. Davis and T. S. Littler, Phil. Mag. iii. p. 177 (Jan. 1927).

the aperture, and the ratio of the intensity in the latter case to that in the former is taken as the reduction factor.

Ideally, the sound reduction factor should be taken as the ratio of the intensity of an incident beam of sound to that of the transmitted beam but it may be shown that the reduction factor, as measured by the method described above, approximates closely to this provided that the rooms are sufficiently non-reverberant. Calculations show that the transmission rooms at the Laboratory approximate to this condition.

It will be noted that in the theoretical section of this paper only the case of a sound wave incident normally was considered. Experimentally neither condition could be fulfilled, since, if the sound was incident normally, it would be reflected back to the loud-speaker and would affect its emission. For this reason the sound is incident obliquely. Since the wave-length is large at most of the test frequencies, it is impossible to use a parallel beam for these. Actually, at the higher frequencies, the radiation from the loud-speaker diaphragm approximates to a parallel beam.

It is not possible to allow for such errors as are introduced by the divergence and oblique incidence of the beam but in practice they do not appear to be very large, as is seen by the fact that the theoretical and experimental values for the sound reduction due to a simple wall are in fair agreement, especially for partitions having a small weight per square foot. In some experiments made some time ago it was shown that the change in measured reduction factor produced by substituting a non-parallel for a parallel beam was negligible. No doubt this is mainly due to the fact that reductions are normally so very large that factors introduced by the above effect are unimportant.

As it was desirable to make the measurements extend over as wide a range of air-spacing as possible, it was important that the component members of the partition should be as flat as possible. This condition was most easily satisfied by using sheets of glass. It was also desirable to use this material on account of the ready application of the results to the practical case of double windows. On the other hand, in order that measurements could be conducted with large air-spacing, it was necessary to choose the panels so that the resulting sound reduction

should not be too great to be measured with sufficient accuracy. It was not possible, owing to technical difficulties, to measure, with any accuracy, a reduction greater than 70 decibels. A preliminary calculation of the sound reduction to be expected showed that the thickest glass which could be used was that known as 21 oz.; $\frac{1}{4}''$ plate glass, which was from all other points of view desirable, had to be ruled out Unfortunately it was not possible to obtain sheets of 21-oz glass which were larger than $4' \times 4'$.

Measurements with spacings of up to $8''$ were contemplated and, with this in view, the following construction was made. The aperture connecting the two experimental rooms was provided with a reveal constructed mainly of brickwork. A sectional plan of this is shown in fig. 5. Since it was not possible to provide a depth to the aperture which was sufficient for an $8''$ air-spacing, an adequate range of spacing was obtained by arranging that for small spacings the two sheets of glass were on the same side of the reveal, whilst for large separations ($>4''$) they were on opposite sides. The two dispositions of the sheets of glass are represented in figs. 6 (*a*) and 6 (*b*).

The experiments were rendered more difficult by the fact that relatively small variations in the reduction factor were being looked for, and that an apparently small alteration in the methods of clamping or sealing the panel can produce variations of the sound transmission which might easily obscure the effects which were expected. These variations are almost certainly due to the number of resonant frequencies which a panel possesses. To avoid this difficulty it was essential that the sealing arrangements should remain as nearly constant as was possible, and the following method of clamping was finally adopted. One sheet of glass was sealed with plasticine to the reveal, whilst the other was sealed to a frame of $2'' \times 2''$ wood which fitted the aperture. Distance-pieces having been put in position, the wooden frame was inserted in the aperture with the glass towards the reveal and all crevices were well sealed. The boundary conditions of the sheets of glass were unaltered by the process of removing the glass on its wooden frame for the purpose of changing the spacing The reduction factor of the sheet which was sealed to the reveal was measured in each of its two positions (figs. 6 (*a*) and 6 (*b*)), and in view

of the fact that but little change was observable it is believed that the clamping arrangements were adequately reproduced.

Ideally the only connexion between the two com-

Fig. 5.

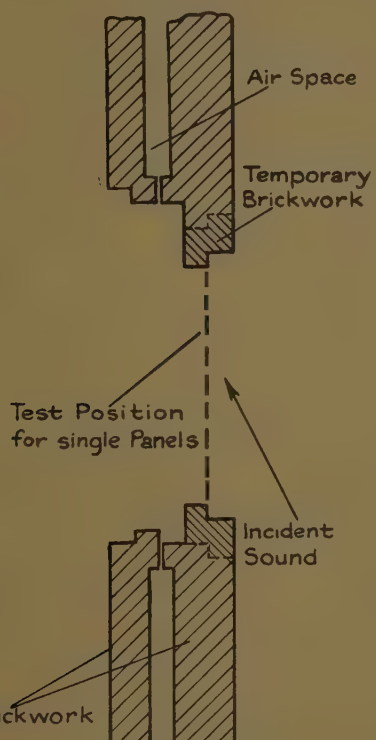

Section through sound-transmission test-aperture.

ponents should be acoustical, but there are three reasons why this was not strictly attained :—

(1) Since both sheets of glass are secured to the same wall, there will inevitably be a mechanical linkage between them.

(2) Some form of distance-piece is desirable and energy will be transferred through this path. This effect was minimized by using only small triangular pieces of wood, one at each corner of the sheet.

(3) The wall to which the partition is secured will be subjected to forces due to the incident sound and in its resultant motion will carry the window with it. This is possibly the most serious of all the errors (though, for the partitions considered,

Figs. 6 (*a*) and 6 (*b*).

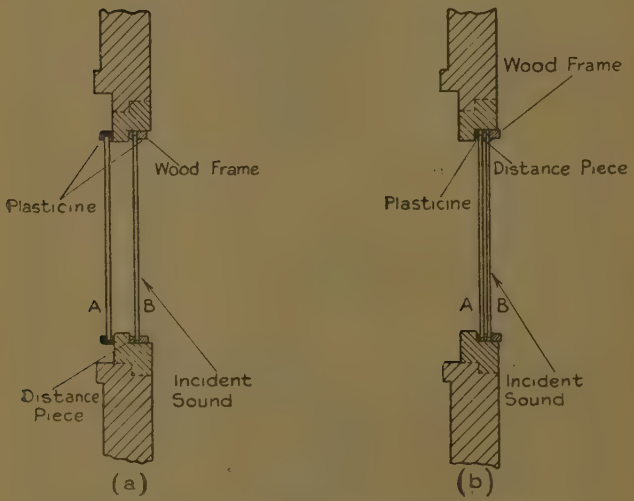

Method of fixing experimental double window into aperture.

it is only serious at the high frequencies at which the sound reduction due to the partition is comparable with that due to the wall). It was rendered more serious by the necessity of reducing the normal aperture of the test-rooms by brickwork in order to accommodate the small size of glass available.

It was thought advisable to attempt to determine the fundamental resonant frequency of the glass panels although this frequency does not explicitly occur in the

final formulæ. The determination was accomplished very simply by attaching a small specially designed coil to the centre of the panel and arranging that it was in the field of a small permanent magnet. When the panel was caused to vibrate by a light blow an alternating potential difference was generated by the coil and, after amplification, was examined with a recording Duddell oscillograph. By using a suitable blow it was possible to obtain the fundamental practically free from overtones. It may be mentioned that it was also possible, using this apparatus, to observe resonances of the panel to incident sound, and in this way a very large number of natural frequencies were detected, their associated damping coefficients being measured in many cases. The fundamental frequency was found to be approximately 17 $\sim$, a value which agrees fairly well with that calculated from a formula given by Franke *. It is obvious that this is very much below any of the experimental frequencies, and α was therefore negative in all measurements.

The graphs in figs. 7–10 are typical of the results which were obtained and are the results of several series of measurements. In each case the theoretical curves are also shown. At the higher frequencies (500 $\sim$ and 1000 $\sim$) the divergence between the curves obtained from formulæ (11) and (16) becomes large and the two curves are shown. The divergence at 100 $\sim$ and 200 $\sim$ was too small to be shown. The experimental curve for 200 $\sim$ has been drawn to show an agreement between its minimum and that of the theoretical curve and it is not justified by the experimental points alone.

It will be seen that, except for fig. 10, the results agree reasonably well with equation (16) and, for small separations, with (11). The experimental curves have, in figs. 9 and 10, a value inserted for zero separation, this being obtained by interpolation from the established (sound reduction)/(mass per unit area) curves for simple partitions. Fig. 10 illustrates the second minimum, which occurs at an increase in the separation of half a wave-length. The first minimum would occur at a separation which is too small to be shown on the graph. The theoretical reduction at 1000 $\sim$ (fig. 10), it will be noted, can be as much as 10 decibels greater than the

* G. Franke, *Ann. d. Phys.* 5, 2, pp. 649–675 (1929).

Fig. 8.

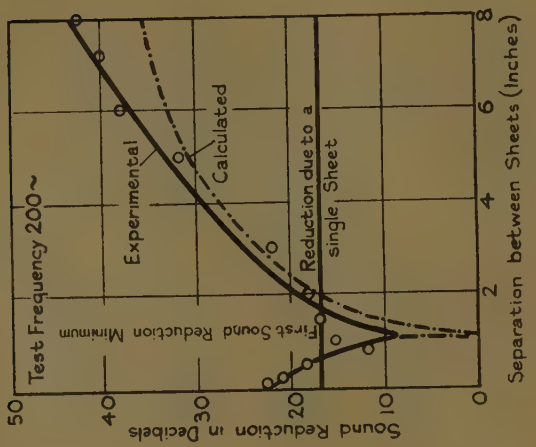
Test Frequency 200~
Experimental
Calculated
Reduction due to a single Sheet
First Sound Reduction Minimum
Sound Reduction in Decibels
Separation between Sheets (Inches)
0
10
20
30
40
50
2
4
6
8

Fig. 7.

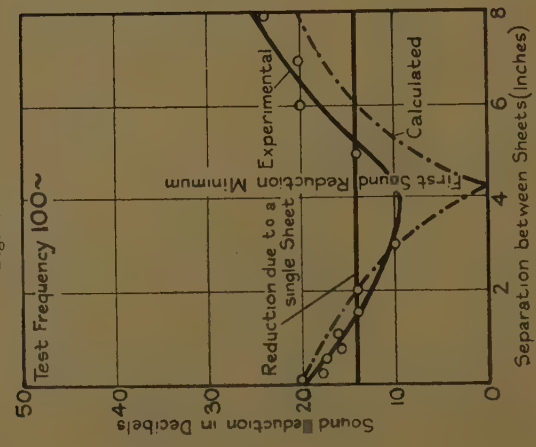
Test Frequency 100~
Experimental
Calculated
Reduction due to a single Sheet
First Sound Reduction Minimum
Sound Reduction in Decibels
Separation between Sheets (inches)
0
10
20
30
40
50
2
4
6
8

Fig. 9.

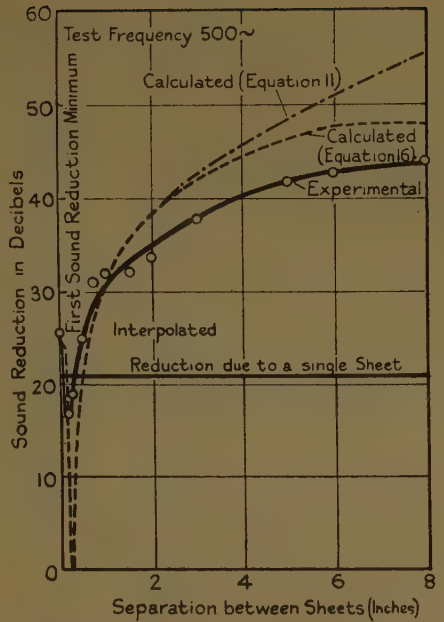

Fig. 10.

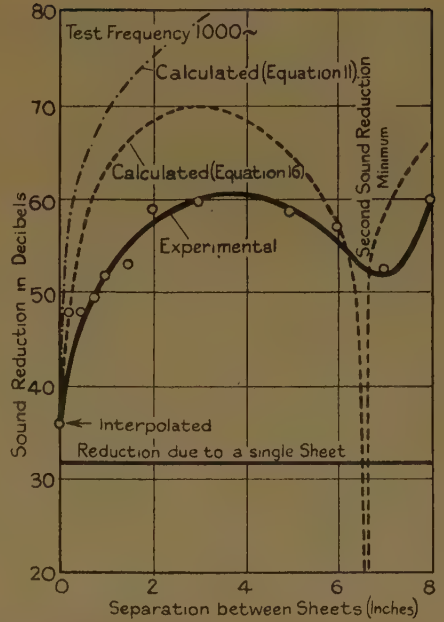

Figs. 7–10.—Comparison between the calculated and experimental variations with spacing of the sound reduction due to two sheets of 21-oz. glass.

experimental values, but a rough calculation showed that this discrepancy could be satisfactorily accounted for by the motion of the supporting wall, as was explained on page 338. It will be noted that the experiments show that the sound reduction due to the double window can, over a range of frequencies, be less than that afforded by one of its components.

Calculation showed that the sound reduction for a single sheet of glass of known weight and fundamental resonance, as calculated from Davis's formula, did not differ greatly from the experimental values. These experiments do not, therefore, provide much information as to whether it would be safe to apply formula (17) to double partitions constructed from panels for which the theoretical and experimental sound reductions differed widely It may be taken as an experimental fact, however, that normally the two values will agree for panels which are lighter than $1\frac{1}{2}$ lb. per sq. ft., and formula (16) should therefore hold for double partitions constructed from these.

Conclusion.

The experiments described above show that the relation between the sound-reduction factor of an idealized double partition and that of one of its components, as expressed by equations (11) and (16), represents, with reasonable accuracy, the experimental results for a rectangular double-glass partition. The relations, which are derived on the assumption of the absence of upper resonances, are offered only as approximations. They appear, however, to have useful practical application, particularly in their bearing on the design of light double partitions for sound insulating purposes. A wider series of measurements is needed upon partitions constructed from materials of other types and greater weights before any claim can be advanced as to the general applicability of the formulæ. It is hoped to carry out such measurements, which will necessarily be somewhat protracted, as the opportunity occurs.

Summary.

A theoretical and experimental study has been made of the acoustical insulation afforded against air-borne sound by double partitions constructed from similar components. In the case of singly resonant rigid

partitions a relation is derived connecting the sound reduction due to a double partition with that due to one of its components. It is shown that the relation represents with reasonable accuracy the results for a rectangular double glass partition studied experimentally. It is deduced and confirmed experimentally that at the lower frequencies an increase of the spacing between two air-separated components may decrease the acoustical insulation. It thus happens with double glass windows, and may occur with other double structures, that there is a range of frequencies over which the acoustical insulation is less than that afforded by one of the components.

The author wishes to express his sincere thanks to Dr. G. W. C. Kaye, O.B.E., Superintendent of the Physics Department, for his encouragement and advice and to Dr. A. H. Davis for many helpful discussions.

XXIX. *The* Cu_2Mg *Phase in the Copper-Magnesium System.*

By V. G. Sederman, *M.Sc., Isaac Roberts Research Scholar* *.

Introduction.

THE copper-magnesium system of alloys has been examined by X-ray methods by Grime and Morris-Jones[1], and independently by Runqvist, Arnfelt, and Westgren[2]. Apart from slight differences in the numerical values of their measurements, their results are essentially the same. The existence of two intermediate phases which had previously been disclosed by metallurgical methods (Sahmen[3], Urazov[4]), corresponding to the intermetallic compounds Cu_2Mg and $CuMg_2$, was confirmed, and a crystal structure assigned in each case. The former was found to be face-centred cubic and the latter hexagonal.

The X-ray analysis also confirmed the existence of a range of solid solution of Mg in Cu, amounting to approximately 3 per cent.; this had previously been indicated by the results of Stepanov[5], who used the electrical resistance method of examination. It disclosed also

* Communicated by Prof. R. T. Dunbar, Ph.D.

a second, and as yet undiscovered, solid solution range, namely, a range extending on each side of the composition Cu_2Mg.

Shortly after the publication of this result by the authors mentioned above[1], [2], there appeared a paper by W. R. D. Jones[6] announcing the results of a very detailed and thorough examination of the copper-magnesium system by metallurgical methods (thermal and microscopic). The elements were of exceptional purity, and the alloys, over one hundred in number, were prepared *in vacuo*, a special device being used for stirring on account of the disparity in density between the two constituents. The

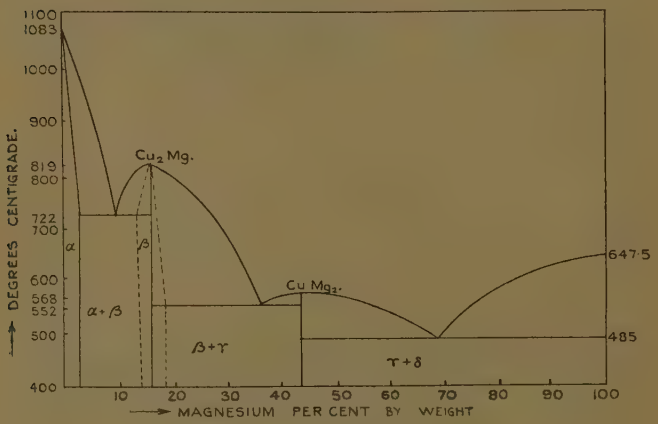

Copper-magnesium equilibrium diagram.

equilibrium diagram that he obtained is reproduced in the figure, with the addition of dotted lines to indicate the homogeneity range which had been disclosed by the X-ray analyses already referred to. Jones confirmed the existence of the solid solution of Mg in Cu (α-phase), and ascribed the value 2·2 per cent. to the range of solubility at 500° C. and 2·7 per cent. at 730° C. In spite, however, of a careful examination of the alloys he had prepared in the neighbourhood of the composition Cu_2Mg, he was unable to detect any evidence for the existence of a range of solubility at this point. Considering the refinement of the method of preparation of his alloys,

and the fact that he had prepared very many more specimens than the X-ray workers, it would appear at first sight that his failure to observe any trace of the solubility range must throw an element of doubt upon the conclusion arrived at from X-ray analysis. It has to be remembered, however, that the detection of a solubility range by X-ray methods is a comparatively simple matter, all that is required being an X-ray analysis of one specimen in each of the mixed phase regions on the two sides of the phase in question. If the lines corresponding to this phase in the two spectrograms differ in spacing, there can be only one conclusion, namely, that a solubility range exists. On the other hand, the metallurgical method entails the preparation of specimens of different constitution within the limits of the homogeneity range itself. In the present instance this appears to present insuperable difficulties, for not only has the metallurgist to contend with (1) the disparity in density, and (2) the high volatility of one of the metals, in the preparation of an alloy of a predetermined composition, but in the annealing process which must precede examination there seems to be no possible hope of preventing segregation and a change in composition for the two reasons, respectively, which have just been mentioned.

It was suggested by Dr. W. R. D. Jones that the author should undertake a fresh examination of the question of the existence of the above homogeneity range, using the X-ray powder method. Dr. Jones kindly offered to provide samples of the alloys that he had prepared. It seemed worth while re-examining the question by the X-ray method, not only on account of the element of doubt which had been raised by Dr. Jones's unsuccessful search for metallurgical confirmation of the existence of the homogeneity range, but also for the following reasons. The actual alloys which had failed to provide confirmatory evidence would be available : the specimens themselves were undeniably of high purity and prepared by the best metallurgical methods : the importance of submitting the specimens to systematic annealing processes had been recognized only since the previous X-ray analyses had been completed. Furthermore, the extrapolation method for the accurate determination of lattice spacings from Debye-Scherrer spectrograms, due to Bradley and Jay[7], would make

possible a precision of measurement some ten times better than had previously been obtained with these alloys. The present paper gives an account of the analysis which was undertaken, and of the results which it yielded.

Experimental.

The procedure observed with each of the specimens was as follows :—A prolonged lump annealing, *in vacuo*, was first given to produce homogeneity. After discarding the surface layers, filings were taken off and annealed, *in vacuo*, at the temperature at which the lattice parameter was required. The filings were then quenched in cold water. This filing annealing had a two-fold significance : (*a*) it had to remove the lattice distortion introduced by the filing process, and (*b*) it had to produce the state of equilibrium corresponding to the temperature of annealing. When the temperature required was below the minimum temperature necessary to remove the lattice distortion in a reasonable time, the filings were first annealed for a short time at a high temperature to remove it, cooled to the desired temperature, and there maintained for a long period to ensure that the required state of equilibrium had been attained. (It is to be noted that an alteration in the composition of the filings during the annealing is immaterial provided that the composition still lies within the mixed-phase region under examination.) A spectrogram of the annealed filings was then obtained with a standard type of Debye-Scherrer powder camera.

An accurate value of the lattice parameter was obtained by employing the procedure described by Bradley and Jay[7]. In this method the film employed is wrapped completely round the camera except for a small space at the entrance-slit. Shrinkage of the film is automatically compensated for by referring all lengths measured on the film to the distance between two fiducial marks, which appear, one at each end of the film. Errors due to eccentricity of the specimen and to absorption are eliminated by graphing the values of the lattice parameter obtained from the various high-order lines against $\cos^2\theta$, and extrapolating to $\cos^2\theta = 0$. The camera used in the present research was standardized with chemically pure sodium chloride by the method given in Bradley and Jay's paper.

An X-ray tube of the gas-filled type was employed, operated by a transformer which, under normal working conditions, supplied a current of 7 ma. at about 40 kv. Copper K radiation was used throughout, since it gave three high-order doublets for the cubic β-phase, namely, (840), (662), and (555), very conveniently placed for the above extrapolation. The specimens were annealed in a Gallenkamp electric furnace, the temperatures being measured to an accuracy of 5° C. by a platinum—platinum-iridium thermocouple.

Experimental Results.

Six alloys were selected for examination, which will be denoted by A. 94, A. 92, A. 86, A. 79, A. 73, A. 66, the numbers indicating the approximate percentage (by weight) of copper contained in them. The composition Cu_2Mg corresponds to 83·94 per cent. Cu (International Atomic Weights, 1927), and consequently, since the homogeneity range (if it exists at all) must be small, the first three alloys were assumed to be in the $(\alpha+\beta)$ mixed region and the last three in the $(\beta+\gamma)$ region. A number of preliminary photographs were taken with the alloys so as to obtain information regarding the periods of annealing necessary. Although it has been shown[8] that, with certain alloy systems, a single annealing of the "as-cast" filings is sufficient both to remove lattice distortion and to produce equilibrium, in the present instance a preliminary lump annealing was found necessary before satisfactory results could be obtained.

The $(\alpha+\beta)$ Mixed-phase Region.

Alloys A. 94, A. 92, and A. 86 were examined after having been annealed at temperatures 600° C., 500° C., and 400° C. The details of the annealing are given in Table I., together with the lattice parameters obtained from measurements of the spectrograms. In each of the spectrograms the β-phase gave three strong doublets, namely, (840), (662), (555), at diffraction angles of about 79°, 73°, and 72°, respectively. As mentioned before, these were very conveniently situated for the extrapolation. The values of the parameter calculated from the two components of a doublet were often found

to differ slightly. This effect has been observed by Bradley and Jay, who consider it due to an optical illusion encountered during the measuring of the doublet. In such cases the extrapolation curve (a straight line) was drawn rather nearer to the $K\alpha_1$ value, $K\alpha_1$ being the more intense line. Another effect of a similar nature was observed: the values obtained from the (662) doublet were sometimes lower than those obtained from the (555) doublet, and, consequently, it was rather difficult to estimate the position of the extrapolation curve. In such cases two straight lines were drawn to act as extrapolation curves, one for the doublets (840) and (662) and one for the doublets (840) and (555). The two extrapolated values obtained differed very little, and their mean was taken as the true value. From considerations of the errors involved in the above procedure, and also of the agreement amongst the results for the various alloys, the accuracy of the determination of the lattice parameter of the β-phase has been estimated to be 1 part in 15,000 or better.

In the case of alloys A. 94 and A. 92 the α-phase was recorded as well. Two high-order doublets appeared, namely, (420) and (331); occasionally (333)$K\beta$ was recorded. Since the diffraction angles for these doublets were approximately 71° and 68°, they were rather close together for a satisfactory extrapolation to 90°. Consequently the results for the α-phase are not so accurate as those for the β-phase parameter. The values for the α-phase parameter are considered to be correct to 1 part in 10,000.

The $(\beta+\gamma)$ *Mixed-phase Region.*

The saturation parameters of the β-phase in the $(\beta+\gamma)$ region were determined for the temperatures 500° C. and 380° C. with the aid of the three alloys A. 79, A. 73, A. 66. Particulars of the annealing given to these specimens, and the results obtained, are given in Table II. Results for alloy A. 79 at 500° C. have not been included, as the spectrograms obtained were not sufficiently sharp for accurate measurements. In addition to the three doublets already mentioned, the line (753)$K\alpha_1$ appeared on several of the spectrograms for this region. Since this line was recorded quite close to the fiducials ($\theta=84°$

TABLE I.—Lattice Parameters of Alloys in $(\alpha+\beta)$ Region.

Alloy.	Lump annealing.	Filing annealing.	Parameter of α-phase.	Parameter of β-phase.
A. 94	130 hrs. 680° C.	2 hrs. 600° C.	3·6368 Å.	7·0087 Å.
A. 92	42 hrs. 600° C.	2 hrs. 600° C.	3·6366 Å.	7·0089 Å.
A. 86	24 hrs. 620° C.	2 hrs. 600° C.	—	7·0084 Å.
		Mean	3·6367 Å. ± ·0004 Å.	7·0087 Å. ± ·0004 Å.
A. 94	130 hrs. 680° C.	5 hrs. 500° C.	3·6260 Å.	7·0134 Å.
A. 92	42 hrs. 600° C.	3 hrs. 500° C.	3·6266 Å.	7·0132 Å.
A. 86	24 hrs. 620° C.	5 hrs. 500° C.	—	7·0133 Å.
		Mean	3·6263 A. ± ·0004 Å.	7·0133 Å. ± ·0004 Å.
A. 94	130 hrs. 680° C.	2 hrs. 500° C. & 20 hrs. 400° C.	3·6178 Å.	7·0182 Å.
A. 92	42 hrs. 600° C.	1 hr. 500° C. & 20 hrs. 400° C.	3·6174 Å.	7·0187 Å.
A. 86	24 hrs. 620° C.	2 hrs. 500° C. & 20 hrs. 400° C.	—	7·0185 Å.
		Mean	3·6176 Å. ± ·0004 Å.	7·0185 Å. ± ·0004 Å.

approx.), the measurement of it gave a very accurate value for the lattice parameter, and consequently due weight was given to this point in the extrapolation.

TABLE II.

Lattice Parameters of Alloys in $(\beta+\gamma)$ Region.

Alloy.	Lump annealing.	Filing annealing.	Parameter of β-phase.
A. 79.....	45 hrs. 500° C.	2 hrs. 500° C.	—
A. 73.....	45 hrs. 500° C.	2 hrs. 500° C.	7·0518 Å.
A. 66.....	24 hrs. 500° C.	2 hrs. 500° C.	7·0517 Å.
		Mean	7·0518 Å. ± ·0004 Å.
A. 79.....	45 hrs. 500° C.	3 hrs. 500° C. & 24 hrs. 380° C.	7·0341 Å.
A. 73.....	45 hrs. 500° C.	2 hrs. 500° C. & 24 hrs. 380° C.	7·0345 Å.
A. 66.....	24 hrs. 500° C.	2 hrs. 500° C. & 25 hrs. 380° C.	7·0343 Å.
		Mean	7·0343 Å. ± ·0004 Å.

TABLE III.

Summary of Results.

Temperature.	$(\alpha+\beta)$ region.		$(\beta+\gamma)$ region.
	Parameter of α-phase.	Parameter of β-phase.	Parameter of β-phase.
600° C.	3·6367 Å.	7·0087 Å.	—
500° C.	3·6263 Å.	7·0133 Å.	7·0518 Å.
400° C.	3·6176 Å.	7·0185 Å.	7·037 Å. (interpolated)
380° C.	—	—	7·0343 Å.

The results of Tables I. and II. have been arranged in Table III. in a form more convenient for examination. Table III. gives the values obtained for the saturation parameters of the β-phase both in the $(\alpha+\beta)$ and $(\beta+\gamma)$

regions : it also shows the values of the saturation parameters of the α-phase for various temperatures.

The differences between the parameters of the β-phase for the $(\alpha+\beta)$ and $(\beta+\gamma)$ regions are seen to be of the order 0·02 Å., while the accuracy of the determination is of the order 0·0004 Å. The existence of a homogeneity range for this phase has thus been confirmed. Moreover, the variations in the parameter with change of temperature for both the regions show that it extends on both sides of the composition Cu_2Mg, and that its extent varies with temperature rather considerably. We see that, if the variation of the parameter in the pure β-phase region is strictly linear, the extent of the range at 500° C. is more than double that at 400° C. It was hoped, originally, to determine definitely the saturation compositions at the various temperatures, but, since this entails an examination of alloys within the homogeneity range itself, it was finally considered impracticable for the reasons already given in the introduction. We can, however, obtain some idea of the composition limits if the results of Dr. W. R. D. Jones are taken into account. He found that alloys containing 82·64 per cent. Cu and 84·27 per cent. Cu exhibited, after annealing at 500° C., the presence of eutectic as well as compound on microscopic examination, while an alloy containing 83·20 per cent. Cu showed no definite eutectic. These observations are consistent with the existence of a homogeneity range lying wholly within the compositions 84·27 per cent. Cu, and 82·64 per cent. Cu, and, therefore, of smaller extent than was suggested by Grime and Morris-Jones, who gave "2 or 3 per cent. on either side of the Cu_2Mg composition." The observed microstructure of the alloy 83·20 per cent. Cu indicates that the range extends to at least 0·74 per cent. (83·94 per cent. to 83·20 per cent.) to the right of the compound Cu_2Mg (83·94 per cent. Cu). Taking Dr. Jones's results into consideration, we therefore conclude that the extent of the range at 500° C. is not more than 1·63 per cent. (84·27 per cent. to 82·64 per cent.), while at lower temperatures it is considerably less.

The variation with temperature in the value of the saturation parameter of the α-phase observed in the present investigation shows that here also there is a marked variation of saturation composition with temperature.

A complete determination of this boundary, however, necessitates an investigation into the variation of the α-phase parameter with composition in the pure phase region. This has not yet been undertaken.

In conclusion, I wish to thank Prof. W. R. D. Jones for kindly placing at my disposal the alloy specimens. I am also indebted to Prof. R. T. Dunbar for his constant interest and advice.

List of References.

(1) Grime & Morris-Jones, Phil. Mag. (7) vii. p. 1113 (1929).
(2) Runqvist, Arnfelt, & Westgren, *Z. Anorg. Chem.* clxxv. p. 43 (1928).
(3) Sahmen, *Z. Anorg. Chem.* lvii. p. 1 (1908).
(4) Urazov, *J. Soc. phys.-chem. russe*, (9) xxxix. p. 1566 (1907).
(5) Stepanov, *J. Soc. phys.-chem. russe*, xli. p. 1383 (1909).
(6) Jones, J. Inst. Met. xlvi. p. 395 (1931).
(7) Bradley & Jay, Proc. Phys. Soc. xliv. p. 563 (1932).
(8) Owen & Pickup, Proc. Roy. Soc. A, cxxxvii. p. 397; cxxxix. p. 526.

Viriamu Jones Research Laboratory,
University College, Cardiff.
June 4, 1934.

XXX. *Photographic Time Registration on a Falling Plate in an Experimental Determination of "g."* *By* E. Langton, *B.Sc., and* E. Tyler, *D.Sc., M.Sc., F.Inst.P., Physics Department, Leicester College of Technology* *.

[Plates VI. & VII.]

Introduction.

WHEN a photographic plate is allowed to fall past a small aperture through which passes light interrupted at a definite frequency development of the plate produces a broken straight line trace consisting of portions (dots), whose lengths depend on the speed of the plate and the time for which the light persists at a single flash, while the spacing of the dots depends in addition on the time interval between the flashes. Thus, as the plate is accelerating the lengths of the dots and the spaces between them increase, and if the time interval

* Communicated by the Authors.

between the beginnings of successive flashes of light is known (*i. e.*, if the frequency of flashing is known) measurement of the distances between successive dots (either upper or lower edge) will enable "g," the acceleration due to gravity, to be calculated.

For accurate evaluation it is preferable to use the expression

$$g=\frac{N^2}{n^2}.(S_2-S_1),$$

where N is the number of flashes per second made by the light falling on the plate, while S_1 is the distance between, say, the lower edges of the first and the $(n+1)$th dots, and S_2 the distance between the lower edges of the $(n+1)$th and $(2n+1)$th; so that S_1 and S_2 are the distances fallen by the plate in successive equal intervals of time $\frac{n}{N}$ secs.

In a previous article * an experiment for deducing "g" was described utilizing this theoretical relationship.

In this method the light produced by a glowing filament "auto" lamp is interrupted by a rotating slotted disk driven at constant speed by an electric motor, the speed of which was adjusted by personal control and measured by a stroboscopic Neon-tube method, using as time standard the frequency of the A.C. mains supply operating the Neon tube.

It was pointed out that greater precision would be obtained if the frequency of the interruption of light falling on the plate were directly controlled by the A.C. supply frequency. Two methods were suggested: (1) the slotted disk acting as the interrupter could be rotated by a synchronous motor whose constant speed would bear a simple relation to the mains frequency, (2) the light falling on the plate could be that produced by an "Osglim" Neon lamp operating from the A.C. mains, and therefore flashing 2N times per second, N being the mains frequency under normal conditions of lamp glow.

The present article describes experiments on both of these methods with computation of "g," and includes details of modifications of the apparatus which make

* Tyler and Langton, 'School Science Review,' xv. (Dec. 1933).

certain the production of straight traces. In addition results are given of a time-base device, employing the flashing "Osglim," operated by a valve oscillator whose frequency is tuned to that of a standard tuning-fork. Certain aspects of the glow condition of the Osglim are also considered.

Experimental Details and Results using Synchronous Motor and Slotted Disk.

In the earlier work the photographic plate was held in contact with a vertical board by a spring clamp,

Fig. 1.

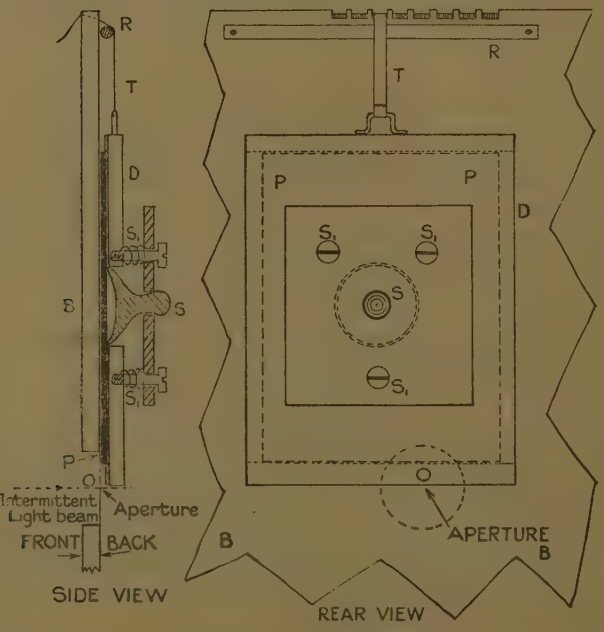

release of which allowed the plate to fall past the aperture. The traces obtained were not always straight, owing to the lightness of the plate and the form of the clamp.

For the series of experiments here described a special holder was designed, and is illustrated in fig. 1.

The plate P is held with its back surface in contact with the metal plate D by the combined action of the rubber " sucker " S and the springs S_1. It is undesirable to use clips for holding the plate, as the front surface of the latter must be as near as possible to the vertical board. In the vertical position the plate is held supported by a tape T, such that its sensitive side is just clear of the front of the board and also with its lower edge a short distance (1 or 2 cm.) above the pin-hole aperture O.

The function of the tape is to permit the plate to take up an initial position of equilibrium with its centre of gravity vertically below the point of support, so that on releasing rotation in a vertical plane is not produced. Tape is preferable to thread, since it resists twisting and assures that the plate in its initial position has its face parallel to the vertical board B. The tape passes over a round rod R, which serves as a distance piece, and then through a slot in the top of the board, where it is held by finger pressure until ready for release. A series of such equally spaced slots enables a number of traces to be obtained on a single plate by dropping the plate and holder successively with the tape in each of the slots. The shortest possible length of tape is used, so that there is no interference with the free fall of the plate-holder by the time it passes the illuminated aperture. Provision could easily be made for mechanical clamping of the tape, but this was considered undesirable in these tests.

The additional procedure is precisely the same as that in the former experiment, except that a synchronous motor * (8 teeth), operated from the A.C. mains at 50 cycles/sec., is employed to drive the slotted disk at constant speed, the latter interrupting the light beam emitted from a 36 watt "auto-lamp." Using a disk with 24 equally spaced radial slots a flashing frequency of 300 per second is obtainable. Typical sets of traces for this flashing frequency is shown in Pl. VI. fig. 1, and specimen observations and results incorporated in Table I.

* Supplied by Messrs. Gent and Co., Leicester.

TABLE I.

Synchronous Motor. Slotted Disk Results.
Typical readings: Fig. 1, Trace 3, Pl. VI.
N=300 per sec.

Number of dot.	Microscope readings. For S_1. cm.	Microscope readings. For S_2. cm.	Differences ($n=12$). S_1. cm.	Differences ($n=12$). S_2. cm.	S_2-S_1. cm.
	(A).				
1.....	·035				
2.....	·268				
3.....	·521				
4.....	·772				
		(B).	(A).	(B).	
13.....	3·575	·037	3·540	5·099	1·559*
14.....	3·937	·399	3·669	5·229	1·560
15.....	4·301	·763	3·780	5·389	1·609
16.....	4·686	1·148	3·914	5·494	1·580
25.....	..	5·136			
26.....	..	5·628			
27.....	..	6·152			
28.....	..	6·642			

* These variations are due to irregularities in the spacings of the slots in the disk. A machine-cut disk is preferable.

Mean value of $S_2-S_1=1{\cdot}577$ cm.,

giving
$$g=\frac{300^2}{12^2}\times 1{\cdot}577$$
$$=986 \text{ cm./sec.}^2.$$

Average values for other traces, Pl. VI. fig. 1; (24 independent values)

1·578, 1·563, 1·593, 1·570, 1·577 cm.

Mean value=1·576 cm.,

giving $g=985$ cm./sec.^{2}.

Method and Results using Flashing Neon Tube as Time Base. A.C. Mains Controlled.

It appears that the light from a "Beehive" Osglim fitted with cap resistance and working direct from the A.C. supply mains at 200 volts is not sufficiently actinic to produce measurable effects with ordinary plates, but much better photographic registration is obtained using either panchromatic or red sensitive plates.

Since the original object was to produce traces sufficiently well defined (as regards the lower edges of the dots) for accurate microscopic measurement of the spacings, certain modifications in procedure were adopted, the results of which follow with discussion bearing thereon, and provide interesting information, particularly from the dot formation. Fig. 3 (Pl. VII.) shows sets of traces

TABLE II.

Flashing Neon, A.C. Mains Controlled Results.
(At 50 cycles/sec. and 200 volts.)
N=100/sec., fig. 5 (Pl. VII.).

Number of trace.	Average microscope readings.		Differences (n=4).		
	For S_1. cm.	For S_2. cm.	S_1. cm.	S_2. cm.	S_2-S_1. cm.
	Number of dot.	Number of dot.			
1.....	(3) 8·215 (7) 4·352	(7) 7·680 (11) 2·238	3·863	5·442	1·579
2.....	(1) 9·039 (5) 5·729	(5) 9·024 (9) 4·150	3·310	4·874	1·564
3.....	(2) 8·736 (6) 5·201	(6) 7·851 (10) 3·735	3·535	5·116	1·581

(The number of the dot is indicated by the figure in the bracket.)
Mean value of S_2-S_1=1·574 cm.,

giving $$g=\frac{100^2}{4^2}\times 1{\cdot}574=984 \text{ cm./sec.}^2.$$

obtained using the "Beehive" glow from an ordinary Osglim lamp and operating direct from the A.C. 200 volt mains, the cap resistance of the lamp as fitted by the makers still being intact and in series with the lamp.

It will be observed the alternate dots differ in intensity because of the asymmetry of the discharge, the greater intensity occurring when the glow fills the spiral (*i. e.*, the spiral is negative). The lower edges of the dots corresponding to the "ignition glow" are more sharply

defined than the upper corresponding to the "extinction glow," thus indicating that the illumination from the discharge builds up more suddenly than it dies away. The actual intensity of the lamp glow will depend on the current consumption of the lamp, this being much greater

TABLE III.

Flashing Neon Results. A.C. and D.C. voltage superposed. Mains A.C. voltage = 200 volts at 50 cycles/sec., D.C. voltage = 100.

Flashing frequency = 50/sec., fig. 6 (Pl. VII.).

Number of trace.	Average microscope readings.		Differences ($n=2$).		
	For S_1. cm.	For S_2. cm.	S_1. cm.	S_2. cm.	S_2-S_1. cm.
	Number of dot. (1) (3)	Number of dot. (3) (5)			
1.....	6·671 3·454	7·758 2·969	3·217	4·789	1·572
2.....	(1) (3) 8·855 5·030	(3) (5) 8·133 2·731	3·825	5·402	1·577
3.....	(1) (3) 7·577 3·693	(3) (5) 7·961 2·500	3·884	5·461	1·575
4.....	(1) (3) 8·670 5·602	(3) (5) 7·186 2·545	3·068	4·641	1·573

Mean value of $S_2-S_1=1{\cdot}574$ cm.,

giving $$g=\frac{50^2}{2^2}\times 1{\cdot}574=984 \text{ cm./sec.}^2.$$

at the ignition or striking voltage than at the extinction voltage. The rate of variation of the light intensity at these critical voltages is thus a function of both lamp current and rate of change of voltage. The definition of the lower edges on A.C. alone, even with the best photographic effects (*i.e.*, intense dots), is not sufficiently good for measurement with the microscope. Measurements are, however, possible if the same lamp is operated from the 200 volt A.C. mains together with a steady

D.C. voltage of, say, 200 volts superposed. Such traces are exhibited in fig. 4 (Pl. VII.).

Very intense dots are obtainable by using the lamp on A.C. 200 volts, with the cap resistance removed, and superposing a steady D.C. voltage of 100 volts. Traces obtained by such an arrangement are shown in figs. 5 and 6 (Pl. VII.) and the corresponding data included in Tables II. and III., together with computed values of "*g*." As an alternative method one could use a higher A.C. voltage, and thus obtain similar effects.

It will be observed from these traces that the dots are much longer and intense (*i. e.*, brighter), and only half the number registered, an effect which is to be expected from a consideration of the striking and extinction voltages of the Osglim, together with a knowledge of the wave-form of the applied A.C. voltage, a fuller interpretation of such being given later.

Method and Results using Flashing Neon controlled by Valve Oscillator.

As an alternative to the foregoing methods, and reverting to the personal adjustment of control, the Osglim is made to flash at any desired frequency over a wide range by transformer coupling it to the plate-circuit of a valve oscillator. Such a device has been employed by one of us * in an evaluation of "*g*" by means of stroboscoping a liquid jet.

A loud-speaker inserted in the Neon lamp circuit serves as a means of ascertaining the flashing frequency of the lamp, the value of which is readily controlled by a variable condenser connected across the transformer windings in the grid circuit of the valve. The note emitted by the loud-speaker is tuned to that of a standardized fork by the beat method. While under this condition and with the Neon illuminating the aperture the plate is dropped past the latter with resulting effects as shown in fig. 2 (Pl. VI.) for a frequency of 256.

The dots in these traces differ somewhat from those of the previous methods, which it to be expected in view of the different wave-form of the voltage output of the oscillator. The dots are sufficiently well defined to permit measurement of the traces with a cathetometer

* Tyler, Phil Mag. (Feb. 1934).

telescope, the results of which are incorporated in Table IV., and show consistency with those obtained by the other methods. Where the effort of manipulation is required on the part of an observer this method is preferable over the two previous, but accuracy of "g" is here dependent on the accuracy of the fork frequency.

TABLE IV.

Flashing Neon. Valve Oscillator Results.

Typical readings: Fig. 2, Trace 4, Pl. VI.

N=256 per sec.

Number of dot.	Microscope readings. For S_1. cm.	Microscope readings. For S_2. cm.	Differences (n=10). S_1. cm.	Differences (n=10). S_2. cm.	S_2-S_1. cm.
	(A).				
1.....	3·055				
2.....	3·290				
3.....	3·540				
4.....	3·807				
5.....	4·087				
		(B).	(A).	(B).	
11.....	6·113	2·464	3·058	4·553	1·495
12.....	6·488	2·861	3·198	4·697	1·499
13.....	6·896	3·258	3·356	4·850	1·494
14.....	7·313	3·676	3·506	5·001	1·495
15.....	7·742	4·112	3·655	5·148	1·493
21.....	..	7·017			
22.....	..	7·558			
23.....	..	8·108			
24.....	..	8·677			
25.....	..	9·260			

Mean value of S_2-S_1=1·495 cm.,

giving $$g=\frac{256^2}{10^2}\times 1{\cdot}495$$

$$=980 \text{ cm./sec.}^2.$$

Average values for other traces, fig. 2, Pl. VI. (24 independent values),

1·495, 1·500. 1·500, 1·496, 1·496, 1·492 cm.

Mean Value=1·496 cm.,

giving g=980 cm./sec.^{2}.

Discussion of Glow Conditions of Neon Lamp under the Experimental Conditions.

As mentioned earlier, the rate of change of "ignition glow" is dependent upon the rate of variation of the applied voltage together with the current strength at this phase of ionization. Since we are only concerned with obtaining well-defined edges of the dots for accurate measurements, and this occurs at the striking voltage, we can confine our attention to this phase of the glow

Fig. 7 (*a*) & (*b*).

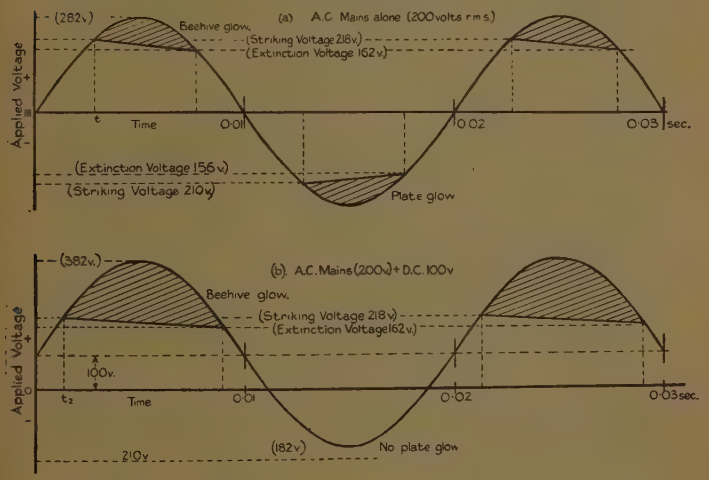

and deal with the Osglim operating without its cap resistance.

The given lamp under a steady applied P.D. glows with "Beehive" illuminated at a striking voltage of 218 volts, and goes out at 162 volts. For reversal of polarity, thus giving "plate glow," the corresponding voltages are 210 and 156 volts respectively.

Representing the wave-form of the applied A.C. voltage by the diagram in fig. 7 (*a*), and inserting the appropriate ignition and extinction voltages (assuming these to remain unchanged), the shaded parts of the loops correspond to the phases of persistence of glow, positive half-cycle

for "Beehive" and negative half-cycle for plate respectively. If, however, we superpose on the 200 volts A.C. a steady D.C. voltage of 100 volts, we obtain the resulting curve shown in fig. 7 (*b*). Such a curve is characteristic of several features consistent with the experimental facts obtained, the following of which are worthy of mention :—(*a*) The shaded area corresponding to the periods of persistence of glow only exist for the beehive glow, thus giving half the number of dots on the photographic plate ; meanwhile the dots corresponding to the plate glow are completely extinguished. (*b*) These same areas are larger with superposed D.C. voltage on A.C. than with A.C. alone, resulting in an increase in the total light emitted during persistence of glow with resulting increase in average intensity of the dots. (*c*) The striking voltage occurs at an earlier stage in the A.C. voltage cycle, whereas the extinction voltage is delayed to a later phase of the cycle ; the time of flash is thus greater, and longer dots are formed on the falling plate. (*d*) The rate of change of the applied voltage is greater at the ignition point in the combined case than with A.C. voltage alone, thereby enhancing the possible formation of dots with more well-defined edges.

Quantitative information substantiating these characteristics may be obtained from a consideration of the wave-form of the applied A.C. voltage in addition to a knowledge of the ignition and extinction voltages of the lamp. Two possible cases arise: (1) effect of increase in A.C. voltage only; (2) effect of superposing D.C. voltage on A.C.

Case 1.—*Effect of increasing A.C. voltage only.*

The curves *a* and *b* shown in fig. 8 correspond to one half-cycle of the applied voltage producing beehive glow, the A.C. voltages being 200 and 250 volts respectively, giving peak values of 282 and 353 volts. Reference to the striking voltage axis indicates that glow begins at an earlier stage in the cycle for the higher applied A.C. voltage. Furthermore, the slope of the higher A.C. curve at the ignition point of the lamp is greater than that for the lower A.C. curve, thus indicating that the greater the applied A.C. voltage the more rapid is the voltage rise. (This is of course obvious from the curves.)

The time of persistence of glow is also longer for the higher A.C. curve, and, in addition, greater areas of the loops between the critical voltages are obtained.

Similar effects in respect of increased brightness and length of the dots are therefore to be expected, to those obtained in the case of A.C. with D.C. voltage superposed. There is one exception, however ; well-defined dots are formed on the photographic plate for both half-cycles of applied A.C. voltage.

Writing the equation for the applied voltage as $E=E_0 \sin wt$. At the striking voltage $E=218$ volts, and the peak voltages for 200 and 250 volts A.C. are such that $E_0=282$ and 353 volts respectively.

Fig. 8.

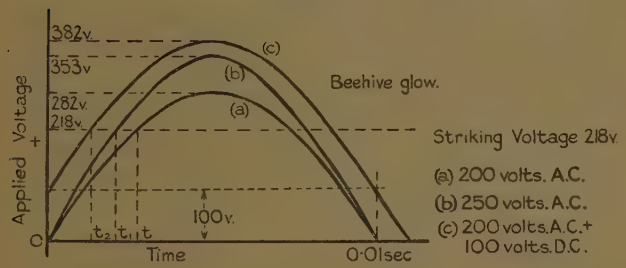

If t and t_1 be the times at which the lamp commences to glow in each case, we have $218=282 \sin w.t$ for the 200 volts A.C. curve, and $218=353 \sin w.t_1$ for the 250 volts A.C. curve. For the A.C. mains operating at 50 cycles/sec. w is 100π.

The values of t and t_1 are therefore obtained from the expressions

$$\sin 100.\pi t = \frac{218}{282} = \cdot 773$$

and

$$\sin 100.\pi t_1 = \frac{218}{353} = \cdot 617.$$

The rise in voltage given as $\frac{dE}{dt} = wE_0 . \cos wt$ thus increases with both rise in mains frequency and applied A.C. voltage. At constant frequency the rate of rise of voltage at lamp ignition is proportional to $E_0 \cos wt$; hence, substituting

numerical values in these two cases under consideration, we obtain the following data :—

(a) *At* 200 *volts A.C. supply.*

$$E_0 = 282 \text{ volts, } \sin wt = \frac{218}{282} = \cdot 773, \cos wt = \cdot 633,$$

whence rise in striking voltage $\propto E_0 \cos wt \propto 282 \times \cdot 633.$
$\propto 178$

(b) *At* 250 *volts A.C. supply.*

$$E_0 = 353 \text{ volts, } \sin wt_1 = \frac{218}{353} = \cdot 617, \cos wt_1 = \cdot 786,$$

whence rise in striking voltage $\propto E_0 \cos w.t_1 \propto 353 \times \cdot 786.$
$\propto 277$

Thus from voltage considerations alone there is an apparent increase in the rate of voltage rise of 55·6 per cent. for an increase of 50 volts A.C. in excess of 200.

Case 2.—*Effect of superposing* 100 *volts D.C. voltage on* 200 *A.C.*

Curve *c* fig. 8 shows the resultant effect of such a combination. The equation of this curve is now given as $E = E_0 \sin wt_2 + E_1$, where E_1 is the applied D.C. voltage of 100 volts.

Again $\frac{dE}{dt} = w.E_0 \cos w.t_2$, and substituting for the applied D.C. voltage, we have $218 = 282 \sin wt_2 + 100$, whereupon $\sin wt_2 = \frac{118}{282} = \cdot 418$, and $\cos wt_2 = \cdot 908$,

whence rise in striking voltage $\propto E_0 \cos w.t_2 \propto 282 \times \cdot 908.$
$\propto 255 \cdot 8$

In this case an apparent increase in the rate of voltage rise of 43·7 per cent. is produced in excess of that for 200 volts A.C. alone. The limiting condition of superposed D.C. voltage on A.C. is obviously when the applied D.C. voltage reaches the striking value of 218 volts, a stage at which the lamp glows continuously.

Although it will be observed that superposed D.C. voltage of 100 volts on 200 A.C. is not so good as the 250 A.C. alone, it has the advantage of eliminating the negative half-cycle due to the plate glow, and hence prevents possible overrunning of the lamp.

The foregoing theory is purely tentative, but its application to the existing experimental conditions is sufficient to account for the observed effects produced without considering the theoretical aspect of the relation between glow and current strength of the lamp. The results obtained for "*g*" by the various methods outlined herein compare favourably with those obtained by other methods involving falling bodies, and the recording of a time base photographically on a falling plate is worthy of recommendation in view of its possible adoption in other directions.

Summary.

As an extension of some earlier work suitable methods of recording a time base on a falling photographic plate in an experimental evaluation of "*g*" are described, employing the use of (*a*) synchronous motor and slotted disk, A.C. mains controlled, (*b*) flashing "Osglim," operated by either the A C mains supply or valve oscillator. Typical traces obtained by each of the methods are included, together with computed values of "*g*."

Certain aspects of the glow condition of the "Osglim" under A.C. and D.C. voltage superposed are also considered, interpreting the photographic effects obtained.

XXXI. *Note on the Electric Arc.* *By* F. H. Newman, *D.Sc., Professor of Physics, University College, Exeter* *.

THE simple theory of normal arcs having cathodes heated by means of an external source, or cathodes of refractory materials which reach a high temperature, is based on the fact that the cathode is at such a high temperature that the thermionic current density is equal to the measured current density, the electron space charge being neutralized by positive ions existing in the neighbourhood of the cathode. Since the mobility of the positive ion is small compared with that of the electron, a relatively small positive ion current suffices to provide

* Communicated by the Author.

the positive space charge, and in the main the current at the cathode is electronic in nature, the positive ions being replenished from the gas or vapour molecules by the ionizing action of the electrons after passing through the cathode fall of potential. Hence the cathode temperature is of such a value that the thermionic current density is equal to that measured.

In the case of the cold cathode or Stolt arc the mechanism of freeing electrons from the cathode is still a subject of diverse opinion. The thermionic theory suggests that the electrons are thermions emitted by the cathode hot spot, but this theory demands that the temperature of the spot shall be high. Unfortunately measurements of the spot temperature are very discordant. For example, from Stark's observation * of a continuous spectrum at the cathode early investigators assumed the mercury cathode temperature to be about 2000° K., whereas Compton † has shown theoretically from the rate of mercury evaporation that the surface temperature of this cathode spot cannot exceed about 200° C. Moreover the author ‡ found that there was little, if any, continuous spectrum at a sodium cathode, and in a 20-ampere copper arc the cathode spot shows only a faint continuous spectrum §, indicating that the cathode temperature is not high.

The high electric field theory of cold arcs was developed originally by Langmuir ‖, who suggested that the positive space charge causing the cathode drop may exert a strong enough field at the cathode surface to cause a large field current from the electrode, even though the latter may be too cool to emit thermions. Compton ¶ has further developed this idea, and from energy considerations suggests that in the mercury arc the electrons emanating from the cathode are due primarily to a high electric field, and not to thermal emission. Numerous writers on this cold emission have mentioned that such electron currents, drawn from cold cathodes by extremely high electric fields of the order of 10^7 volts per cm., are much larger than is expected on the wave-mechanical calculation

* *Ann. d. Phys.* xii. p. 692 (1903).
† Phys. Rev. xxxvii. p. 1077 (1931).
‡ Phil. Mag. xiv. p. 718 (1932).
§ See Tanberg and Berkey, Phys. Rev. xxxvii. p. 1679 (1931).
‖ Gen. Elec. Rev. xxvi. p. 734 (1923).
¶ Jour. Amer. Inst. Elec. Eng. xlvi. p. 1192 (1927).

by Fowler and Nordheim*. To account for this it is usually assumed that there are submicroscopic sharp points on the cathode at which the field is much more intense than the average value in the vicinity. In connexion with this effect Bennett† has shown that this is not the only factor to be considered, and that if the emitted electrons can strike glass, substances which are removed from such a target can be ionized and then move back along the electron stream. They are deposited on the cathode surface and reduce the work-function of the cathode, so that much larger currents than those calculated for a clear surface are obtained in practice. Hence the emission is apt to be characteristic of a contaminated surface.

It has been shown by Mason‡ from the quantum theory of electron emission from a cold surface under the action of a sufficiently high field that, so long as the production mechanism of positive ions is similar in the hot and cold cathode arcs and that mechanism depends upon electron energy, the arc produced by a high field must have a cathode fall several volts greater than a thermionic arc. He has calculated that if the positive ion current is greater than 10^3 amperes per sq. cm. an equal electron current will consist of electrons of energies less than the cathode fall by an amount exceeding 3 volts in the case of mercury, so that the cathode fall must be greater than 13·4 volts if ions are to be produced at a single impact. The measured fall is only about 10 volts, and the author§ has shown that with a sodium cathode the fall is approximately equal to the ionization potential of sodium vapour, viz., 5·1 volts. It must be remembered, however, that many examples have been found in practice where there is an abnormally low cathode fall; for example, Compton‖ noted a cathode fall of 5·5 volts in the low voltage mercury arc with thermionic current, such a low value being accounted for by supposing that the positive ions are produced by cumulative ionization. Mason's reasoning does not preclude, therefore, the existence of the high field action.

* Proc. Roy. Soc. A, cxix. p. 173 (1928).
† Phys. Rev. xliv. p. 859 (1933).
‡ *Ibid.* xxxviii. p. 427 (1931).
§ Phil. Mag. xv. p. 601 (1933).
‖ Trans. Amer. Inst. Elect. Eng. xlvi. p. 868 (1927).

The cold cathode arc with different metals investigated by the author * shows the existence of cathode spots. With iron and tungsten electrodes there is evidence that these spots arise at submicroscopic points on the cathode surface—probably impurities—since it is very difficult to start the arc with pure metal electrodes or if the electrode surface is covered with an oxide film which completely masks these active points. Electrons are freed from the latter and produce ionization which is localized near the spots. Due to the high mobilities of the electrons a dense positive space charge results which increases the electric field near the active spots, and consequently the number of electrons emitted therefrom. This process is cumulative, and proceeds rapidly until the field at the spot increases sufficiently to produce field electrons from the cathode due to the high electric field, and an arc results. Such is the process on the field theory. On the other hand, if ordinary thermionic emission occurs, these active spots must develop a high temperature, and the electron emission is due entirely to this temperature. It is certain that the metal in the immediate neighbourhood of the active spots, if the latter are at very high temperatures, is comparatively cold, since in experiments the cathode temperature rises slowly, and spectroscopic examination shows no trace of volatilization of the more refractory metals. Even with sodium, potassium, and mercury there is little volatilization. Although this does not preclude high temperatures of the active spots, the high field theory with lowered work function due to the impurities may also hold.

The starting of an arc under conditions where the electrodes are separated and a momentary electrical discharge is passed probably occurs in the following manner. When the high tension (electrical discharge) is suddenly applied, the bombardment of the cathode active spots by the positive ions results in thermionic emission therefrom. Ionization occurs in the cathode fall space with the high applied field, and the positive ions form a dense positive space charge which produces the requisite electric field for cold emission. This does not preclude some thermionic emission from the active spots.

* Phil. Mag. ii. p. 796 (1926); vi. pp. 807 & 811 (1928); vii. p. 1085 (1929); xiv. pp. 712 & 718 (1932).

XXXII. *The Influence of Electric Waves on the Ionosphere.* *By* V. A. Bailey, *M.A., D.Phil., Associate Professor of Physics, University of Sydney, and* D. F. Martyn, *Ph.D., Research Physicist, Commonwealth Radio Research Board* *.

1. *Introduction.*

In current investigations of the passage of radio waves through the ionosphere it is generally assumed that the mean velocity of agitation u and the collision frequency ν of the electrons are independent of the intensity of the waves. That these assumptions may be notably in error will be shown in the following investigation of the disturbances in the ionosphere produced by electric waves. This analysis applies the methods and results of Townsend and his associates concerning the motions of electrons in gases. From the same analysis a number of interesting consequences emerge, which bear on the phenomenon recently observed by Tellegen †, whereby there appeared to be an interaction of radio waves in the ionosphere.

Recently a considerable amount of evidence has been obtained which shows that some correlation exists between the ionization density in the ionosphere and the prevalence of thunderstorms ‡, in the lower atmosphere. Various possible explanations of this connexion have been examined, but so far no consideration seems to have been given to the radiation field from the lightning flashes. It will appear from the analysis that the effect of this field cannot be neglected.

2. *Average Work done, over a Mean Free Path, by an Alternating Electric Force acting on an Electron in a Magnetic Field.*

We choose a right-handed system of axes such that the x-axis is parallel to the electric force E, and the magnetic force H lies in the xz-plane.

The component of H which is parallel to E has no effect on the motion in that direction, and so does not enter

* Communicated by Prof. J. S. Townsend, M.A., F.R.S.

† 'Nature,' cxxxi. p. 840 (1933).

‡ Appleton and Naismith, Proc. Phys. Soc. xlv. p. 389 (1933); Watson Watt, Proc. Roy. Soc. A, cxli. p. 715 D (1933).

into the energy-relations. Thus only the effect of H_p, the component perpendicular to E, need be considered.

Let

$E=A \sin pt$ (e.m.u.).

$Z=$root mean square of $E=A\sqrt{2}$.

$\tau=$free time, *i. e.*, the interval of time between two given successive collisions of an electron.

$\delta/p=$the time at which the first collision occurs.

$e=$the charge on an electron,

$\rho=e/m$, the specific charge of an electron in e.m.u., $=1{\cdot}77\times10^7$.

$\omega=H_p\rho=H_pe/m$.

$U=\dot{x}$.

$V=\dot{y}$.

$\nu=$number of collisions per second made by an electron.

In the interval $t=\delta/p$ to $t=\tau+\delta/p$ the equations of motion of the electron are

$$\dot{U}=\rho E+\omega V, \quad . \quad . \quad . \quad . \quad . \quad . \quad (1)$$

$$\dot{V}=-\omega U. \quad . \quad . \quad . \quad . \quad . \quad . \quad . \quad (2)$$

Therefore

$$\ddot{U}+\omega^2U=\rho Ap\cos pt. \quad . \quad . \quad . \quad . \quad . \quad (3)$$

Thus the complete solution of the system (1) and (2) is

$$\left.\begin{aligned} U&=B\cos pt+b\cos\omega t+c\sin\omega t,\\ V&=-C\sin pt-b\sin\omega t+c\cos\omega t,\end{aligned}\right\} \quad . \quad . \quad (4)$$

where

$$B=\frac{\rho Ap}{\omega^2-p^2} \quad \text{and} \quad C=\frac{\rho A\omega}{\omega^2-p^2}.$$

The initial velocities U_0, V_0 occur at time $t=\delta/p$, and so

$$\left.\begin{aligned} U_0-B\cos\delta&=b\cos(\delta\omega/p)+c\sin(\delta\omega/p),\\ V_0+C\sin\delta&=-b\sin(\delta\omega/p)+c\cos(\delta\omega/p),\end{aligned}\right\} \quad . \quad (5)$$

The work done on the electron in the free time τ is, therefore,

$$w_\tau=\int_{\delta/p}^{\tau+\delta/p} EeU\,dt=\phi(\tau)-\phi(0), \quad \text{say}, \quad . \quad (6)$$

where

$$\phi(\tau) = \int^{\tau+\delta/p} Ae \sin pt(B \cos pt + b \cos \omega t + c \sin \omega t)\, dt$$

$$= -\frac{AeB}{4p} \cos 2p(\tau + \delta/p) + Ae\psi(\tau) \quad . \quad . \quad . \quad . \quad . \quad . \quad (7)$$

and

$$\psi(\tau) = \frac{1}{2}\int^{\tau+\delta/p} \{b(\sin \overline{p-\omega}.t + \sin \overline{p+\omega}.t) + c(\cos \overline{p-\omega}.t - \cos \overline{p+\omega}.t)\}\, dt$$

$$= \frac{1}{2}\left[-\frac{b \cos \overline{p-\omega}.t}{\overline{p-\omega}} - \frac{b \cos \overline{p+\omega}.t}{\overline{p+\omega}} + \frac{c \sin \overline{p-\omega}.t}{\overline{p-\omega}} - \frac{c \sin \overline{p+\omega}.t}{\overline{p+\omega}}\right]^{\tau+\delta/p}$$

$$= (p^2-\omega^2)^{-1}[p \cos \overline{p\tau+\delta} \times (-b \cos \overline{\omega\tau+\delta\omega/p} - c \sin \overline{\omega\tau+\delta\omega/p}) + \omega \sin \overline{p\tau+\delta} \times (-b \sin \overline{\omega\tau+\delta\omega/p} + c \cos \overline{\omega\tau+\delta\omega/p})]$$

$$= (p^2-\omega^2)^{-1}[p \cos \overline{p\tau+\delta} \times \{-(U_0 - B \cos \delta) \cos \omega\tau - (V_0 + C \sin \delta) \sin \omega\tau\} + \omega \sin \overline{p\tau+\delta} \times \{(V_0 + C \sin \delta) \cos \omega\tau - (U_0 - B \cos \delta) \sin \omega\tau\}] \quad (8)$$

on using (5) at the last transformation.

The time $t = \delta/p$ of the beginning of a free path may occur with equal probability at any part of the period of oscillation $2\pi/p$ of the electric force E.

Thus, of all the free paths having the same free time τ, the fraction whose beginnings lie in the interval of time δ/p to $(\delta + d\delta)/p$ is $d\delta/2\pi$. The average value of w_τ is, therefore,

$$\bar{w}_\tau = \frac{1}{2\pi}\int_0^{2\pi} w_\tau\, d\delta$$

$$= \frac{Ae}{2\pi}\left[\int_0^{2\pi} \psi(\tau)\, d\delta - \int_0^{2\pi} \psi(0)\, d\delta\right] \quad . \quad . \quad (9)$$

by (6) and (7).

But from (8) we find that

$$\int_0^{2\pi} \psi(\tau)\, d\delta = (p^2-\omega^2)^{-1} \times \left[B(p\cos p\tau\cos\omega\tau + \omega\sin p\tau\sin\omega\tau)\int_0^{2\pi} \cos^2\delta\, d\delta + C(p\sin p\tau\sin\omega\tau + \omega\cos p\tau\cos\omega\tau)\int_0^{2\pi} \sin^2\delta\, d\delta \right],$$

all other terms vanishing,

$$= -\frac{\pi\rho A}{(\omega^2-p^2)^2}[(p^2+\omega^2)\cos p\tau\cos\omega\tau + 2p\omega\sin p\tau\sin\omega\tau],$$

$$= -\frac{\pi\rho A}{2}\left[\frac{\cos\overline{p-\omega}.\tau}{(p-\omega)^2} + \frac{\cos\overline{p+\omega}.\tau}{(p+\omega)^2}\right].$$

So (9) becomes

$$\overline{w}_\tau = \tfrac{1}{4}\rho e A^2\left[\frac{1-\cos\overline{p-\omega}.\tau}{(p-\omega)^2} + \frac{1-\cos\overline{p+\omega}.\tau}{(p+\omega)^2}\right].$$

Since the number of free paths which have free times lying between τ and $\tau+d\tau$ is the fraction $e^{-\nu\tau}d(\nu\tau)$ of all the free paths, the average $\overline{w}$ done over a mean free path is

$$\overline{w} = \int_0^\infty \overline{w}_\tau e^{-\nu\tau}\, d\tau = \frac{1}{2}\left(\frac{Z^2e^2}{m}\right)\left[\frac{1}{\nu^2+(p-\omega)^2} + \frac{1}{\nu^2+(p+\omega)^2}\right].$$

In the above theory it has been tacitly assumed that the electrons have no velocity distribution. If a Maxwellian distribution be adopted, this will introduce into the last formula a factor approximately equal to 0·815 when $p+\omega$ is small compared with ν. We may, without much error, introduce this factor quite generally, and so we have

$$\overline{w} = 0{\cdot}815\left(\frac{Z^2e^2}{m}\right)\frac{1}{2}\left[\frac{1}{\nu^2+(p-\omega)^2} + \frac{1}{\nu^2+(p+\omega)^2}\right]. \quad (10)$$

3. *Determination of the Velocity of Agitation and the Collision Frequency.*

Let u=mean velocity of agitation of an electron.

L=mean free path of an electron in the gas at 1 mm. pressure.

P=pressure of the gas in mm. of Hg.

l=mean free path of an electron at the pressure P.

g=proportion of its own energy lost by an electron at a collision.

In general the quantities L, l, and g will be functions of u. Their values for different values of u are given for many different gases by the researches of Townsend and Bailey and their associates.

We now apply the principle of the conservation of energy to the motion of an electron during a small interval of time dt. The number of collisions or of free paths occurring in the interval dt is $\nu\,dt$, so, in the same interval,

the work done by the field $=\bar{w}\nu\,dt$,
the loss of energy in collisions $=g(\frac{1}{2}mu^2)\nu\,dt$,
the increase of kinetic energy $=d(\frac{1}{2}mu^2)$.

Therefore

$$mu\dot{u}+g(\tfrac{1}{2}mu^2)\nu=\bar{w}\nu. \quad . \quad . \quad . \quad . \quad . \quad (11)$$

But $u=lv$ and $l=\mathrm{L}/p$; so by eliminating ν and u in turn from (11) we can obtain the equations for determining u and ν respectively.

It is more convenient, however, to determine u and ν from the quantity n, defined as follows:

$$n=\nu/\mathrm{P}=u/\mathrm{L},$$

i. e., n is the collision frequency for a gas-pressure of 1 mm.

From (11) we thus obtain the following equation for determining n:

$$\frac{1}{\mathrm{P}}\left(1+\frac{n}{\mathrm{L}}\frac{d\mathrm{L}}{dn}\right)\frac{dn}{dt}+\tfrac{1}{2}gn^2=\frac{\bar{w}}{m\mathrm{L}^2}.$$

For a given gas n depends on u alone, so g and L may be regarded as functions of n alone. If the gas be air it is known from the observations of Townsend and Tizard* that L does not change very rapidly with u, and as the present discussion will be concerned with air alone, we may here accordingly set $d\mathrm{L}/dn=0$ in the last equation.

On substituting the expression for $\bar{w}$ given by (10), and replacing ν by $n\mathrm{P}$, the equation for n finally takes this form:

$$\frac{dn}{d\theta}+\tfrac{1}{2}gn^2=\tfrac{1}{2}a\zeta^2\left[\frac{1}{n^2+(q-r)^2}+\frac{1}{n^2+(q+r)^2}\right], \quad (12)$$

* See Table I.

where $\theta=Pt$, $\zeta=Z/P$, $a=0{\cdot}81\rho^2/L^2$,
$q=p/P$, $r=w/P$, $n=\nu/P$.

If the initial value of n is specified, this equation gives the value at any later time t, and the corresponding values of u and ν are then easily obtained.

4. *The Steady State.*

Corresponding to $\zeta=\zeta_0$, a constant, let n_0, g_0, u_0, and ν_0 be the steady values of n, g, u, and ν respectively. From (12) we then have

$$\tfrac{1}{2}g_0{n_0}^2=\tfrac{1}{2}a{\zeta_0}^2\left[\frac{1}{{n_0}^3+(q-r)^2}+\frac{1}{{n_0}^2+(q+r)^2}\right]. \quad (13)$$

Values of L_0 and g_0 in terms of u_0, as determined by means of the observations of Townsend and Tizard * on air, are given in the table.

$u_0\times10^{-6}$	18·5	27	38	54
$L_0\times10^{2}$	3·22	3·37	3·30	3·28
$g_0\times10^{4}$	18	26	26	26
$n_0\times10^{-8}$	5·75	8·0	11·5	15·5

u_0 in cm./sec., L_0 in cm.

The values of $n_0(=u_0/L_0)$ are shown in the last row of the table.

No values of L_0 and g_0 corresponding to values of u_0 lower than $18{\cdot}5\times10^6$ are available, and, as such will be needed later, we can make approximate estimates of them as follows.

Pidduck † has given a theory of the motions of electrons in a gas which assigns a coefficient of elasticity f to the collisions between electrons and molecules, and which regards f as variable with the velocity of collision u.

From his theory the following relation can be derived :

$$g_0=C(f^{-1}-1)+C(f^{-1}-k^{-1})m\mathrm{M}^{-1},$$

where m is the mass of an electron, M the mass of a molecule, k is the ratio of their respective mean energies of agitation, and C is a constant.

* J. S. Townsend and H. T. Tizard, Proc. Roy. Soc. A, lxxxviii. p. 336 (1913). See also J. S. Townsend, 'Motion of Electrons in Gases,' p. 32 (Clarendon Press).

† F. B. Pidduck, Proc. Lond. Math. Soc. ser. 2, xv. pt. 2, p. 89 (1915).

By means of this formula it is found that for the smaller velocities f is nearly constant and is about 0·99895. The above table also shows that L_0 is nearly constant at about the value $3{\cdot}3\times10^{-2}$ for the smaller velocities. We may thus suppose, without serious error, that f and L_0 are constant for values of u_0 less than $18{\cdot}5\times10^6$. The following relation can then easily be derived from the previous one :

$$g_0=G\left(1-\frac{n_1^2}{n_0^2}\right), \quad . \quad . \quad . \quad . \quad . \quad (14)$$

where G and n_1 are constants.

G is the value of g when n_0/n_1 is large, so from the table we conclude that $G\doteq26\times10^{-4}$. Also since $g_0=18\times10^{-4}$ when $n_0=5{\cdot}75\times10^8$, we find that $n_1\doteq3{\cdot}2\times10^8$; hence $u_0\doteq10{\cdot}6\times10^6$ when $g_0=0$, *i. e.*, in the absence of an electric field.

So for a given value of ζ_0 the lower values of n_0 and g_0 can be determined by means of (13) and (14).

5. *Effects produced by a Modulated Wave.*

We now consider the effects produced when $Z=Z_0(1+s)$ with $s=M\sin ft$ and $M<1$, $f<<p$.

Hence

$$\zeta=\zeta_0(1+s) \quad \text{and} \quad n=n_0(1+\sigma),$$

where σ is a function of t to be determined.

If M be sufficiently small, or if f be sufficiently large, then n will not vary much, *i. e.*, we will have

$$|\sigma|<<1.$$

When such is the case, since g is a function $g(n)$ of n, we must have

$$g=g(n)=g(n_0+n_0\sigma)=g(n_0)+n_0\sigma g(n_0),$$

by Taylor's Theorem, *i. e.*,

$$g=g_0(1+K\sigma),$$

where

$$g_0=g(n_0) \quad \text{and} \quad K=\left(\frac{n_0}{g_0}\right)\frac{dg_0}{dn_0}.$$

We can now, on substituting for n, g, and ζ in (12), and subtracting from its two sides the corresponding sides

of equation (13), neglect the terms containing powers of σ higher than the first. This leads to the following equation:

$$\frac{d\sigma}{d\theta}+\beta b_0\sigma=b_0(s+\tfrac{1}{2}s^2), \quad . \quad . \quad . \quad . \quad (15)$$

where

$$b_0=g_0n_0, \quad \beta=1+\tfrac{1}{2}\mathrm{K}+(1+s)^2\chi,$$

and

$$\chi=\frac{n_0^2[(n_0^2+\overline{q-r}^2)^{-2}+(n_0^2+\overline{q+r}^2)^{-2}]}{[(n_0^2+\overline{q-r}^2)^{-1}+(n_0^2+\overline{q+r}^2)^{-1}]}.$$

The principal application of these calculations is to situations in which $p\neq\omega$ and $\nu<<|p-\omega|$, i.e., $q\neq r$ and $n>>|q-r|$.

Accordingly, in place of (12) and (13) we may adopt the following as sufficiently close approximations:

$$\frac{dn}{d\theta}+\tfrac{1}{2}gn^2=a\zeta^2\mathrm{Q} \quad . \quad . \quad . \quad . \quad . \quad (16)$$

and

$$\tfrac{1}{2}g_0n_0^2=a\zeta_0^2\mathrm{Q}, \quad . \quad . \quad . \quad . \quad . \quad (17)$$

where

$$\mathrm{Q}=(q^2+r^2)/(q^2-r^2)^2,$$

and in (15) we will have $\chi\doteq 0$, *i. e.*,

$$b_0=g_0n_0, \quad \beta=1+\tfrac{1}{2}\mathrm{K}. \quad . \quad . \quad . \quad (18)$$

If we neglect the harmonic $\frac{1}{2}s^2$, in comparison with the fundamental s, (15) then becomes

$$\frac{d\sigma}{dt}+\mathrm{R}\sigma=\mathrm{SM}\sin ft, \quad . \quad . \quad . \quad . \quad . \quad (19)$$

where

$$\mathrm{R}=(1+\tfrac{1}{2}\mathrm{K})g_0\nu_0 \quad \text{and} \quad \mathrm{S}=g_0\nu_0. \quad . \quad (20)$$

Therefore

$$\sigma=\mu\sin(ft-\phi)+\mathrm{A}^{-\mathrm{R}t}, \quad . \quad . \quad . \quad (21)$$

where A is an arbitrary constant, $\tan\phi=f/\mathrm{R}$, and

$$\mu=\frac{\mathrm{SM}}{\sqrt{f^2+\mathrm{R}^2}}. \quad . \quad . \quad . \quad . \quad (22)$$

By means of (14) and (17) we can now examine how μ depends on the mean electric force Z_0.

Thus (dropping the subscript in Z_0),

$$\nu_0=\sqrt{\nu_1^2+b\mathrm{Q}\mathrm{Z}^2}, \quad . \quad . \quad . \quad . \quad . \quad (23)$$

$$g_0\nu_0 = \frac{2aQZ^2}{\sqrt{\nu_1^2+bQZ^2}}, \quad \ldots \quad (24)$$

where

$$a = \cdot 81\rho^2/L^2 \quad \text{and} \quad b = 2a/G.$$

Also

$$K = \frac{n_0}{g_0}\frac{dg_0}{dn_0} = 2\frac{Gn_1^2}{g_0 n_0^2}$$

by (14); therefore,

$$1+\tfrac{1}{2}K = G/g_0,$$

and so by (20) and (23) in succession we have

$$R = G\nu_0 = \sqrt{G^2\nu_1^2+cQZ^2},$$

where

$$c = 2aG.$$

So (22) may be written as

$$\mu = \frac{2aQZ^2M}{\sqrt{\nu_1^2+bQZ^2}\sqrt{f^2+G^2\nu_1^2+cQZ^2}}, \quad \ldots \quad (25)$$

where

$$Q = P^2(p^2+\omega^2)/(p^2-\omega^2)^2 \quad \ldots \quad (26)$$

and

$$2a = 4\cdot 7\times 10^{33}, \qquad b = 1\cdot 8\times 10^{36},$$
$$G = 2\cdot 6\times 10^{-3}, \qquad c = 1\cdot 2\times 10^{31},$$

Z being in volts/cm.

The formula (25) holds for values of Z up to about

$$2\times 10^{-10}\,|\,p^2-\omega^2\,|\,/\sqrt{p^2+\omega^2}.$$

6. *Modulation impressed on a Second Wave.*

We now consider a homogeneous volume of ionized air in which the collision frequency of an electron with the molecule is modulated throughout according to equation (21).

When an electric wave of initial intensity $E_0 = A_0 \sin p_1 t$ traverses this volume of ionized air in a direction nearly transverse to the earth's magnetic field the intensity of the emergent wave will be given by

$$E_1 = E_0 \exp\left(-\int k.ds\right),$$

where, if $p_1^2 >> \nu^2$,

$$k = \nu(1-\mu_0^2)/6\times 10^{10}\mu_0,$$
$$\mu_0^2 = 1-4\pi Ne^2/mp_1^2; \quad \ldots \quad (27)$$

N is the number of electrons per c.c. and s is the length of path in the ionized air.

For an actual wave, which follows a curved trajectory in the ionosphere, the above equation reduces to

$$E_1 = E_0 \exp(-C_0 \nu), \quad . \quad . \quad . \quad . \quad . \quad (28)$$

where C_0 depends on the frequency of the wave, the length of path, and the density and gradient of ionization in the ionosphere.

When the ionized gas has been subjected to the modulating agency for a time sufficient to reduce the term representing decay in equation (21) to a negligible quantity, (28) becomes

$$E_1 = E_0 \exp[-C_0 \nu_0 (1 + u \sin(ft - \phi)]. \quad . \quad (29)$$

It follows that the amplitude of the emergent wave is modulated at the angular frequency f.

Therefore, when $C_0 \nu_0$ is of order unity *,

$$E_1 = E_3 e^{-C_0 \nu_0}(1 + M' \sin ft - \phi), \quad . \quad . \quad . \quad (30)$$

$$M' = C_0 \nu \mu_0 = 4{\cdot}6 \times 10^{16} \frac{(p^2+\omega^2) C_0 \nu_1^2 Z^2 M}{(p^2-\omega^2)^2 \sqrt{f^2 + G^2 \nu_1^2} + cQZ^2}. \quad (31)$$

We thus see that the coefficient of the modulation impressed on the emergent wave is M′, given by the above expression.

7. *Application to the Observations of Tellegen in Radio Transmission.*

Let us consider a radio emitter of radiated power W watts operating on a wave-length in the broadcasting wave-bands ($10^6 < p < 10^7$), and whose carrier-wave is modulated as in section 5 above. This will modulate the velocity of agitation of the electrons in the part of the ionosphere above the emitter to an extent the effect of which we now proceed to examine.

If the emitting aerial behaves as a Hertzian dipole then we have

$$Z = 0{\cdot}95 \times 10^{-4} \sqrt{W} (\sin i)/r, \quad . \quad . \quad . \quad (32)$$

where Z is the field-intensity at a point on the under-surface of the ionosphere distant r km. from the emitter

* See footnote †, p. 379.

and i is the angle of incidence of the wave on the surface of the ionosphere at this point.

It is easy to show that the maximum value of Z occurs when $i=45°$, so if we assume, in accordance with the measurements of Appleton * and others, that the under-surface of the ionosphere lies at a height of about 100 km., then

$$Z(\text{max.})=4{\cdot}7\sqrt{W}\times10^{-7}\text{ volts/cm.} \quad . \quad . \quad (33)$$

Since in general the aerials used in broadcasting emitters have an appreciable part of their length in the horizontal, a greater upward radiation occurs in the immediate vicinity of the emitter than is expressed by equation (32). There will not, therefore, be much error if we assume that the field-intensity over a circular horizontal area of diameter 100 km. centred at a point 100 km. vertically above the emitter is substantially uniform and is given by (33). It follows that the field-intensity over such an area due to an emitter of power 200 kw. may be taken as about 2×10^{-4} volts/cm.

We now examine the modulation M′ impressed on a second wave traversing this region of the ionosphere. We choose $p=1{\cdot}58\times10^{6}$($\lambda=1190$ m.), $P=8\times10^{-4}$ mm. corresponding to $\nu_1=3{\cdot}0\times10^{5}$ collisions per second $C_0\nu_1=1$ corresponding to average night-time broadcasting transmission †, $f=2\pi\times256$ (middle C), and $M=\frac{1}{3}$ (a common average modulation coefficient). The value of ω under European conditions may range from 10^{7} to zero, according to the direction of propagation of the wave (*vide* section 8.2 below). For the purposes of the present calculation we take $\omega=10^{7}$, thereby finding a lower limit to the impressed modulation. On substituting these values in equation (31) we find

$$M'=10^{-3}.$$

If now we take $M_1=\frac{1}{3}$ as the average coefficient of a modulation already present in the second wave, then $M'/M_1=3\times10^{-3}$. The average level of the impressed modulation is, therefore, 50 decibels below that already

* Proc. Roy. Soc. A, cxxvi. p. 542 (1930).

† This expresses the observed fact that the reflexion coefficient of the ionosphere (*vide* equation (28)) is of the order 30 per cent. under these conditions.

See also Martyn, 'The Propagation of Medium Radio Waves in the Ionosphere.' (In the press.) This contains a detailed discussion of several points in the theory of propagation of broadcasting waves, and is frequently referred to below.

present, and so the interference with the signals or programme given by M_1 is just audible, and may reach annoying intensity when M_1 falls.

Mention has been made in section 1 above of a recent discovery by Tellegen, who found, when listening in Holland to transmissions of the Swiss emitter at Beromünster (650 kc./sec.), that the modulation of the Luxembourg emitter appeared to be superposed thereon. From the above calculation, which has been carried out for the wave-length and power of the Luxembourg station, it follows that the theory developed here is adequate to explain Tellegen's results. The latter has not yet given a sufficiently quantitative account of his results to enable us to compare them in detail with our theory.

In the following sections some experimentally verifiable consequences of this theory are discussed.

8. *Variation of Impressed Modulation with Conditions.*

8.1. *Spatial Considerations.*

Let T denote the emitter of frequency p (the interfering station), and T_1 the second emitter whose signals it is desired to receive.

It is clear that the interference will be greatest when the receiving station is so situated that the ground projection of the point of reflexion in the ionosphere of the signals from T_1 is within 100 km. of T. For distances greater than this the interference will at first fall off slowly, but for distances greater than about 200–300 km. equations (31) and (32) show that the interference will begin to fall off according to the square of the distance.

In order that interference may occur it is also necessary that the signals from T should penetrate to that region of the ionosphere which absorbs the waves from T_1. Waves from any emitter of frequency p penetrate to the region of ionization density

$$N=mp^2\cos^2 i/4\pi^2,$$

given by setting $\mu_0=\sin i$ in (27), where i is the angle of incidence of the wave at the ionosphere.

Thus * for T to interfere notably with the signals from T_1 it is desirable that

$$N \doteqdot N_1,$$

i. e.,

$$p^2\cos^2 i \doteqdot p_1^2\cos^2 i_1. \quad . \quad . \quad . \quad . \quad (34)$$

* See footnote †, p. 379.

For the instance investigated by Tellegen we have

$$p^2 \cos^2 i = 1{\cdot}3 \times 10^{12},$$

$$p_1^2 \cos^2 i_1 = 2{\cdot}3 \times 10^{12},$$

so that

$$N = 0{\cdot}56\, N_1.$$

It follows that the conditions for most notable interference are not here satisfied, and so the value for M′ calculated in section 7 must be reduced. In view of the uncertainty regarding the precise values of some of the quantities involved, it does not seem profitable here to evaluate the consequent correction to M′. It need only be remarked that an appreciable reduction in the modulation factor obtained in section 7, would still give interference of "at times annoying strength," as observed by Tellegen.

It is probable that in the relation (34) lies the explanation of the fact that interference in broadcasting channels has not been experienced from the powerful telegraph stations at Rugby and Nauen. The very long waves emitted by these stations are reflected from regions of the ionosphere below those which absorb waves of broadcasting frequencies. At the same time appreciable interference with other long-wave channels may not necessarily be anticipated, since the greater part of the energy received on such wave-lengths is due either to the ground wave or to a wave which is little absorbed in the affected regions.

8.2. *Influence of the Frequency of* T.

The effect of the frequency of T on the impressed modulation is given by equation (31) when $p \neq \omega$. When $p \doteqdot \omega$ the collision frequency ν cannot now be neglected in deriving (31). Since ω depends on the direction of travel of the wave, therefore, the quasi-resonant state $p = \omega$ can occur only in limited regions of the ionosphere, and since the absorption of the waves from T_1 occurs over several kms. of path, we may consequently neglect the effect of quasi-resonance in producing interference.

If the condition $p \doteqdot \omega$ be neglected, it is clear from equation (31) that the impressed modulation will tend to be greatest when both p and ω are small. It then follows that in the broadcasting wave-band ($10^6 < p < 10^7$) the impressed modulation will tend to be greatest when $p \to 10^6$, provided that simultaneously $\omega << 10^7$ over an

appreciable part of the wave's path. The magneto-ionic theory * shows that $\omega << 10^7$ over an appreciable portion of the upper part of the trajectory of a wave of this frequency under European conditions. At the lower end of the band of broadcasting wave-lengths, however, p is greater, and the same theory shows that $\omega << 10^7$ over a much smaller portion of the waves' trajectory. It follows that the modulation impressed on the ionosphere is greater for the longer broadcasting waves. Also consideration of (34) shows that since $\cos i > \cos i_1$ interference is likely to be most notable when $p < p_1$.

So for these two reasons we may expect that interference will be observed mainly from long-wave broadcasting emitters.

For the very long waves used in commercial telegraphy ($p < 10^6$) the impressed modulation probably tends to a constant value determined by the value of ν_1, while the factors mentioned in 8.1 above will tend to prevent the occurrence of appreciable interference with other transmissions.

For the short waves ($p >> 10^7 p^2$) is always much greater than the maximum value of ω^2. It follows from equation (26) that the impressed modulation varies inversely as the square of the frequency, so that no appreciable interference is likely to be observed from even the most powerful current short-wave emitters.

8.3. *Influence of the Modulation Frequency.*

From equation (31) it follows that the impressed modulation is proportional to $(f^2+780^2+1{\cdot}9\times10^{10}Z^2)^{-\frac{1}{2}}$. For the values of Z obtaining in practice the last term is negligible, so the impressed modulation is proportional to $(f^2+780^2)^{-\frac{1}{2}}$. There is thus an inherent distortion of the impressed modulation in the range of the higher audible frequencies.

The impressed modulation is received over several kms. of path, so a possibility exists of interference between the modulations impressed at different points of the trajectory of the ray from T_1. It is, however, easy to show that this effect is unimportant for the audible frequencies.

* Appleton, J. I. E. E. lxxi. p. 642 (1932).

8.4. *Diurnal Variation of Impressed Modulation.*

From equation (31) it appears that the impressed modulation is approximately proportional to ν_1^2. Also it is well known that the value of ν_1 in the reflecting regions of the ionosphere undergoes a diurnal variation as follows : towards sunset the level of maximum ionization * rises and ν_1 decreases, with a resultant decrease of absorption of radio waves ; at sunrise the reverse occurs, and the level of ionization falls so low that upgoing radio waves may become completely absorbed. The value of C_0, however, does not undergo marked diurnal variations †.

It follows that the impressed interference is least during the night and early morning, but increases towards sunrise. Towards noon, if signals due to downcoming waves are still audible, the interference is greatest, while towards sunset it decreases steadily.

8.5. *Variation of Interference with the Power and Modulation of* T.

From equation (31) it follows that the impressed modulation is proportional to the square of the electric intensity produced by T, and so is proportional to the power radiated from its aerial.

We further conclude from equation (31) that the degree of interference is directly proportional to M, the modulation coefficient of T.

9. *Ionization by Collision due to a Strong Wave.*

In this section we shall examine the effect on the ionosphere of a strong wave of very long wave-length. We suppose that the wave lasts for a brief period, of the order 0·001 sec., so that the discussion may be regarded as a first approximation to the more complex case where a short, powerful pulse of radiated energy, such as originates from a lightning flash, acts upon the ionosphere.

If, for simplicity, we suppose that a steady state exists equation (13) is applicable, and since we have $p<<\nu$, i. e., $n>>q$, equation (13) becomes

$$\tfrac{1}{2}g_0 n_0^2 = a\zeta^2/(n_0^2+r^2), \quad . \quad . \quad . \quad . \quad (35)$$

where $a = 2{\cdot}56\times10^{14}/L_0^2$.

* Chapman, Proc. Phys. Soc. xliii. p. 26 (1931).

† See footnote †, p. 379.

There are good grounds *† for supposing that under undisturbed conditions in the lower regions of the ionosphere $\nu=3\times10^5$. In such circumstances $u=11\times10^6$ and $L=3{\cdot}3\times10^{-2}$, and so $P=\nu L/n=8{\cdot}7\times10^{-4}$ mm.

In Townsend's experiments on ionization by collision of electrons in air the rate of generation of fresh electrons per second is

$$\gamma=\alpha W=P(\alpha/P)W,$$

where α/P and the drift velocity W correspond to a given value of u. Again we have

$$dN=N\gamma\,dt,$$

so that

$$N=N_0e^{\gamma t},$$

where N_0 and N are the initial and final ionization densities respectively and t is the time during which ionization by collision is occurring. In the situation here considered t is therefore 0·001 sec.

We now choose a value for u_0 and proceed to examine the resultant increase in ionization, and the field-intensities necessary to produce this result.

If we take $u_0=120\times10^6$, then from the results of Townsend and Tizard ‡ we have

$$L_0=2{\cdot}75\times10^{-2}, \qquad g_0=6{\cdot}5\times10^{-2},$$

so that by equation (35)

$$Z=1{\cdot}35\sqrt{\nu^2+\omega^2}$$

$$=1{\cdot}35\times10^{-3}\sqrt{9\times10^{10}+\omega^2}\ \text{mv./m.}$$

It follows that a field ranging from 400 to 15,500 mv./m., according as ω ranges from 0 to 10^7, will be required to produce the assumed value of u_0.

Also for this value of u_0 we have § $W=19{\cdot}5\times10^6$, $X/P=60$, and consequently $\alpha/P=0{\cdot}11$. Hence $\gamma=1870$ and $N=6{\cdot}5\,N_0$.

Thus for the condition postulated we obtain an increase of ionization up to 6·5 times that initially existing.

Recent observations have shown that sudden increases in the ionization of the E layer in the ionosphere of this order of magnitude are correlated with the presence of

* See footnote †, p. 379.
† Appleton, J.I.E.E. lxxi. p. 642 (1932).
‡ See Table, p. 374.
§ Townsend, 'Electricity in Gases' (Clarendon Press), pp. 180 and 282.

nearby thunderstorms. Now the observations of Appleton, Watson Watt, and Herd * on the intensities of the radiation fields of lightning flashes enable us to determine the peak-field strength of the pulse at the E layer. This field proves to be of the order 600 mv./m. The pulses observed by these workers lasted for several milliseconds, and normally took the form of a highly damped oscillation. Since the present treatment considers only the effect of an undamped oscillation, we have taken the duration of this pulse to be but one millisecond in order to ensure an approximate equality of the energies in our short pulse and in an actual atmospheric, and to allow for the time required for the steady state to be approached. A fuller investigation of the effect of a damped pulse on the ionosphere will be given elsewhere.

From the above example it is therefore very probable that the pulse radiated by a lightning flash in certain directions making favourable angles with the earth's magnetic field can produce a notable effect on the ionization of the ionosphere.

Another effect which can be produced by such a pulse is the production of " atmospherics " in a radio receiver by modulation of a received carrier-wave which passes through regions of the ionosphere acted on by the pulse. Calculations similar to those already given show that such " atmospherics " may be appreciable.

In conclusion we desire to acknowledge our indebtedness to Drs. G. Builder and A. L. Green for their helpful criticisms, and to the former for having carefully checked all our calculations.

10. *Summary.*

The application of the methods and results of Townsend and his associates shows that a powerful radio emitter is capable of appreciably modifying the collision frequency of electrons with the molecules in the ionosphere. In this way are explained the observations of Tellegen, in which the powerful Luxembourg station interfered with the signals received in Holland from Beromünster in Switzerland. Some observable consequences of the theory are predicted. It is also shown that a short undamped pulse,

* Proc. Roy. Soc. A, cxi. p. 615 (1926).

comparable in intensity with an atmospheric, is able to produce a notable increase in the ionization of the ionosphere.

Addendum.

Since the above was written two further instances of interference of the type discussed in this paper have been found ('World Radio,' xviii. p. 132 (1934)). In each case the interference was caused by an emitter using a wave-length in the long end of the broadcasting spectrum. These additional experimental facts appear to confirm Tellegen's observations and to support the arguments developed in section 8.2 above on the variation of the impressed modulation with the wave-length of the interfering emitter.

XXXIII. *The Magneto-Optical Dispersion of Organic Liquids in the Ultra-Violet Region of the Spectrum.—* Part VIII. *The Magneto-Optical Dispersion of Normal Butyl Acetate, Methyl Acetate and Ethyl Acetate. By* G. E. Jones, *M.Sc., and* Prof. E. J. Evans, *D.Sc., Physics Department, University College of Swansea* *.

Introduction.

THE experimental methods employed in the measurements of the magneto-optical rotations and the refractive indices of the three liquids have been previously described in detail †. The magneto-optical and ordinary dispersions of methyl and ethyl acetates ‡ have already been determined in this laboratory, but, as the results were not altogether satisfactory, it was decided to repeat the measurements under better conditions.

The results have been examined in relation to Larmor's theory § of magnetic rotation. According to this theory Verdet's constant δ for a wave-length λ is given by the expression

$$\delta = \frac{e}{2mC^2} \cdot \lambda \cdot \frac{dn}{d\lambda}, \quad \ldots\ldots (1)$$

* Communicated by the Authors.

† Stephens and Evans, Phil. Mag. x. p. 759 (1930).

‡ Evans and Evans, Phil. Mag. viii. p. 137 (1929).

§ 'Æther and Matter,' Appendix F, p. 352.

where n is the refractive index, e/m is the ratio of the charge to the mass of the resonators, and c the velocity of light.

In the above expression the charge e is measured in electrostatic units and the magnetic field in electromagnetic units.

If the ordinary dispersion of each liquid is represented by an equation of the type

$$n^2-1=b_0+\frac{b_1}{\lambda^2-\lambda_1^2}+\frac{b_2}{\lambda^2-\lambda_2^2} \quad . \quad . \quad . \quad (2)$$

and the magneto-optical dispersion over the range of spectrum investigated is controlled by one absorption band in the ultra-violet, it can be shown that

$$\phi=n\delta\lambda^2=\mathrm{K}\left(\frac{\lambda^2}{\lambda^2-\lambda_1^2}\right)^2, \quad . \quad . \quad . \quad . \quad . \quad . \quad (3)$$

where K is a constant, and λ_1 the wave-length of the absorption band. In addition, the value of e/m deduced from the above three equations is given by the expression

$$-\frac{2\mathrm{K}C^2}{b_1}.$$

Each of the three liquids employed in this investigation was subjected to a process of fractional distillation before use, and the fraction which distilled over in the neighbourhood of the accepted boiling-point was employed in the determinations of the refractive indices.

The refractive indices given in Table I. were determined at temperatures in the neighbourhood of 20° C., and were corrected to the temperatures at which the magneto-optical rotations were measured by means of the known values of the temperature coefficients of the three liquids. It was found that the refractive indices of normal butyl, methyl, and ethyl acetates diminished by $\cdot 0004_6$, $\cdot 0004_1$, and $\cdot 0004_1$ respectively for one degree C. rise of temperature. The refractive indices of the three liquids for various wave-lengths are plotted in fig. 1.

Magneto-Optical Dispersion.

The normal butyl acetate employed for the magneto-optical experiments distilled over between 126·7° C. and 126·9° C. at a pressure of 782 mm. of mercury.

Experimental Results.

Ordinary Dispersion.

Table I.

Normal butyl acetate at 18·5° C.		Methyl acetate at 22° C.		Ethyl acetate at 20·9° C.	
Wave-length in microns.	Refractive index.	Wave-length in microns.	Refractive index.	Wave-length in microns.	Refractive index.
·6678	$1{\cdot}3930_6$	·6678	$1{\cdot}3582_4$	·6678	$1{\cdot}3700_8$
·6563	$1{\cdot}3934_5$	·5893	$1{\cdot}3603_8$	·5893	$1{\cdot}3719_5$
·5893	$1{\cdot}3953_1$	·5876	$1{\cdot}3604_4$	·5876	$1{\cdot}3721_1$
·5876	$1{\cdot}3953_9$	·5016	$1{\cdot}3639_9$	·5218	$1{\cdot}3749_9$
·5016	$1{\cdot}3993_8$	·4922	$1{\cdot}3645_8$	·5153	$1{\cdot}3751_7$
·4922	$1{\cdot}3999_3$	·4713	$1{\cdot}3656_9$	·5016	$1{\cdot}3757_7$
·4861	$1{\cdot}4003_5$	·4704	$1{\cdot}3658_2$	·4922	$1{\cdot}3763_9$
·4713	$1{\cdot}4013_1$	·4674	$1{\cdot}3660_6$	·4651	$1{\cdot}3781_3$
·4535	$1{\cdot}4027_0$	·4651	$1{\cdot}3662_2$	·4472	$1{\cdot}3793_4$
·4472	$1{\cdot}4031_5$	·4587	$1{\cdot}3666_5$	·4400	$1{\cdot}3800_4$
·4427	$1{\cdot}4035_0$	·4535	$1{\cdot}3670_1$	·4308	$1{\cdot}3809_3$
·4341	$1{\cdot}4042_4$	·4480	$1{\cdot}3674_8$	·4062	$1{\cdot}3832_0$
·4329	$1{\cdot}4044_0$	·4472	$1{\cdot}3674_6$	·4056	$1{\cdot}3832_3$
·4248	$1{\cdot}4051_8$	·4378	$1{\cdot}3682_8$	·3860	$1{\cdot}3854_9$
·4177	$1{\cdot}4059_0$	·4275	$1{\cdot}3691_4$	·3825	$1{\cdot}3860_2$
·4063	$1{\cdot}4071_0$	·4177	$1{\cdot}3700_6$	·3688	$1{\cdot}3881_0$
·3947	$1{\cdot}4085_0$	·4062	$1{\cdot}3711_1$	·3654	$1{\cdot}3884_0$
·3860	$1{\cdot}4095_3$	·3861	$1{\cdot}3733_6$	·3627	$1{\cdot}3887_9$
·3801	$1{\cdot}4104_0$	·3688	$1{\cdot}3757_8$	·3533	$1{\cdot}3904_3$
·3737	$1{\cdot}4113_6$	·3654	$1{\cdot}3763_2$	·3337	$1{\cdot}3940_0$
·3688	$1{\cdot}4120_0$	·3627	$1{\cdot}3768_5$	·3308	$1{\cdot}3946_0$
·3619	$1{\cdot}4131_7$	·3533	$1{\cdot}3783_5$	·3282	$1{\cdot}3951_5$
·3536	$1{\cdot}4145_8$	·3337	$1{\cdot}3820_1$	·3247	$1{\cdot}3959_8$
·3520	$1{\cdot}4148_7$	·3308	$1{\cdot}3825_4$	·3208	$1{\cdot}3969_6$
·3476	$1{\cdot}4155_2$	·3208	$1{\cdot}3847_6$	·3140	$1{\cdot}3984_0$
·3457	$1{\cdot}4159_2$	·3140	$1{\cdot}3865_1$	·3127	$1{\cdot}3988_0$
·3404	$1{\cdot}4169_1$	·3127	$1{\cdot}3867_1$	·3116	$1{\cdot}3991_0$
·3381	$1{\cdot}4174_0$	·3092	$1{\cdot}3875_9$	·3063	$1{\cdot}4005_8$
·3363	$1{\cdot}4178_0$	·3010	$1{\cdot}3898_5$	·3036	$1{\cdot}4012_3$
·3337	$1{\cdot}4184_6$	·2997	$1{\cdot}3900_8$	·3022	$1{\cdot}4016_0$
·3312	$1{\cdot}4190_6$	..	..	·3010	$1{\cdot}4019_8$
·3278	$1{\cdot}4197_7$	..	..	·2986	$1{\cdot}4029_0$
				·2961	$1{\cdot}4035_0$
				·2911	$1{\cdot}4051_0$
				·2883	$1{\cdot}4060_0$
				·2824	$1{\cdot}4081_0$
				·2766	$1{\cdot}4105_0$
				·2724	$1{\cdot}4122_3$

The experimental results are given in Table II. (*a*) and fig. 2.

Fig. 1.

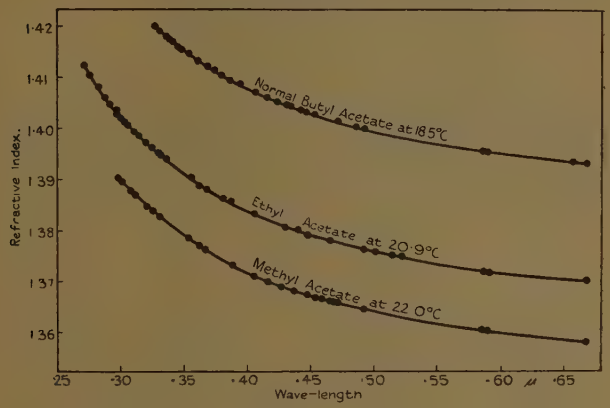

Fig. 2.

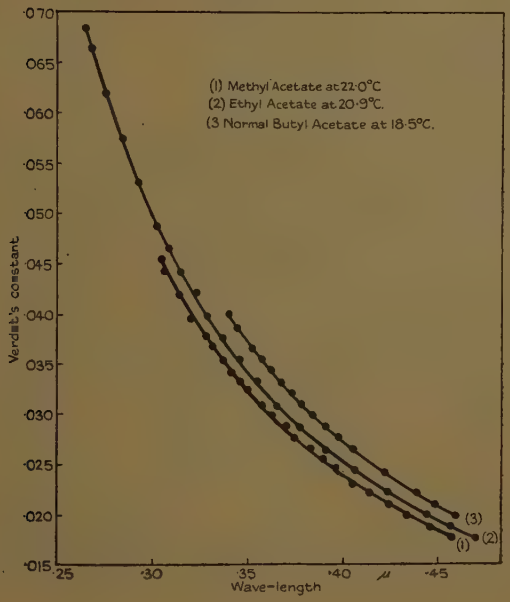

TABLE II. (*a*).

Verdet's constant of *n*-butyl Acetate at various wave-lengths.

[Temperature 18·5° C.]

Wave-length in microns.	Verdet's constant in min./cm. gauss.	Wave-length in microns.	Verdet's constant in min./cm. gauss.
·4606	$\cdot0198_7$	·3787	$\cdot0309_3$
·4496	$\cdot0209_8$	·3731	$\cdot0320_4$
·4394	$\cdot0220_8$	·3677	$\cdot0331_4$
·4300	$\cdot0231_9$	·3625	$\cdot0342_5$
·4212	$\cdot0242_9$	·3578	$\cdot0353_6$
·4130	$\cdot0254_0$	·3532	$\cdot0364_6$
·4053	$\cdot0265_1$	·3488	$\cdot0375_6$
·3979	$\cdot0276_1$	·3446	$\cdot0386_7$
·3912	$\cdot0287_2$	·3406	$\cdot0397_8$
·3847	$\cdot0298_3$		

Table II. (*b*) contains results taken from fig. 1 and Table II. (*a*), and these were employed in determining the constants of the magneto-optical dispersion equation of *n*-butyl acetate.

TABLE II. (*b*).

	λ microns.	*n*.	δ min./cm. gauss.
(*a*)	·4496	$1\cdot4029_5$	$\cdot0209_8$
(*b*)	·3847	$1\cdot4097_3$	$\cdot0298_3$
(*c*)	·3488	$1\cdot4154_6$	$\cdot0375_6$

From (*a*) and (*b*), $\lambda_1=\cdot1076_4\ \mu$ and $K=5\cdot275_7\times10^{-3}$.
,, (*a*) ,, (*c*), $\lambda_1=\cdot1085_1\ \mu$,, $K=5\cdot271_1\times10^{-3}$.
,, (*b*) ,, (*c*), $\lambda_1=\cdot1095_0\ \mu$,, $K=5\cdot274_8\times10^{-3}$.

The mean values of λ_1 and K are $\cdot1086\ \mu$ and $5\cdot27_4\times10^{-3}$ respectively, and the equation representing the magneto-optical dispersion of *n*-butyl acetate over the region $\cdot4606\ \mu$ to $\cdot3406\ \mu$ is

$$n\delta=5\cdot27_4\times10^{-3}\frac{\lambda^2}{\{\lambda^2-(\cdot1086)^2\}^2}.$$

The accuracy of the representation of the experimental results by the above equation is shown in Table II. (*c*), which gives a comparison of the observed and calculated values of Verdet's constant at certain wave-lengths.

TABLE II. (*c*).

λ.	δ (observed).	δ (calculated).	λ.	δ (observed).	∂ (calculated).
·4300	$\cdot0231_9$	$\cdot0231_7$	·3731	$\cdot0320_4$	$\cdot0320_4$
·4212	$\cdot0242_9$	$\cdot0242_7$	·3677	$\cdot0331_4$	$\cdot0331_5$
·3979	$\cdot0276_1$	$\cdot0276_2$	·3625	$\cdot0342_5$	$\cdot0342_8$
·3912	$\cdot0287_2$	$\cdot0287_2$	·3578	$\cdot0353_5$	$\cdot0353_4$
·3787	$\cdot0309_3$	$\cdot0309_5$	·3532	$\cdot0364_6$	$\cdot0364_5$

Methyl Acetate.

The specimen of methyl acetate employed in the magneto-optical experiments distilled over between 57·4° C. and 57·8° C. at a pressure of 782 mm. of mercury.

The experimental results are collected in Table III. (*a*) and plotted in fig. 2.

From the values of Verdet's constants and the refractive indices at $\cdot4452\ \mu$, $\cdot4138\ \mu$, $\cdot3688\ \mu$, $\cdot3213\ \mu$, and $\cdot3078\ \mu$ the constants λ_1 and K of the magneto-optical dispersion equation

$$n\delta=\mathrm{K}\frac{\lambda^2}{(\lambda^2-\lambda_1^2)^2}$$

were calculated.

The mean values of λ_1 and K were found to be $\cdot1054\ \mu$ and $4\cdot523\times10^{-3}$ respectively, and the equation representing the magneto-optical dispersion of methyl acetate at 22° C.

over the range of spectrum investigated (·4576 μ to ·3047 μ) is therefore

$$n\delta = 4{\cdot}52_3 \times 10^{-3} \frac{\lambda^2}{\{\lambda^2 - (\cdot 1054^2)\}^2}.$$

TABLE III. (*a*).

Verdet's constant of Methyl Acetate at various wave-lengths.

[Temperature = 22·0° C.]

Wave-length in microns.	Verdet's constant in min./cm. gauss.	Wave-length in microns.	Verdet's constant in min./cm. gauss.
·4576	$\cdot 0176_3$	·3629	$\cdot 0297_7$
·4452	$\cdot 0187_3$	·3572	$\cdot 0308_7$
·4337	$\cdot 0198_3$	·3519	$\cdot 0319_8$
·4235	$\cdot 0209_3$	·3470	$\cdot 0330_8$
·4138	$\cdot 0220_4$	·3420	$\cdot 0341_9$
·4046	$\cdot 0231_4$	·3374	$\cdot 0352_9$
·3964	$\cdot 0242_5$	·3213	$\cdot 0397_2$
·3890	$\cdot 0253_5$	·3143	$\cdot 0419_3$
·3820	$\cdot 0264_5$	·3078	$\cdot 0441_4$
·3747	$\cdot 0275_6$	·3047	$\cdot 0452_5$
·3688	$\cdot 0286_6$		

This equation was employed to compare the calculated values of Verdet's constant at different wave-lengths with those determined experimentally, and the result of the comparison is shown in Table III. (*b*).

The value of Verdet's constant of methyl acetate at 22° C. for sodium light was also calculated from the magneto-optical dispersion equation, and was found to be $\cdot 0102_2$. Perkin's * value of the specific rotation of methyl acetate for sodium light at 22° C. is ·7792. Taking the value of Verdet's constant of water for sodium light to be ·01308, the value of Verdet's constant of methyl acetate deduced from Perkin's observations is ·01019.

* Perkin, Journ. Chem. Soc. xlv. p. 493 (1884).

TABLE III. (*b*).

λ.	δ (observed).	δ (calculated).	λ.	δ (observed).	δ (calculated).
·4576	$·0176_3$	$·0176_2$	·3629	$·0297_7$	$·0297_5$
·4235	$·0209_3$	$·0209_3$	·3519	$·0319_8$	$·0319_7$
·3964	$·0242_5$	$·0242_9$	·3420	$·0341_9$	$·0342_0$
·3890	$·0253_5$	$·0253_5$	·3374	$·0352_9$	$·0353_2$
·3820	$·0264_5$	$·0264_3$	·3143	$·0419_3$	$·0419_3$
·3747	$·0275_6$	$·0276_3$	·3047	$·0452_5$	$·0452_6$

Ethyl Acetate.

The specimen of ethyl acetate employed in the measurements of the magneto-optical rotations distilled over between 76·6° C. and 77·1° C. at a pressure of 753 mm. of mercury.

The experimental results are given in Table IV. (*a*) and fig. 2.

TABLE IV. (*a*).

Values of Verdet's constant of Ethyl Acetate at various wave-lengths.

[Temperature = 20·9° C.]

Wave-length in microns.	Verdet's constant in min./cm. gauss.	Wave-length in microns.	Verdet's constant in min./cm. gauss.
·4692	$·0176_4$	·3290	$·0397_4$
·4564	$·0187_4$	·3220	$·0419_5$
·4445	$·0198_4$	·3149	$·0441_6$
·4240	$·0220_5$	·3088	$·0463_8$
·4064	$·0242_6$	·3031	$·0485_9$
·3909	$·0264_8$	·2928	$·0530_3$
·3776	$·0286_9$	·2839	$·0574_3$
·3657	$·0308_9$	·2755	$·0619_0$
·3553	$·0331_0$	·2686	$·0663_4$
·3457	$·0353_2$	·2654	$·0685_4$
·3367	$·0375_2$		

From the values of Verdet's constants and the refractive indices at ·4445 μ, ·3657 μ, ·3149 μ, and 2686 μ the constants λ_1 and K of the magneto-optical dispersion equation

$$n\delta = K\frac{\lambda^2}{(\lambda^2-\lambda_1^2)^2}$$

were calculated.

It was found that the equation representing the magneto-optical dispersion of ethyl acetate at 20·9° C. over the range of spectrum investigated (·4692 μ to ·2654 μ) is

$$n\delta = 4{\cdot}80_5\times10^{-3}\frac{\lambda^2}{\{\lambda^2-(\cdot1065)^2\}^2}.$$

This equation was used to calculate the values of δ for some wave-lengths at which determinations had been carried out, and a comparison of the observed and calculated values is given in Table IV. (*b*).

TABLE IV. (*b*).

λ.	δ (observed).	δ (calculated).	λ.	δ (observed).	δ (calculated).
·4240	$\cdot0220_5$	$\cdot0220_4$	·3290	$\cdot0397_4$	$\cdot0397_1$
·4064	$\cdot0242_6$	$\cdot0242_5$	·3220	$\cdot0419_6$	$\cdot0418_3$
·3909	$\cdot0264_8$	$\cdot0264_9$	·3088	$\cdot0463_3$	$\cdot0463_7$
·3776	$\cdot0286_9$	$\cdot0286_8$	·3031	$\cdot0485_9$	$\cdot0485_7$
·3553	$\cdot0331_0$	$\cdot0330_5$	·2928	$\cdot0530_3$	$\cdot0529_9$
·3457	$\cdot0353_2$	$\cdot0352_6$	·2839	$\cdot0574_8$	$\cdot0573_5$
·3367	$\cdot0375_2$	$\cdot0375_6$	·2755	$\cdot0619_0$	$\cdot0620_1$

The magneto-optical dispersion equation was also employed to calculate Verdet's constant for sodium light, and the value obtained was $\cdot0107_7$ at 20·9° C. Perkin * found the specific rotation of ethyl acetate to be ·8315 at 10·5° C. and ·8277 at 17·75° C. From the value of the temperature coefficient deduced from the above observations it follows that the specific rotation of ethyl acetate at 20·9° C. is ·8260. The value of Verdet's constant of ethyl acetate for sodium light at 20·9° C. deduced from Perkin's value of the specific rotation and the known

* *Loc. cit.* p. 491.

value of Verdet's constant of water at the same wave-length is ·01080.

Ordinary Dispersion.

The experimental results have shown that the magneto-optical dispersion of each of the three liquids can be represented by an equation involving the presence of one absorption band of wave-length λ_1, situated in the Schumann-Lyman region of the spectrum.

It will be shown that the ordinary dispersion of each liquid can be represented within experimental error by the equation

$$n^2-1=b_0+\frac{b_1}{\lambda^2-\lambda_1^2},$$

where λ_1 has the same value as that deduced from the magneto-optical experiments. The values of the constants b_0 and b_1 can be determined from two values of the refractive index corresponding to two known wave-lengths.

Normal Butyl Acetate.

The following pairs of values of λ and n were used to calculate the constants b_0 and b_1 of the ordinary dispersion equation of normal butyl acetate. In these calculations λ_1 was taken to be ·1086 μ, the value deduced from the magneto-optical experiments. The results are collected in Table V. (*a*).

TABLE V. (*a*).

λ in microns.	n.	$b_1\times10^3$.	b_0.
·5016 ·3860	$1{\cdot}3993_8$ $1{\cdot}4095_2$	$9{\cdot}133_2$	$\cdot9201_8$
·4861 ·3688	$1{\cdot}4003_5$ $1{\cdot}4120$	$9{\cdot}111_4$	$\cdot9203_9$
·4341 ·3312	$1{\cdot}4042_4$ $1{\cdot}4190_6$	$9{\cdot}188_6$	$\cdot9198_7$

The mean values of b_1 and b_0 are $9{\cdot}14_4\times10^{-3}$ and $\cdot9201_5$ respectively, and the dispersion of n-butyl acetate at 18·5° C. is represented by the equation

$$n^2=1{\cdot}9201_5+\frac{9{\cdot}14_4\times10^{-3}}{\lambda^2-(\cdot1086)^2}.$$

A comparison of the values of the refractive indices calculated from the above equation with those determined experimentally is given in Table V. (*b*).

TABLE V. (*b*).

λ.	n (observed).	n (calculated).
·4535	1·4027	$1{\cdot}4026_1$
·4427	1·4035	$1{\cdot}4034_6$
·4248	$1{\cdot}4051_6$	$1{\cdot}4051_2$
·4063	1·4071	$1{\cdot}4070_6$
·3870	1·4094	$1{\cdot}4094_0$
·3619	$1{\cdot}4131_7$	$1{\cdot}4131_1$
·3520	$1{\cdot}4148_7$	$1{\cdot}4148_2$
·3404	$1{\cdot}4169_1$	$1{\cdot}4170_4$
·3337	$1{\cdot}4184_8$	$1{\cdot}4184_5$

Methyl Acetate.

The pairs of values of λ and n employed in the calculation of the constants b_1 and b_0 of the dispersion equation are given in Table VI. (*a*). The value of λ_1 was taken as ·1054 μ.

TABLE VI. (*a*).

λ (microns).	n.	$b_1 \times 10^{-3}$.	b_0.
·6678 ·4275	$1{\cdot}3582_4$ $1{\cdot}3691_4$	$8{\cdot}430_6$	$\cdot 8254_3$
·5893 ·3627	$1{\cdot}3603_8$ $1{\cdot}3768_5$	$8{\cdot}461_2$	$\cdot 8254_6$
·5016 ·2997	$1{\cdot}3639_9$ $1{\cdot}3900_8$	$8{\cdot}407_3$	$\cdot 8255_1$

The mean values of b_1 and b_0 are $8{\cdot}43_3 \times 10^{-3}$ and $\cdot 8254_7$ respectively, and the ordinary dispersion equation of methyl acetate at 22·0° C. is

$$n^2 = 1{\cdot}8254_7 + \frac{8{\cdot}43_3 \times 10^{-3}}{\lambda^2 - (\cdot 1054)^2}.$$

A comparison of the values of the refractive indices calculated from this equation and the experimental results is given in Table VI. (*b*).

TABLE VI. (*b*).

λ.	n (observed).	n (calculated).
·4674	$1{\cdot}3660_6$	$1{\cdot}3660_7$
·4587	$1{\cdot}3666_5$	$1{\cdot}3666_7$
·4378	$1{\cdot}3682_8$	$1{\cdot}3682_7$
·3688	$1{\cdot}3757_8$	$1{\cdot}3758_6$
·3533	$1{\cdot}3783_5$	$1{\cdot}3782_7$
·3308	$1{\cdot}3825_4$	$1{\cdot}3824_8$
·3127	$1{\cdot}3867_1$	$1{\cdot}3866_4$
·3010	$1{\cdot}3898_5$	$1{\cdot}3898_0$

Ethyl Acetate.

The constants b_1 and b_0 of the ordinary dispersion equation of ethyl acetate were calculated from the pairs of values of λ and n given in Table VII. (*a*). The value of λ_1 employed in these calculations was ·1065 μ

TABLE VII. (*a*).

λ (microns).	n.	$b_1 \times 10^{-3}$.	b_0.
·6678 ·4400	$1{\cdot}3700_8$ $1{\cdot}3800_4$	$8{\cdot}597_7$	$\cdot 8573_4$
·4922 ·3627	$1{\cdot}3763_9$ $1{\cdot}3887_6$	$8{\cdot}597_2$	$\cdot 8572_2$
·4587 ·2724	$1{\cdot}3789_4$ $1{\cdot}4122_3$	$8{\cdot}597_2$	$\cdot 8576_3$

The mean values of b_1 and b_0 are $8{\cdot}59_7 \times 10^{-3}$ and $\cdot 8574_0$ respectively, and the equation representing the dispersion of ethyl acetate at 20·9° C. is

$$n^2 = 1{\cdot}8574 + \frac{8{\cdot}59_7 \times 10^{-3}}{\lambda^2 - (\cdot 1065)^2}.$$

Table VII. (*b*) gives a series of values of the refractive indices calculated from the above equation, and also the experimental results.

TABLE VII. (*b*).

λ.	*n* (observed).	*n* (calculated).
·5153	$1{\cdot}3751_7$	$1{\cdot}3752_2$
·4651	$1{\cdot}3781_3$	$1{\cdot}3781_7$
·4306	$1{\cdot}3809_3$	$1{\cdot}3808_4$
·4062	$1{\cdot}3832$	$1{\cdot}3832_4$
·3825	$1{\cdot}3860_2$	$1{\cdot}3860_4$
·3533	$1{\cdot}3904_2$	$1{\cdot}3903_8$
·3247	$1{\cdot}3959_8$	$1{\cdot}3960_0$
·3063	$1{\cdot}4005_3$	$1{\cdot}4005_9$
·2911	$1{\cdot}4051$	$1{\cdot}4051_8$
·2766	$1{\cdot}4105$	$1{\cdot}4104_4$

Calculation of $\frac{e}{m}$.

The value of e/m is given by the equation

$$\frac{e}{m} = -\frac{2KC^2}{b_1},$$

and can therefore be deduced from the results of the magneto-optical and ordinary dispersion experiments. In the above equation e is expressed in electrostatic units and the magnetic field in electromagnetic units.

The values of K for *n*-butyl, methyl, and ethyl acetates when δ is expressed in radians per cm. gauss are $1{\cdot}53_4\times10^{-14}$, $1{\cdot}31_6\times10^{-14}$, and $1{\cdot}39_8\times10^{-14}$ respectively.

Similarly, the values of b_1 for the three liquids when λ is expressed in cm. are $\cdot914_4\times10^{-10}$, $\cdot843_3\times10^{-10}$, and $\cdot859_7\times10^{-10}$ The values of e/m for *n*-butyl, methyl, and ethyl acetates are therefore $1{\cdot}01\times10^7$, $\cdot93_6\times10^7$, and $\cdot94_2\times10^7$ e.m.u. respectively.

DISCUSSION OF RESULTS.

The experimental results show that the magneto-optical dispersion of normal butyl, methyl, and ethyl acetates over the ranges of spectrum examined, can be represented by an equation of the type

$$n\delta = K\frac{\lambda^2}{(\lambda^2-\lambda_1^2)^2},$$

where n and δ are the values of the refractive index and Verdet's constant for a wave-length λ, and λ_1 is the

Table VIII.

Liquid.	Molecular weight.	λ_1 (microns).	e/m.	K.	Constants of ordinary dispersion equation.		Verdet's constant (sodium light), calculated.	Verdet's constant (sodium light), Perkin.	Temp. in ° C.
					b_0.	b_1.			
Acetic acid : $(C_2H_4O_2)$.....	60	·1042	$\cdot 91_6 \times 10^7$	$4\cdot 71_3 \times 10^{-3}$	$\cdot 8557_5$	$8\cdot 98_1 \times 10^{-3}$	$\cdot 0105_1$	$\cdot 0105_1$	19·5
Methyl acetate : $(C_3H_6O_2)$	74	·1054	$\cdot 93_6 \times 10^7$	$4\cdot 52_3 \times 10^{-3}$	$\cdot 8254_7$	$8\cdot 43_3 \times 10^{-3}$	$\cdot 0102_2$	$\cdot 0101_9$	22·0
Ethyl acetate : $(C_4H_8O_2)$	88	·1065	$\cdot 94_2 \times 10^7$	$4\cdot 80_5 \times 10^{-3}$	$\cdot 8574_0$	$8\cdot 59_7 \times 10^{-3}$	$\cdot 0107_7$	$\cdot 0108_0$	20·9
n-Propyl acetate : $(C_5H_{10}O_2)$	102	·1077	$1\cdot 01 \times 10^7$	$5\cdot 12_2 \times 10^{-3}$	$\cdot 8978_5$	$8\cdot 85_5 \times 10^{-3}$	$\cdot 0113_8$	·01137	13·0
n-Butyl acetate : $(C_6H_{12}O_2)$	116	·1086	$1\cdot 01 \times 10^7$	$5\cdot 27_4 \times 10^{-3}$	$\cdot 9201_5$	$9\cdot 14_4 \times 10^{-3}$	$\cdot 0116_6$	..	18·5
Isobutyl acetate : $(C_6H_{12}O_2)$	116	·1080	$1\cdot 01_5 \times 10^7$	$5\cdot 37_1 \times 10^{-3}$	·9151	$9\cdot 24 \times 10^{-3}$	$\cdot 0118_3$	·01191	11·4

wave-length of the absorption band situated in the Schumann-Lyman region of the spectrum. The values of the constants K and λ_1 vary from liquid to liquid.

Similarly, the refractive indices of the three liquids can be represented within experimental error by the equation

$$n^2-1=b_0+\frac{b_1}{\lambda^2-\lambda_1^2},$$

where λ_1 has the same value as that deduced from the magneto-optical experiments. The values of the constants b_0 and b_1 depend on the nature of the liquid.

The results obtained in this laboratory for acetic acid and several acetates are collected in Table VIII.

An examination of the Table shows that λ_1 for substances of the same structure increases by about $\cdot 0011\ \mu$ for every addition of CH_2. It is also seen that the position of the absorption band of isobutyl acetate is not far removed from that of normal butyl acetate, which has a different structure. Again, comparing the normal acetates it is found that K, b_0, and b_1 increase progressively with increase of molecular weight. This statement holds even when the effect of temperature on the magneto-optical rotation and refractive index is taken into account. It is, however, noticeable that there is a diminution in the values of K, b_0, and b_1 in passing from acetic acid to methyl acetate. The values of Verdet's constant given in column 8 were not determined experimentally, but were calculated from the magneto-optical dispersion equation deduced from experimental results for wave-lengths below $\cdot 46\ \mu$. The agreement between these calculated values and those obtained by Perkin is very satisfactory. The value of e/m tends to increase with increasing molecular weight, but is in all cases well below $1{\cdot}77\times 10^7$.

These experiments show that Larmor's theory satisfactorily accounts for the variation in the magneto-optical rotation with wave-length, but leads to a very low value of e/m. It is, however, possible that the magneto-optical dispersion equation involving only one absorption band in the ultra-violet would have to be modified if rotations could be measured for smaller wave-lengths.

February, 1934.

XXXIV. *On Parabolic Cylinder Functions.*

By S. C. Dhar, *D.Sc.*, *and* N. A. Shastri, *M.Sc.**

1. VARIOUS methods† have been employed to study the properties of Parabolic Cylinder Functions, but it is the purpose of this paper to study some of these by contour integration.

Integral Equation.

Take the following differential equation of the second order which comes so often in problems of mathematical physics, viz.,

$$(ax^2+c)\frac{d^2y}{dx^2}+ax\frac{dy}{dx}+(c\kappa^2x^2+b)y=0. \quad . \quad . \quad (1)$$

Suppose that a solution of the above equation exists in the form

$$y=\lambda\int e^{\kappa\theta x}\frac{\phi(\theta)}{\sqrt{a\theta^2+c}}\,d\theta,$$

where the form of $\phi(\theta)$ and the limits of integration have to be determined.

Substituting in (1), we get

$$\int\{(ax^2+c)\kappa^2\theta^2+(ax)\kappa\theta+(c\kappa^2x^2+b)\}e^{\kappa\theta x}\frac{\phi(\theta)}{\sqrt{a\theta^2+c}}d\theta=0$$

or

$$\int\{\kappa^2x^2(a\theta^2+c)+a\kappa\theta x+(c\kappa^2\theta^2+b)\}e^{\kappa\theta x}\frac{\phi(\theta)}{\sqrt{a\theta^2+c}}d\theta=0.$$

Integrating by parts, we get

$$[\{\kappa x\phi(\theta)-\phi'(\theta)\}e^{\kappa\theta x}\sqrt{a\theta^2+c}]+\int e^{\kappa\theta x}\left\{\sqrt{a\theta^2+c}\,\phi''(\theta)+\frac{a\theta}{\sqrt{a\theta^2+c}}\phi'(\theta)+\frac{c\kappa^2\theta^2+b}{\sqrt{a\theta^2+c}}\phi(\theta)\right\}d\theta=0,$$

or

$$[\{\kappa x\phi(\theta)-\phi'(\theta)\}e^{\kappa\theta x}\sqrt{a\theta^2+c}]+\int\frac{e^{\kappa\theta x}}{\sqrt{a\theta^2+c}}\{(a\theta^2+c)\phi''(\theta)+(a\theta)\phi'(\theta)+(c\kappa^2\theta^2+b)\phi(\theta)\}d\theta=0.$$

* Communicated by the Senior Author.

† Whittaker, Proc. London Math. Soc. xxxv.; Adamoff, *Annales de l'Institute Polytechnique de St. Petersburg*, v.; Watson, Proc. London Math. Soc. ser. 2, viii. & xvii.; Curzon, Proc. London Math. Soc. xii.; Milne, Proc. Edin. Math. Soc. xxxii. & xxxiii.; Mitra, Proc. Edin. Math. Soc. ser. 2, iv. (1934).

If $\phi(\theta)$ be the same function of θ as y is of x, $y(x)$ being a solution of (1), then

$$y(x)=\lambda\int e^{\kappa\theta x}\frac{y(\theta)}{\sqrt{a\theta^2+c}}d\theta=0, \quad . \ . \ . \quad (2)$$

provided the limits of integration be found such that

$$\left[\{\kappa x\phi(\theta)-\phi'(\theta)\}e^{\kappa\theta x}\sqrt{a\theta^2+c}\right]=0. \quad . \ . \quad (3)$$

Relation (3) will hold if the limits are the roots of either

$$a\theta^2+c=0 \ . \ . \ . \ . \ . \ . \ . \quad (4)$$

or

$$\kappa x\phi(\theta)-\phi'(\theta)=0, \quad . \ . \ . \ . \ . \quad (5)$$

provided $e^{\kappa\theta x}\neq\infty$ at the limits of θ.

Taking the roots of (4), we obtain the homogeneous integral equation which will satisfy (1), viz.,

$$G(x)=\lambda\int_{-i\sqrt{\frac{c}{a}}}^{i\sqrt{\frac{c}{a}}}e^{\kappa\theta x}\frac{G(\theta)}{\sqrt{a\theta^2+c}}d\theta, \quad . \ . \ . \quad (6)$$

$G(x)$ being a solution of (1).

By choosing a, b, c properly we shall get by this the well-known *Mathieu Functions* *.

Now, if θ_1 and θ_2 be the two values of θ which satisfy (5), then the solution of (1) will be given by

$$\phi(x)=\lambda\int_{\theta_1}^{\theta_2}\frac{e^{\kappa\theta x}}{\sqrt{a\theta^2+c}}\phi(\theta)d\theta. \ . \ . \ . \ . \quad (7)$$

If we take $a=0$, $c=1$, $\lambda=n+\frac{1}{2}$, and $\kappa=\frac{1}{2}i$, the equation (1) will reduce to the form (when z is put for x)

$$\frac{d^2y}{dz^2}+(n+\tfrac{1}{2}-\tfrac{1}{4}z^2)y=0, \quad . \ . \ . \ . \ . \quad (8)$$

whose solutions are the Weber's cylinder functions $D_n(z)$, and we also know that $D_n(z)$ and $D'_n(z)$ vanish at $\pm\infty$. Hence the integral equation of the parabolic cylinder function † is given by

$$D_n(z)=\lambda\int_{-\infty}^{\infty}e^{\frac{i\theta z}{2}}D_n(\theta)d\theta. \ . \ . \ . \ . \quad (9)$$

* Dhar, Jour. of the Dept. of Science (Calcutta University), vol. ix.

† Milne, Proc. Edin. Math. Soc. xxxii. p. 8.

Evaluation of λ.

2. The value of λ in the integral equation (9) has been obtained by Milne * by the method of Fourier's Double-Integral Theorem. We will, however, proceed to find the value of λ by the method of contour integration.

Take the contour integral for $D_n(x)$ †, viz. :

$$D_n(\theta) = -\frac{\lfloor\overline{n+1}}{2\pi i} e^{-\frac{1}{4}\theta^2} \int_{\infty}^{(0+)} e^{-t\theta - \frac{1}{2}t^2} (-t)^{-n-1} dt. \quad .$$

By deforming the path and making $(-t)^{-n-1}$ one-valued function, it can easily be shown that the contour integral is equal to

$$2i \sin n\pi \int_0^{\infty} e^{-\theta x - \frac{1}{2}x^2} x^{-n-1} dx,$$

where $-\pi < \arg(-t) \leq \pi$, and x being the real part of t.

Hence

$$D_n(\theta) = \frac{\lfloor\overline{n+1} \sin(-n\pi)}{\pi} e^{-\frac{1}{4}\theta^2} \int_0^{\infty} e^{-\theta x - \frac{1}{2}x^2} x^{-n-1} dx$$

$$= \frac{e^{-\frac{1}{4}\theta^2}}{\lfloor -n} \int_0^{\infty} e^{-\theta x - \frac{1}{2}x^2} x^{-n-1} dx.$$

Now substitute this value in (9) and change the order of integration, which is permissible. We obtain

$$D_n(z) = \frac{\lambda}{\lfloor -n} \int_0^{\infty} \left\{ \int_{-\infty}^{\infty} e^{\frac{i\theta z}{2} - \theta x - \frac{1}{4}\theta^2} d\theta \right\} e^{-\frac{1}{2}x^2} x^{-n-1} dx.$$

Now

$$\int_{-\infty}^{\infty} e^{\frac{i\theta z}{2} - \theta x - \frac{1}{4}\theta^2} d\theta = e^{\frac{1}{4}(2x-iz)^2} \int_{-\infty}^{\infty} e^{-\frac{1}{4}[\theta + (2x-iz)]^2} d\theta.$$

$$= 2\sqrt{\pi} e^{\frac{1}{4}(2x-iz)^2}.$$

Hence $$D_n(z) = \frac{\lambda 2\sqrt{\pi}}{\lfloor -n} \int_0^{\infty} e^{x^2 - ixz - \frac{1}{2}z^2 - \frac{1}{2}x^2} x^{-n-1} dx$$

$$= \frac{\lambda 2\sqrt{\pi}}{\lfloor -n} e^{-\frac{1}{4}z^2} \int_0^{\infty} e^{-ixz + \frac{1}{2}x^2} x^{-n-1} dx. \quad . \quad . \quad (10)$$

* Milne, *loc. cit.*

† Whittaker and Watson, ' Modern Analysis,' p. 349 (1927).

Again, putting $t=i\varpi$ in the contour integral for $D_n(z)$, we get

$$D_n(z)=-\frac{\lfloor n+1}{2\pi i}i^{-n}e^{-\frac{1}{4}z^2}\int_{\infty}^{(0+)}e^{iz\omega+\frac{1}{2}\omega^2}(-\omega)^{-n-1}d\omega\ *.$$

The transformation $t=i\omega$ changes the real axis in the t-plane into the imaginary axis in the ω-plane and the imaginary axis into the real axis in the ω-plane. The new figure is obtained by rotating the plane through a right angle in the positive sense. Hence the contour in the ω-plane will also be $(\infty, 0+)$.

Hence

$$D_n(z)=-\frac{\lfloor n+1}{2\pi i}e^{-\frac{1}{4}z^2}i^{-n}2i\sin n\pi\int_0 e^{-ixx'+\frac{1}{2}x'^2}(x')^{-n-1}dx' \quad (11)$$

by deforming the contour and making $(-\omega)^{-n-1}$ one-valued. Here the real part of ω is x' and $-\pi\leq\arg(-\omega)\leq\pi$.

Hence for (10) and (11)

$$-\lfloor n+1\frac{\sin n\pi}{\pi}i^{-n}=\frac{\lambda}{\lfloor -n}2\sqrt{\pi}$$

or

$$\lambda=\frac{\lfloor 1+n\,\lfloor -n\sin n\pi}{\pi}\frac{1}{2\sqrt{\pi}}i^{-n}=\frac{1}{2\sqrt{\pi}i^n}. \quad . \quad (12)$$

The change of the order of integration can be very easily justified.

Addition Formula.

3. When n is a positive integer

$$D_n(z)=-n!\frac{e^{-\frac{1}{4}z^2}}{2\pi i}\int^{(0+)}e^{-zt-\frac{1}{2}t^2}(-t)^{-n-1}dt.$$

Put $t=\sqrt{2}u$ and $z=x+y$,

then

$$D_n(x+y)=-\frac{n!}{2\pi i}e^{-\frac{1}{4}(x+y)^2}\int^{0+}e^{-(\sqrt{2}x+\sqrt{2}y)u-u^2}(-\sqrt{2}u)^{-n-1}\sqrt{2}du,$$

$$=-\frac{n!}{2\pi i}\frac{1}{(\sqrt{2})^n}e^{-\frac{1}{4}(x^2+2xy-y^2)}\int^{0+}e^{-\frac{1}{2}u^2-\sqrt{2}xu}\times\sum_{m=0}^{\infty}\frac{D_m(y\sqrt{2})}{m!}(-u)^{-n+m-1}du.$$

For we know $e^{zt-\frac{1}{2}t^2-\frac{1}{4}z^2}=\sum_0^{\infty}\frac{D_m(z)}{m!}t^m$.

* This can be proved independently as in §16.6 in 'Modern Analysis,' by Whittaker and Watson.

Hence

$$D_n(x+y)=-\frac{n!}{2\pi i}\frac{1}{(\sqrt{2})^n}e^{-\frac{1}{2}(x^2+2xy-y^2)}\sum_{m=0}^{\infty}\frac{D_m(y\sqrt{2})}{m!}\int^{0+}e^{-\frac{1}{2}u^2-\sqrt{2}xu}(-u)^{m-n-1}du.$$

Now

$$\int^{0+}e^{-\sqrt{2}xu-\frac{1}{2}u^2}(-u)^{m-n-1}du=0, \quad \text{when } m>n.$$

Therefore

$$\begin{aligned}&D_n(x+y)\\&=\frac{n!}{(\sqrt{2})^n}e^{\frac{1}{2}(x^2-2xy+y^2)}\sum_{m=0}^{n}\frac{D_m(y\sqrt{2})}{m!}\frac{D_{n-m}(x\sqrt{2})}{(n-m)!}\\&=\frac{n!}{(\sqrt{2})^n}e^{\frac{1}{2}(x-y)^2}\sum_{m=0}^{n}\frac{D_m(y\sqrt{2})}{m!}\frac{D_{n-m}(x\sqrt{2})}{(n-m)!}. \quad . \quad . \quad (13)\end{aligned}$$

The term-by-term integration which we have carried out above is permissible. For we know *

$$\left|\frac{D_n(z)}{n!}\right|\leq e^{\frac{1}{2}(x^2+y^2)}e^{y\sqrt{n}-\frac{1}{2}n}n^{\frac{1}{2}n+\frac{1}{2}n}(2\pi)^{\frac{1}{2}}e^{\theta\,12n},$$

where $0<\theta<1$.

Therefore $\Sigma\frac{D_m(z)}{m!}$ and $\Sigma\frac{D_m(z)}{m!}R^m$ are convergent series where R is finite.

Hence $\Sigma\frac{D_m(\sqrt{2}y)}{m!}(-u)^{m-n-1}$ is uniformly convergent in the region $|u|\leq R$, and term-by-term integration is justifiable.

College of Science,
Nagpur, India.

XXXV. *Notices respecting New Books*

Planetary Theory. By E. W. Brown and C. A. Shook. [Pp. xii+302.] (Cambridge University Press, 1933. Price 15*s.* net.)

THE requirements of a purely theoretical worker in dynamical astronomy are very different from those of anyone engaged in computing the general orbit of a particular

* Gorak Prasad, Proc. Benares Math. Soc. vols. vii.–viii. § 8.

planet, and it is with the latter case that this book is mainly concerned. Thus, the volume is not merely an orthodox treatise on celestial mechanics, and does not attempt to describe the classical theories of Leverrier, Hansen, and Newcomb. In actual computation, economy of time and labour and the provision of adequate checks are all-important, and these considerations have largely determined the scope and plan of the book. Thus, such questions as existence theorems and the validity of the expansions used are not treated. Much of the content is original, either in its methods and results or in the adaptation of known lines of attack.

Two main ways of approach are followed: in the more classical method the theory of canonical variables is followed; by means of a transformation of variables the short-period terms are eliminated, leaving for separate treatment the long-period terms and the secular terms. The other principal method involves the calculation of the coordinates directly in terms of the true longitude; this is the method that has been pursued particularly by Professor E. W. Brown, and the development of the disturbing function is greatly facilitated by the tables recently published by Brown and Brouwer. There is a very useful chapter on "Methods for the Expansion of a Function," and the development of the disturbing function is treated in considerable detail. Schedules are given to facilitate harmonic analysis, and it is worth while quoting a remark made by the authors:—"Harmonic analysis is usually so much more accurate with respect to convergence, and is so much more easily controlled than literal expansions, that it should be used whenever possible."

Apart from its practical value the great importance of this book is the collecting together in one volume of much of the modern work, particularly that of Professor Brown. This is particularly seen in the last two chapters, on Resonance and on The Trojan Group of Asteroids, which are of great theoretical interest and comprise mainly the results of Professor Brown's own researches. The former chapter has cosmological implications; in view of the possibilities of resonance relations of very long period within the solar system inferences based on expansions in powers of the time may have some value in deciding the configuration some 10^8 years ago, but if an interval of 10^9 years is considered, some doubt arises concerning the validity of the inferred possible ranges of the eccentricities and the inclinations.

The perturbations of the Trojan planets by Saturn afford an interesting general result. The difficulty of this problem is enhanced by the fact that the action of Jupiter cannot be neglected in computing even the first approximation to these

perturbations. In addition to the direct effect of Saturn's orbital motion (which is in turn disturbed by the action of Jupiter) there is an indirect perturbation transmitted through the perturbation of Jupiter. Actually it is shown that the perturbations of the longitude of Jupiter by other planets, if of period long compared with that of the libration of the asteroid (about 150 years), are directly impressed on the longitude of the asteroid. Further: "Jupiter not only impresses on the asteroid its own inequalities of period long in comparison with that of the libration, but it also prevents the asteroid from having any very large terms of this nature arising from the action of another planet."

It remains only to add that the typography is excellent and the formulæ well set out.

Analytic and Vector Mechanics. By H. W. Edwards. [Pp. x+428.] (McGraw-Hill Book Company, Inc., New York and London, 1933. Price 24*s*.)

This book gives a very useful introduction to the study of mechanics, suitable for students intending to take a university honours course in physics or mathematics. It will be particularly interesting to those not accustomed to using vector methods in mechanics. In the second chapter the writer gives an account of vectors, including the scalar and vector products and the differentiation of a vector with respect to a scalar—in particular, time. Throughout the development of his subject the author often uses both vectorial and analytical methods. In the numerous problems worked out in the book an attempt is made to assist the student to regard the mathematical expressions as the representation of physical relations rather than groups of symbols to be manipulated according to rules.

The topics discussed include those one would expect to meet in a book of this kind, but the treatment is unusual. After chapters dealing with fundamental subjects come harmonic motion, translation, rotation, statics, attractions, and potentials, central forces, motion with resistance and damped harmonic motion. The chapter on central forces includes the problems of the deflexion of an alpha particle by a stationary and a moving nucleus, while the development of Kepler's laws by vector methods is very interesting. Several examples are solved in a chapter on vector fields, in which Stokes's theorem is used to find the curl of the velocity at a point of a rotating disk. Numerous problems illustrating the fundamental principles of mechanics follow, and the last two chapters deal with systems of particles, rigid systems, the principles of d'Alembert and Hamilton, and the use of Lagrange's equations.

This excellent volume will be of considerable value to many students and teachers. An adverse criticism should be mentioned—it may be considered that the price is rather high for a book of an introductory nature.

Funktionentafeln, Tables of Functions. (German and English text.) By E. JAHNKE and F. EMDE. [Pp. xviii+330, with 171 text-figures.] (Teubner, Leipzig and Berlin, 1933. Price R.M. 16.00.)

THE first edition of this book appeared in 1909, and it has been twice reprinted. This collection of tables of functions, formulæ, and graphs is known to applied mathematicians and physicists throughout the world. Owing to the death of Professor Jahnke in 1921 Professor Emde has been responsible for the preparation of this second edition. Some of the less useful matter has been eliminated, and new tables which appear include powers, circular and hyperbolic functions of a complex variable, tables and graphs for the solution of equations, tables relating to heat conduction, and Planck's radiation function. The tables of Bessel functions have been extended. Where it has not been possible to include a table, curves have been plotted to such a scale that the numerical values can be read off with some accuracy. A very important and interesting feature of the new edition is the introduction of relief representations of complex functions, such as elliptic, Bessel, and Zeta functions.

Emde expresses his indebtedness to the work of the Mathematical Tables Committee of the British Association, and numerous references to other sources are given. A list of useful books for the computer is given at the end of the volume. Much care has been taken to eliminate the errors in the first edition, so that the new collection reaches a high standard of accuracy and reliability. The volume is indispensable to those engaged in the solution of physical, technical, and mathematical problems, and no doubt the English translation which appears side by side with the German explanatory text will lead to an increased popularity in this country and in America.

[*The Editors do not hold themselves responsible for the views expressed by their correspondents.*]

Fig. 5.

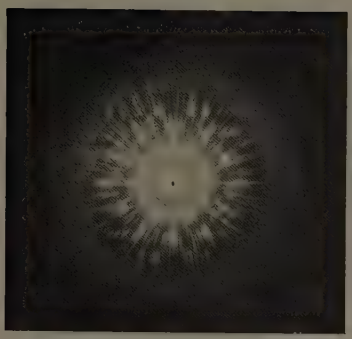

Celluloid. Multiple pattern, including eight principal patterns.

Fig. 6.

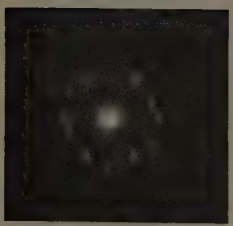

First ring of pattern of fig. 5.

Fig. 8.

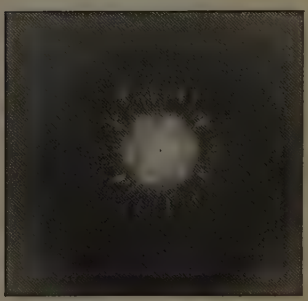

Multiple pattern, including a quadruple pattern.

FIG. 2.

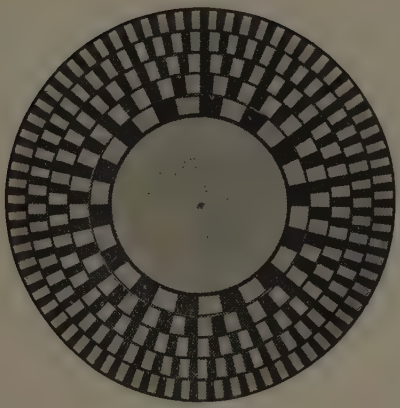

FIG. 3.

FIG. 4.

FIG. 5.

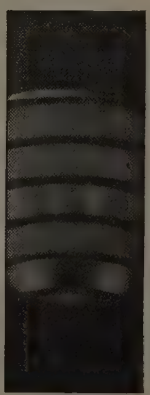

Fig. 2.—Stroboscopic disk for the first five harmonics.
3.—Image of the disk when the slot is completely open.
4.—Image of the disk when one of the slot's ends is covered.
5.—Image of the disk when both ends of slot are symmetrically covered.

Flashing Neon-Valve Oscillator Results.
N=256 per sec.

Synchronous Motor Results.
N=300 per sec.

A.C. 200 volts.
Osglim with
cap resistance.

A.C. 200 volts + 200 volts D.C.
Osglim with cap resistance.

A.C. 200 volts.
Cap resistance
removed.

A.C. 200 volts + 100 volts D.C.
Cap resistance removed.

Flashing Neon Results. A.C. and A.C. + D.C. controlled.